



TECHNISCHE UNIVERSITÄT MÜNCHEN

Fakultät für Medizin

**The role of serine racemase, glypican 4 and accelerated  
aging on pancreatic beta cell function**

**Xue Liu**

Vollständiger Abdruck der von der Fakultät für Medizin der Technischen Universität München zur Erlangung des akademischen Grades einer Doktorin der Naturwissenschaften genehmigten Dissertation.

Vorsitz: Prof. Dr. Dieter Saur

Prüfer\*innen der Dissertation:

1. TUM Junior Fellow Dr. Siegfried Ussar
2. Prof. Dr. Martin Klingenspor

Die Dissertation wurde am 15.12.2022 bei der Technischen Universität München eingereicht und durch die Fakultät für Medizin am 21.03.2023 angenommen.



# Abstract

## Abstract

Obesity and aging are costly worldwide public health problems, and well-known risk factors for developing insulin resistance and type 2 diabetes (T2D). However, preventive and effective therapeutic strategies for halting pancreatic beta-cell dysfunction progression or improving aging-associated development of T2D are not solved yet. Recently, two single nucleotide polymorphisms (SNPs) associated with insulin secretion have been identified in serine racemase (SRR). SRR is an enzyme that converts L-serine to D-serine, which is a co-agonist for the NMDA receptor. However, little is known about the role of SRR in pancreatic islets. Here, it was shown that loss of SRR in beta cells increased alpha cell numbers and impaired the overall islet architecture. However, the loss of SRR in beta cells does not impair glucose-stimulated insulin secretion *in vivo* and *ex vivo* and leads to overall improved glucose tolerance in chow diet-fed mice. In contrast, tested *ex vivo*, loss of SRR elevates basal insulin secretion under the low-glucose condition. Furthermore, SRR inhibition enhances ATP production and consequently increases the membrane potential of isolated pancreatic islets. Insulin potently suppresses lipolysis. Mice with serine racemase deficiency in pancreatic beta cells under high-fat diet treatment display hyperinsulinemia and insulin resistance. Moreover, proteomic analysis of subcutaneous adipose tissue revealed the down-regulation of insulin signaling components. Interestingly, proteomics of pancreatic islets lacking serine racemase in beta cells showed that glypican 4 (Gpc4) was downregulated compared to controls. Gpc4 is best studied in adipose tissue where it interacts with the insulin receptor, enhancing insulin signaling. Furthermore, loss of the insulin receptor in pancreatic beta cells promotes insulin secretion. Here, I show that loss of Gpc4 in pancreatic beta cells leads to an impairment in pancreatic islet architecture, impaired glucose tolerance and reduced insulin secretion after high glucose stimulation under chow diet treatment. Mice lacking Gpc4 in pancreatic beta cells displayed insulin resistance and greater fat mass gain under HFD.

Glucose tolerance and insulin sensitivity gradually decline with aging, and a high incidence of type 2 diabetes is observed in the elderly population. Moreover, a feature of aging is the progressive telomere shortening. Here, it was demonstrated

## *Abstract*

the metabolic consequences of moderate telomere shortening using the second-generation loss of telomerase activity in mice (Terc KO). Surprisingly, moderate telomere shortening in aged mice improves oral glucose tolerance and insulin sensitivity. Furthermore, the gut microbiota composition of Terc KO mice demonstrates significant alterations with an increase in *Bifidobacteriaceae* and *Erysipelotrichaceae*, which can potentially contribute to improved glucose metabolism.

Findings in this thesis may guide future work toward D-serine or NMDAR-targeting, maintaining glypican 4 level, or alteration of microbiota composition as treatments for metabolic diseases. Additionally, data in this thesis provides new insights into reconsidering the interplay between insulin and body fat, contributing to a better understanding of the causes of obesity and aging, and ultimately helping find appropriate and effective treatments for T2D.

## **Zusammenfassung**

Fettleibigkeit und Überalterung sind weltweit kostspielige Probleme der öffentlichen Gesundheit und bekannte Risikofaktoren für die Entwicklung von Insulinresistenz und Typ-2-Diabetes (T2D). Präventive und wirksame therapeutische Strategien, die das Fortschreiten der Beta-Zell-Dysfunktion der Bauchspeicheldrüse aufhalten oder die altersbedingte Entwicklung von T2D verbessern, sind jedoch noch nicht entwickelt. Kürzlich wurden zwei Einzelnukleotid-Polymorphismen (SNPs), die mit der menschlichen Insulinsekretion in Verbindung stehen, in der Serin-Racemase (SRR) identifiziert, einem Enzym, das L-Serin in D-Serin umwandelt. D-Serin ist ein Co-Agonist für den NMDA-Rezeptor, der die Funktion der Inselzellen und das Überleben der Zellen verbessert und damit zu einem neuen Ziel für Antidiabetika wird. Über die Rolle von SRR in Betazellen ist jedoch wenig bekannt. Hier zeige ich, dass der Verlust von SRR in Betazellen die Anzahl der Alphazellen erhöht und die gesamte Inselarchitektur beeinträchtigt. Der Verlust von SRR in Betazellen beeinträchtigt jedoch nicht die glukosestimulierte Insulinsekretion in vivo und ex vivo und führt zu einer insgesamt verbesserten Glukosetoleranz bei Mäusen, die mit Chow-Diät gefüttert werden. Im Gegensatz dazu erhöht der Verlust von SRR bei Ex-vivo-Tests die basale Insulinsekretion unter glukosearmen Bedingungen. Darüber hinaus steigert die Hemmung der SRR die ATP-Produktion und erhöht folglich das Membranpotenzial isolierter Pankreasinseln. Insulin unterdrückt die Lipolyse in hohem Maße. Mäuse mit Serin-Racemase-Mangel in den Betazellen der Bauchspeicheldrüse zeigen unter einer fettreichen Diät Hyperinsulinämie und Insulinresistenz. Darüber hinaus ergab eine Proteomanalyse des subkutanen Fettgewebes eine Herunterregulierung von Insulinsignalkomponenten. In der Proteomik Daten von Pankreasinseln in denen die Serin-Racemase in Betazellen fehlt, war Glypican 4 (Gpc4) im Vergleich zu den Kontrollen herunterreguliert. Interessanterweise wurde Gpc4 im Fettgewebe untersucht, wo es mit dem Insulinrezeptor interagiert, was die Insulinsignalisierung verstärkt. Außerdem fördert der Verlust des Insulinrezeptors in den Betazellen der Bauchspeicheldrüse die Insulinsekretion. Hier konnte gezeigt werden, dass der Verlust von Gpc 4 in den Betazellen der Bauchspeicheldrüse zu einer Beeinträchtigung der Architektur

## *Abstract*

der Pankreasinseln, einer gestörten Glukosetoleranz und einer verringerten Insulinsekretion nach Stimulation mit hoher Glukose führt. Mäuse, denen Gpc4 in den Betazellen der Bauchspeicheldrüse fehlte, zeigten eine Insulinresistenz und eine größere Zunahme der Fettmasse unter HFD.

Die Glukosetoleranz und die Insulinsensitivität nehmen mit zunehmendem Alter allmählich ab, und in der älteren Bevölkerung wird eine hohe Inzidenz von Typ-2-Diabetes beobachtet. Ein Merkmal des Alterns ist außerdem die fortschreitende Verkürzung der Telomere. Hier wurden die metabolischen Folgen einer moderaten Telomerverkürzung durch den Verlust der Telomerase-Aktivität der zweiten Generation bei Mäusen (Terc KO) nachgewiesen. Überraschenderweise verbessert eine moderate Telomerverkürzung bei älteren Mäusen die orale Glukosetoleranz und die Insulinsensitivität. Darüber hinaus weist die Zusammensetzung der Darmmikrobiota von Terc-KO-Mäusen signifikante Veränderungen mit einer Zunahme von Bifidobacteriaceae und Erysipelotrichaceae auf, die möglicherweise zu einem verbesserten Glukosestoffwechsel beitragen können.

Die in dieser Arbeit gewonnenen Erkenntnisse können für künftige Arbeiten in Richtung D-Serin- oder NMDAR-Targeting, Aufrechterhaltung des Glypican-4-Niveaus oder Veränderung der Mikrobiota-Zusammensetzung als Therapien zur Behandlung von Diabetes hilfreich sein. Darüber hinaus bieten die Daten in dieser Arbeit neue Einblicke in das Zusammenspiel zwischen Insulin und Körperfett, was zu einem besseren Verständnis der Ursachen von Fettleibigkeit und Alterung beiträgt und letztlich hilft, geeignete und wirksame Behandlungen für T2D zu finden.

# Table of content

## Contents

<b>Abstract</b> .....	<b>1</b>
<b>List of Figures</b> .....	<b>8</b>
<b>Abbreviations</b> .....	<b>9</b>
<b>1. Introduction</b> .....	<b>11</b>
1.1 <i>Pancreas structure and function in mice</i> .....	11
1.2 <i>Diabetes</i> .....	14
1.3 <i>Risk factors of T2D</i> .....	16
1.3.1 <i>Obesity and T2D</i> .....	16
1.3.2 <i>Gut microbiota and T2D</i> .....	17
1.3.3 <i>Aging and T2D</i> .....	18
1.4 <i>Mechanism of Insulin secretion</i> .....	21
1.5 <i>Effect of insulin on metabolism</i> .....	26
1.6 <i>Insulin and fat metabolism</i> .....	27
1.7 <i>Role of serine racemase and NMDARs in regulating insulin secretion</i> .....	31
1.8 <i>Role of glypican 4</i> .....	34
1.9 <i>Aims of the thesis</i> .....	36
<b>2. Material and Methods</b> .....	<b>38</b>
2.1 <i>Animals</i> .....	38
2.2 <i>In vivo experiment</i> .....	39
<i>Glucose tolerance test (GTT)</i> .....	39
<i>Glucose-stimulated insulin secretion test (GSIS)</i> .....	39
<i>Insulin tolerance test (ITT)</i> .....	40
<i>Pyruvate tolerance test (PTT)</i> .....	40
<i>Body composition and energy metabolism</i> .....	40
<i>Energy metabolism studies</i> .....	40
<i>Glycosylated hemoglobin (HbA1c) measurement</i> .....	40
2.3 <i>Ex vivo experiment</i> .....	41
<i>Pancreatic islets isolation</i> .....	41
<i>Ex vivo Glucose stimulated insulin secretion (GSIS) from pancreatic islets</i> .....	41
<i>Pancreatic islets mitochondrial stress test</i> .....	42
<i>Electrophysiological recordings</i> .....	43
2.4 <i>Staining and imaging</i> .....	44
<i>Cryo-embedded sections preparation</i> .....	44
<i>Immunofluorescence staining and imaging</i> .....	44
<i>Histology and imaging</i> .....	45

# Table of content

2.5 Adipocyte size quantification.....	45
2.6 Hormone and triglyceride measurement.....	45
2.7 Proteomics and analysis.....	46
2.8 RNA isolation and cDNA preparation and real-time PCR.....	48
2.8 Protein extraction and western blot.....	48
2.9 Telomere length quantification.....	49
DNA extraction for telomere length quantification.....	49
Telomere length quantification.....	49
2.10 Microbiota measurement and analysis.....	49
2.11 Statistics.....	50
<b>3. Results.....</b>	<b>51</b>
3.1 Genetic deletion of <i>Srr</i> in pancreatic beta cells impairs islets architecture and improves glucose tolerance under CD.....	51
3.2 Loss of <i>SRR</i> in pancreatic beta cells promotes basal insulin secretion from pancreatic islets with enhanced ATP production and potassium channel trafficking observed under chow diet.....	54
3.3 Mitochondria function related ABC transporters, glycine-serine metabolism and amino acid metabolic process in islets were most affected after the loss of <i>SRR</i> in pancreatic islets observed in proteomics..	57
3.4 <i>Srr<sup>Ins1cre</sup></i> mice showed insulin resistance, glucose intolerance and an impaired islets architecture under HFD.....	60
3.5 Proteomic analysis of islet indicates an upregulation in PPAR signaling and the biosynthesis of unsaturated fatty acids pathway.....	63
3.6 <i>Srr<sup>Ins1cre</sup></i> mice show greater fat mass gain and reduced energy expenditure under HFD.....	66
3.7 <i>Ins1 cre</i> mice does not show greater fat mass gain and reduced energy expenditure under HFD.....	68
3.8 Proteomic analysis of subcutaneous adipose tissue from <i>Srr<sup>Ins1cre</sup></i> under HFD indicates a downregulation in fatty acid metabolism and insulin signaling.....	70
3.9 Proteomic analysis of liver from <i>Srr<sup>Ins1cre</sup></i> under HFD indicates fatty acid metabolism and pyruvate metabolism was top affected.....	73
3.10 Loss of <i>Gpc4</i> in pancreatic beta cells does not affect body weight and body composition under CD.....	76
3.11 Loss of <i>Gpc4</i> in pancreatic beta cells impairs islets architecture and impairs glucose stimulate insulin secretion in vivo but not in vitro under CD.....	77
3.12 <i>Gpc4<sup>Ins1cre</sup></i> mice show greater fat mass gain and insulin resistance under HFD.....	79
3.13 <i>Terc</i> KO mice show greater endocrine homeostasis with reduced telomere length.....	81
3.14 <i>Terc</i> KO mice display improved glucose and insulin tolerance.....	83
3.15 Shorter telomere length results in a reconfiguration of the gut microbiome.....	86
<b>4. Discussion.....</b>	<b>89</b>
4.1 Serine racemase regulates insulin secretion and HFD-induced fat mass gain.....	89
<i>SRR</i> in pancreatic beta cells affects islet architecture and regulates glucose homeostasis.....	90
<i>SRR</i> in pancreatic beta cells promotes basal insulin secretion from isolated pancreatic islets with enhanced ATP production and potassium channel trafficking.....	93

# Table of content

<i>Srr<sup>Ins1cre</sup></i> mice showed insulin resistance, glucose intolerance and a greater fat mass gain with inhibited fat metabolism under HFD .....	94
4.2 Glypican 4 in pancreatic beta cells associates insulin secretion and insulin resistance .....	96
4.3 Alteration in microbiota composition results in improved glucose tolerance and insulin sensitivity in <i>Terc</i> KO mice.....	98
<b>5. Conclusion and perspectives .....</b>	<b>100</b>
<b>References .....</b>	<b>102</b>
<b>Acknowledgements.....</b>	<b>115</b>
<b>Publications and presentations .....</b>	<b>118</b>

# List of Figures

## List of Figures

<b>Figure 1. Anatomy of pancreas</b> .....	11
<b>Figure 2. Immune response in Type 1 Diabetes</b> .....	15
<b>Figure 3. Telomere becomes shorter with cell division</b> .....	19
<b>Figure 4. Telomere and telomerase</b> .....	20
<b>Figure 5. Mechanism of insulin secretion</b> .....	21
<b>Figure 6. Paracrine signaling network</b> .....	24
<b>Figure 7. Effect of insulin on carbohydrate Metabolism</b> .....	26
<b>Figure 8. Main enzymes of breaking down triglycerides in lipolysis</b> .....	29
<b>Figure 9. Mechanism of lipolysis in adipocyte</b> .....	31
<b>Figure 10. Genetic deletion of <i>Srr</i> in pancreatic beta cells impairs islets architecture and improve glucose tolerance under chow diet</b> .....	51
<b>Figure 11. Seahorse and electrical physiological tests of pancreatic islets in low glucose condition under chow diet</b> .....	54
<b>Figure 12. Proteomics analysis of isolated pancreatic islets of <i>Srr<sup>ins1cre</sup></i> under chow diet.</b>	58
<b>Figure 13. <i>Srr<sup>ins1cre</sup></i> mice under HFD showed insulin resistance and impaired glucose tolerance with impaired islets architecture under HFD</b> .....	60
<b>Figure 14. Proteomics analysis of pancreatic islets from <i>Srr<sup>ins1cre</sup></i> under HFD</b> .....	64
<b>Figure 15. <i>Srr<sup>ins1cre</sup></i> mice showed gain higher fat mass and reduced energy expenditure under HFD</b> .....	66
<b>Figure 16. <i>Srr<sup>ins1cre</sup></i> mice showed gain higher fat mass and reduced energy expenditure under HFD</b> .....	69
<b>Figure 17. Proteomics analysis of subcutaneous white adipose tissue from <i>Srr<sup>ins1cre</sup></i> under HFD</b> .....	72
<b>Figure 18. Proteomics analysis of liver from <i>Srr<sup>ins1cre</sup></i> under HFD</b> .....	75
<b>Figure 19. Genetic deletion of <i>Gpc4</i> and it does not affect body weight, body composition development and insulin sensitivity under chow diet</b> .....	76
<b>Figure 20. <i>Gpc4<sup>ins1cre</sup></i> mice shows impaired islets architecture and less glucose stimulated insulin secretion in vivo</b> .....	77
<b>Figure 21. <i>Gpc4<sup>ins1cre</sup></i> mice has greater fat mass gain and insulin resistance in vivo under HFD</b> .....	79
<b>Figure 22. Telomere shortening and metabolic characterization of <i>Terc</i> KO mice</b> .....	81
<b>Figure 23. <i>Terc</i> KO male mice show improved insulin sensitivity and glucose tolerance.</b>	83
<b>Figure 24. Shorter telomere length results reconfiguration of the gut microbiome via 16S rRNA sequencing analysis</b> .....	86

# *Abbreviations*

## Abbreviations

Actb	Beta actin
ATGL	Adipose triglyceride lipase
ATP	Adenosine triphosphate
BMI	Body mass index
BSA	Bovine serum albumin
DAG	Diacylglycerol
DPP-4	Incretin-degrading dipeptidyl peptidase-4
DXM	Dextromethorphan
EE	Energy expenditure
FA	Fatty acid
FDA	Food and drug administration
GIP	Glucose-dependent insulinotropic polypeptide
GLP-1	Glucagon-like peptide 1
GLUT 2	Sodium-independent glucose transporter 2
Gpc4	Glypican 4
GPI	Glycosylphosphatidylinositol
GSIS	Glucose-stimulated insulin secretion
GTT	Glucose tolerance test
HDL	High density lipoprotein
H&E	Hematoxylin and Eosin
HSL	Hormone sensitive lipase
IDL	Intermediate density lipoproteins
IF	Immunofluorescence staining
ITT	Insulin sensitive test
K <sub>ATP</sub>	ATP-sensitive potassium channels
LDL	Low density lipoprotein
MG	Monoacylglycerol
MGL	Monoacylglycerol lipase
MPCs	Multipotent pancreatic progenitors
NEFA	Non-esterified free fatty acids

## *Abbreviations*

NMDAR	N-methyl-D-aspartate receptor
oGSIS	Oral gavage glucose-stimulated insulin secretion
oGTT	Oral gavage glucose tolerance test
PDE3B	Phosphodiesterase 3B
PHGDH	Phosphoglycerate dehydrogenase
PKA	Protein kinase A
PTT	Pyruvate tolerance test
RER	Respiratory exchange ratio
SNP	Single nucleotide polymorphisms
SRR	Serine racemase
Sub WAT	Subcutaneous white adipose tissue
TG	Triglycerides
T1D	Type 1 diabetes
T2D	Type 2 diabetes
Tert	Telomerase reverse transcriptase
Terc	Telomerase RNA component
Terc KO	Second-generation of inbred Terc <sup>-/-</sup> mice
VLDL	Very low density lipoprotein
WAT	White adipose tissue
WHR	Waist-to-hip

# Introduction

## 1. Introduction

### 1.1 Pancreas structure and function in mice

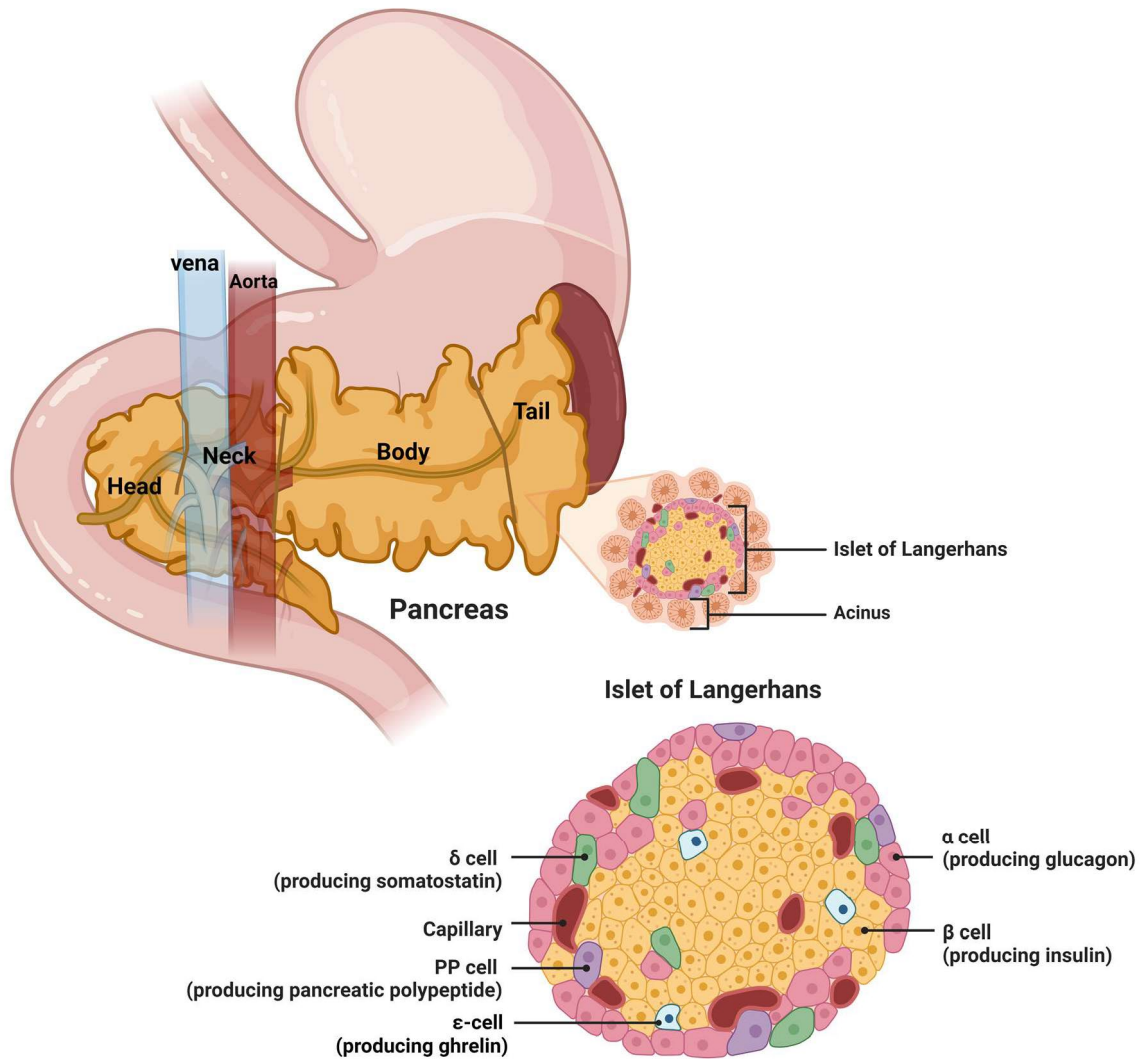


**Figure 1. Anatomy of pancreas.**

Pancreas is physically closely connected to the stomach, spleen, and intestine, divided into head, neck, body and tail four parts. Pancreatic islets are the endocrine compartment of the pancreas, which is mainly comprised of alpha cells (10-20%), beta cells (65-80%), delta cells (~5%), epsilon cells and PP cells (~1%). (Created with BioRender.com)

Systemic regulation of the body glucose homeostasis and energy homeostasis is critically reliant on the pancreas (Bakhti et al., 2019). The pancreas is a large compound gland that lies posterior to the stomach, and is anatomically divided

## *Introduction*

into four parts: head, neck, body and tail (Fig. 1). This organ closely connects with the stomach, duodenum, mesenteric adipose tissue, liver and spleen. The head of the pancreas lies within the C-shaped concavity of the duodenum, while, the neck is anterior to the superior mesenteric vessels. The tail of the pancreas connects the spleen passing between layers of the splenorenal ligament.

In mice, the development of the embryonic pancreas consists of two phases: primary transition, which occurs between embryonic day 8.5 (E8.5) to E12.5, and second transition, which occurs between E12.5 to E15.5. Pancreas development starts around E8.5, originating from the dorsal and ventral buds in the foregut endoderm. In this primary phase, multipotent pancreatic progenitors (MPCs) proliferate extensively (Burlison et al., 2008). During cell proliferation, the size of the dorsal and ventral buds elongate and fuse into one organ along the stomach and duodenum at E12.5 (Pan and Wright, 2011; Villasenor et al., 2010). The glucagon-producing  $\alpha$ -cells are the first to develop in the dorsal bud within the primary phase (Herrera, 2000).

During the secondary transition, MPCs segregate into pancreatic tip and trunk domains where the differentiation of acinar, ductal and endocrine cells take place. Moreover, among these three pancreatic lineages, endocrine cells cluster with endothelial cells, neurons and mesenchymal cells to form the islets of Langerhans (Cleaver and Dor, 2012; Thorens, 2014).

Physiologically, the pancreas is composed of two main distinct compartments: the exocrine compartment which is responsible for digestive functions, and the endocrine compartment which is critical for the regulation of systemic glucose, lipid and protein metabolism. The exocrine compartment is comprised of acinar cells and ductal cells. Pancreatic acini secrete multiple digestive enzymes like trypsin, chymotrypsin, pancreatic amylase, pancreatic lipase, phospholipase and cholesterol esterase for the digestion of all three major macronutrients, which are proteins, carbohydrates and fats. The ductal cells secrete digestive enzymes and sodium bicarbonate into the duodenum via small ductules and larger ducts to aid in nutrient absorption.

## *Introduction*

The pancreatic endocrine compartment is the islets of Langerhans, which was first discovered in 1869 by Paul Langerhans (Sakula, 1988). Each islet of Langerhans comprises approximately 2000 endocrine hormone-secreting cells. These populations are mainly composed of five different cells types with distinguishable morphological characteristics: alpha cells, beta cells, delta cells, PP cells, and epsilon cells. (Bakhti et al., 2019; Islam, 2010; Pan et al., 2015; Zhou and Melton, 2018). In mice, beta cells produce insulin and amylin, account for 65-80% of the cell population within the islet and are mainly distributed in the middle of the pancreatic islets. In detail, the ratio of amylin to insulin secretion of beta cells is 1:100. The alpha cells produce glucagon, and constitute about 10-20% of all cells of the islets, while the delta cells produce somatostatin, and account for approximately 5 % of the total islet cell population. The PP cells produce pancreatic polypeptide and epsilon cells produce ghrelin, in which both cell types together make up about 1% of the cell population within the islet (Campbell and Newgard, 2021; Dolensek et al., 2015a).

The endocrine hormones secreted by pancreatic islets are translocated directly into the blood, which differs to the secreted components of the exocrine compartment that enter into the intestine. Insulin secreted by beta cells activates peripheral organs rapidly and facilitates the uptake of glucose from circulation and the lowering the glucose levels after food intake to maintain systemic glucose homeostasis (Cerf, 2013; Eizirik et al., 2020; Islam, 2010). Glucagon secreted by alpha cells is generally viewed to have the opposite effect of insulin, in that glucagon release stimulates an increase in blood glucose levels. The major pathways of glucagon on glucose production are the breakdown of liver glycogen (glycogenolysis) and increased gluconeogenesis (Briant et al., 2016; Wendt and Eliasson, 2020). Delta cells secrete somatostatin, a 14-amino acid polypeptide, and has a half-life of 3 minutes. The increases in circulating glucose, increased amino acid and fatty acids could promote somatostatin secretion. In turn, somatostatin has multiple inhibitory functions including depressing both insulin and glucagon secretion, inhibiting stomach and duodenum motility, and decreasing secretion into the gastrointestinal tract (Briant et al., 2018; Hauge-Evans et al., 2009; Rorsman and Huising, 2018). Pancreatic polypeptide secreted

# *Introduction*

by PP cells plays an important role in regulating glucose tolerance in mice, shown as an inhibitor of glucagon release under low-glucose conditions (Fukaishi et al., 2021; Lin and Chance, 1974; Moran, 2003; Zhao et al., 2022). The pancreatic polypeptide has been associated with regulating energy metabolism (Batterham et al., 2003; Jesudason et al., 2007; Kojima et al., 2007). Ghrelin was secreted by epsilon cells that were first identified in 2002 (Wierup et al., 2002). Recent studies have demonstrated that ghrelin acts specifically on delta cells within pancreatic islets to elicit somatostatin secretion, which in turn inhibits insulin and glucagon release. (Adriaenssens et al., 2016). However, the precise function of both PP secreted by PP cells and ghrelin secreted by epsilon cells still remains unclear.

## **1.2 Diabetes**

Diabetes mellitus is a chronic metabolic disease characterized by hyperglycemia with loss of functional beta cell mass. Diabetes mellitus consists of two main types, type 1 diabetes (T1D) and type 2 diabetes (T2D). Diabetes has become a pandemic worldwide and almost 1 in 10 people are living with diabetes. In 2021, over 537 million people suffer from diabetes and the total number of people living with diabetes is predicted to rise to 643 million by 2030 and 783 million by 2045 (International Diabetes Federation, 10<sup>th</sup> edition 2021).

T1D is mediated by autoimmune beta cell destruction, leading to a complete or near complete lifelong insulin deficiency. The autoimmunity of T1D mainly originates from CD8<sup>+</sup> T cells that recognize and target specific antigens expressed on the beta cell surface, HLA class I. The attack of T cells results in the death of a massive number of pancreatic beta cells which causes insulin deficiency, whereas, alpha cells and delta cells are still functional to produce glucagon and somatostatin (Eizirik et al., 2020) (Fig. 5). A new study has shown that an antibody drug (teplizumab) targeting CD3 can prevent T1D in mice (Kuhn et al., 2011). Just recently, in 2022, US Food and Drug Administration (FDA) approved teplizumab, the first injectable T1D prevention drug that can delay the diagnosis of T1D. This is a new treatment strategy thus most patients still require an exogenous insulin therapy now. Intensive insulin treatment results in greater weight gain with higher levels of triglyceride, total cholesterol, and low-density lipoprotein cholesterol for

# Introduction

T1D patients (Purnell et al., 1998). Studies suggested that the primary cause of weight gain with insulin therapy might be the lipogenic effect of insulin which induces an increase in fat mass instead of affecting energy intake or appetite (Jacob et al., 2006).

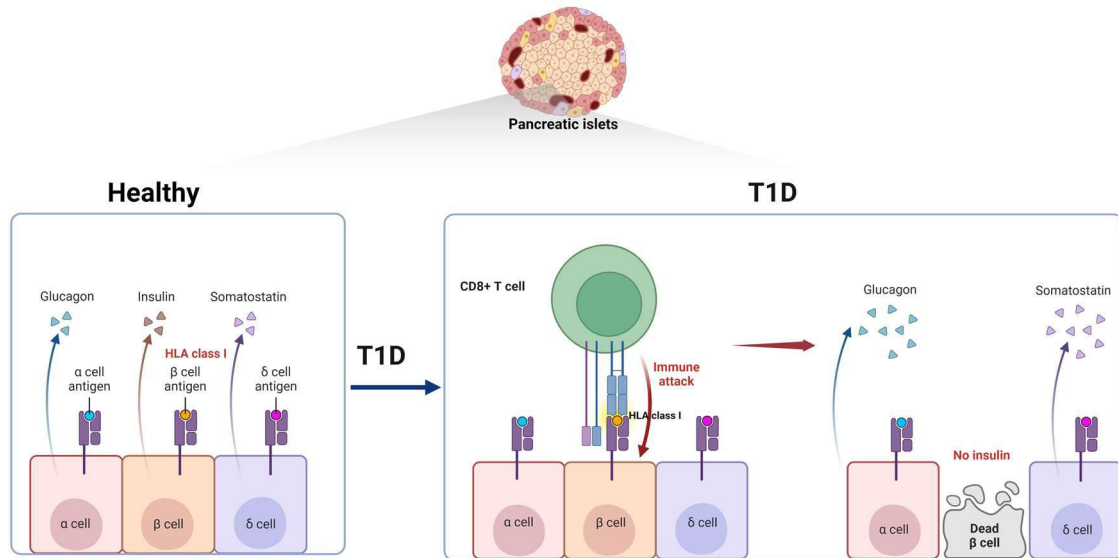


**Figure 2. Immune response in Type 1 Diabetes.**

Under the healthy condition, each endocrine cell type in pancreatic islets secretes a distinct hormone and expresses different tissue-specific proteins. In T1D, CD8+ cytotoxic T cell recognizes and targets the specific antigens, HLA class I of  $\beta$  cell, and kills the  $\beta$  cell leading to insulin deficiency. Whereas, the production of glucagon and somatostatin is not affected by alpha cells and delta cells. (Adapted from 'Immune Response in Type 1 Diabetes', by BioRender.com. Retrieved from <https://app.biorender.com/biorender-templates>)

T2D is the most common type of diabetes and accounts for around 90% of all diabetic cases. In T2D, genetic, environmental, and metabolic factors together induce pancreatic beta cell dysfunction and a progressive loss of pancreatic beta cell mass causing T2D in the end. T2D is often associated with obesity, which involves impaired control of hepatic glucose production and insulin resistance. Insulin resistance refers to the diminished metabolic effect of insulin on the target cell as a result of an impaired lowering of blood glucose by circulating insulin or injected insulin. Insulin resistance is often the earlier stage of the development of T2D. To compensate against the decreased metabolic response to insulin, greater insulin secretion is demanded. Long term increases in total insulin secretion

# *Introduction*

overburdens pancreatic beta cells leading to islet dysfunction and beta cell mass loss (Eizirik et al., 2020). Besides, insulin treatment, lifestyle intervention such as dietary modification and exercise training is indicated to improve glucose homeostasis and metabolic health of T2D (Kolb et al., 2018). T2D development can be proactively treated with pharmacological compounds such as metformin, tirzepatide, sulfonylureas and glitazones. Among them, metformin is the most common antidiabetic drug, which is known to improve insulin sensitivity in liver, muscle and adipose tissue and help to reduce body weight (Bauer et al., 2018; Coll et al., 2020). Moreover, the FDA has just approved the first dual GIP/GLP-1 agonist, tirzepatide injection, for the treatment of adults T2D patients in 2022. Tirzepatide is derived from an intermixed sequence of GLP-1 and GIP, which provides greater antihyperglycemic and insulinotropic efficacy than the monoagonism, and without apparent gastrointestinal discomfort (Finan et al., 2013).

## **1.3 Risk factors of T2D**

### **1.3.1 Obesity and T2D**

Obesity is a costly worldwide public health problem, and a well-known risk factor for the development of type 2 diabetes (T2D) and insulin resistance. Obesity-associated diabetes is known to progress other morbidities such as hepatic steatosis, cardiovascular diseases (CVDs), angiopathy, and nephropathy, which consequently lead to higher mortality risk. The WHO reported more than 1.9 billion adults were overweight (BMI  $\geq 25$ ) in 2016. Of these, greater than 650 million individuals were obese (BMI  $\geq 30$ ). The increasing prevalence of obesity sparked great interest in understanding the causes and physiological mechanisms underlying obesity, and potential treatments. However, the detailed mechanisms underlying the development of human obesity remain uncertain.

There are several explanatory models of obesity. The carbohydrate insulin model (CIM) is one of the well-known models. In this model, adipose tissue is not only a storage site for excess calories but also plays a central role in body fat gain. The CIM model focuses on the direct action of postprandial insulin on adipose tissue. Body fat gain results from the consumption of high carbohydrate stimulating

## *Introduction*

postprandial insulin, which acts to suppress the release of fatty acids from adipose tissue, inhibit the production of ketones in the liver, and promote fat and glycogen deposition (Ludwig and Ebbeling, 2018).

However, this CIM model was refuted by some studies both in humans and mice. Recently, a large dietary study reported that mice fed with varied diets of carbohydrate content but constant protein composition demonstrated a phenotype that opposes the CIM prediction regarding carbohydrate-dependent insulin effect on fat metabolism. Mice on diets with a higher proportion of carbohydrates took in fewer calories and gained less body weight but with higher postprandial insulin (Hu et al., 2020). The CIM model failed, however, it does not discount the importance of insulin in regulating body fat. In 2021, J. Speakman and K. Hall proposed that the carbohydrate-independent actions of insulin on multiple tissues may provide a better target to explore the role of insulin in obesity, and suggested that changes in basal insulin levels may be more important than adipose tissue lipolysis in providing a highly sensitive marker to changes in insulin levels (Speakman and Hall, 2021). Therefore, reconsidering the interplay between insulin and body fat will help us to better understand the cause of obesity and find a proper treatment.

### **1.3.2 Gut microbiota and T2D**

Obesity has been associated with the alteration of intestinal microbiota composition. Germ-free mice that are transplanted with the gut microbiota of normal mice gain more body fat without any increase in food consumption (Backhed et al., 2004). Microbiota refers to all microorganisms that colonize the body. They reside on all surfaces with the highest numbers in the gut (Gill et al., 2006). Gut microbiota contains 150 times more genes than our genome (Qin et al. 2010). Bacteroidetes and Firmicutes are the two dominant groups of beneficial bacteria. The obese mice (*ob/ob*) show 50% reduction of the relative abundance of the Bacteroidetes, and correspondingly show an increased Firmicutes, than the lean mice (Ley et al., 2005). Similar findings have been found in humans. People with obesity contain a less proportion of Bacteroidetes compared to lean individuals, and an increased proportion with weight loss (Ley et al., 2006). Intestinal microbiota influence host metabolism through degradation of dietary

## *Introduction*

compounds, the production of metabolites, and modulation of hormone-producing enteroendocrine cells within the intestinal mucosa, thereby shaping host physiology. A growing number of studies show that intestinal microbiota play an important role in regulating host metabolism and physiology, like modulating GLP-1 secretion and insulin sensitivity (Grasset et al. 2017; Kundu P et al. 2017; Muhammad et al. 2014; Tremaro et al. 2012; Ussar S. et al. 2015; Ussar S. et al. 2016;). *Bifidobacterium longum* APC1472 supplementation has shown improved glucose tolerance in obese mice and lowered fasting glycemia in obese/overweight individuals (Schellekens et al., 2021).

The gut microbiota composition remains relatively stable from 2 years of age onwards in healthy individuals (Borre et al. 2014; Favier et al. 2002). However, as the host ages, it is exposed to various infections or dietary changes which can significantly alter the composition of the intestinal microbiota (Kundu P et al. 2017). The core microbiota composition and diversity levels in older people (>65 years old) differ from younger adults. Further, the microbiota of older people exhibits greater variation between individuals than that of younger adults (Claesson et al., 2012). However, the interplay between microbiota and endocrine cells on effects on insulin secretion and glucose homeostasis in the context of accelerated aging is poorly understood.

### **1.3.3 Aging and T2D**

The National Health and Nutrition Examination Survey (NHANES) shows a significant linear correlation by age for total, diagnosed, and undiagnosed diabetes. The prevalence of total diabetes was 3.5% among adults aged 20–39, 16.3% among adults aged 40–59, and 28.2% among adults aged 60 and over. Several factors associated with aging contribute to the high prevalence of type 2 diabetes and the phenomenon of glucose tolerance progressively declining in the older population. These include increased adiposity, medications, decreased physical activity, deficiency of insulin secretion and beta cell dysfunction (Chia et al., 2018; DeFronzo, 1981; Monickaraj et al., 2012). Additionally, age-related alterations in the incretin hormones such as glucose-dependent insulinotropic polypeptide (GIP) and glucagon-like peptide 1 (GLP-1), have been shown as possible contributing

## Introduction

factors to the glucose intolerance seen with advancing age (Korosi et al., 2001; Scrocchi and Drucker, 1998).

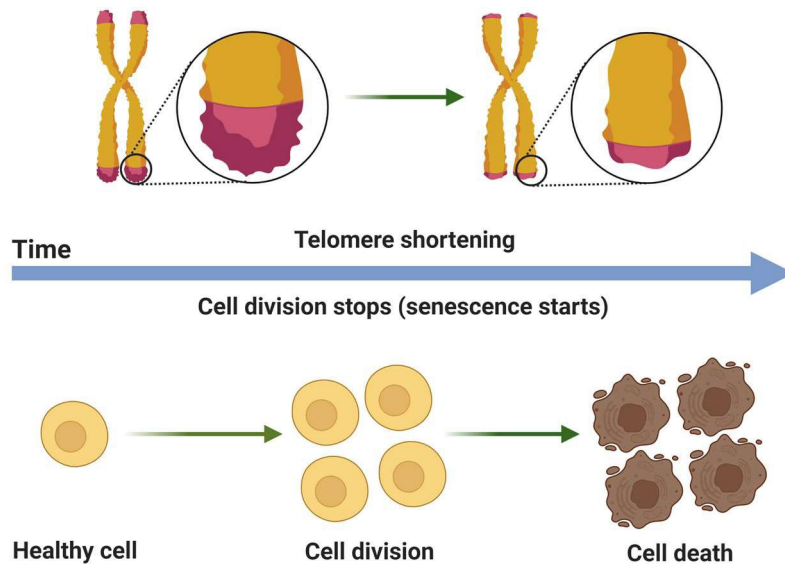


**Figure 3. Telomere becomes shorter with cell division.**

(Adapted from 'Telomere Biology in Cancer Cells', by BioRender.com, Retrieved from <https://app.biorender.com/biorender-templates>)

A factor leading to aging is telomere shortening. Reduced telomere length and impaired telomerase activity relate to senescence and aging-associated diseases (Chia et al., 2018; Kam et al., 2021). Eukaryotic chromosomes carry tandemly repeated terminal sequences, 'TTAGGG', called telomeres, which are essential for chromosome stability. They serve as a protective cap during cell division to prevent the degradation of genes near the ends of chromosomes. Telomeres protect chromosomes from damage and end-to-end fusion to assure the integrity of chromosomes. Moreover, the linear chromosomes with telomeric structures can be distinguished from double-strand DNA breaks, which avoid being attacked by initiating DNA damage response, senescence, apoptosis or chromosomal rearrangement signaling. However, telomeres are consumed gradually during repeated cell divisions. After each cell division, an average person loses 30-200 base pairs from the end of those cells' telomeres (Fig. 6). In human blood cells, the length of telomeres ranges from 8000 base pairs to as low as 1500 in elderly people. Therefore, telomere length is an important marker for aging (Levy et al., 1992; Saretzki, 2018).

# Introduction

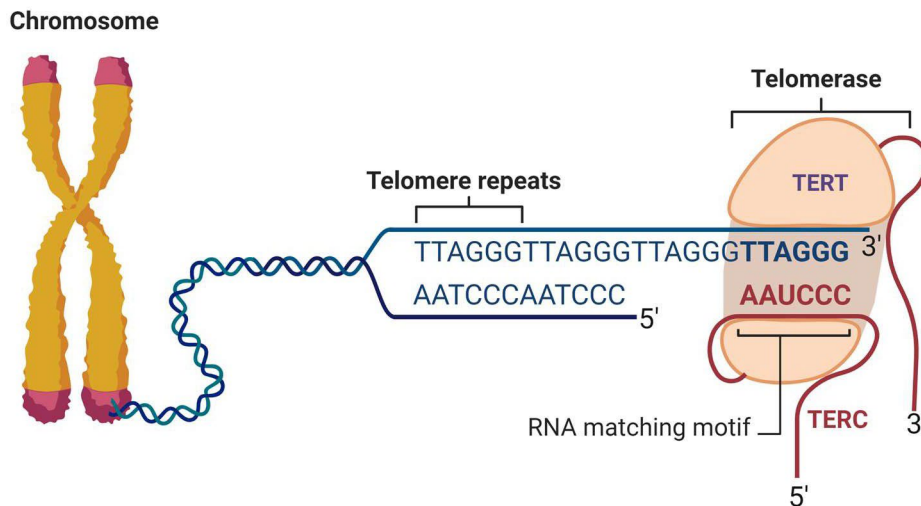


**Figure 4. Telomere and telomerase.**

*Telomerase elongates telomeres through TERT and TERC two units. The reverse transcriptase TERT use TERC as a template which carries the RNA matching motif of the telomere to extend the telomere. (Adapted from 'Telomeres and Telomerase', by BioRender.com, Retrieved from <https://app.biorender.com/biorender-templates>)*

Further, telomerase activity can potentially counteract telomere shortening when it is able to access and interact with telomeres. Telomerase is a ribonucleoprotein enzyme complex that contains two main components, telomerase reverse transcriptase (TERT) and telomerase RNA component (TERC). TERC carries a short RNA motif, which cognate telomeres repeat. TERT uses TERC as a template for reverse transcription to elongate telomeres (Autexier and Lue, 2006) (Fig. 7). Thus, genetic knockout of *Terc* in mice (*Terc*<sup>-/-</sup>) leads to an accelerated telomere length shortening. Furthermore, *Terc*<sup>-/-</sup> mice exhibit progressive telomere shortening with each successive generation arising from *Terc*<sup>-/-</sup> intercrosses (Blasco et al., 1997; Huang et al., 1998). Therefore, *Terc*<sup>-/-</sup> mice are used as an aging model to study the effects of aging. Many disease-associated mutations in telomerase have been identified (Kam et al., 2021; Podlevsky et al., 2007). Single nucleotide polymorphisms in TERC significantly increase the risk of diabetes (Al Khaldi et al., 2015). Studies also suggested that telomerase deficiency promotes metabolic dysfunction in mice, and likely impairs both glucose metabolism and insulin secretion (Alves-Paiva et al., 2018; Kuhlow et al., 2010).

# Introduction

## 1.4 Mechanism of Insulin secretion

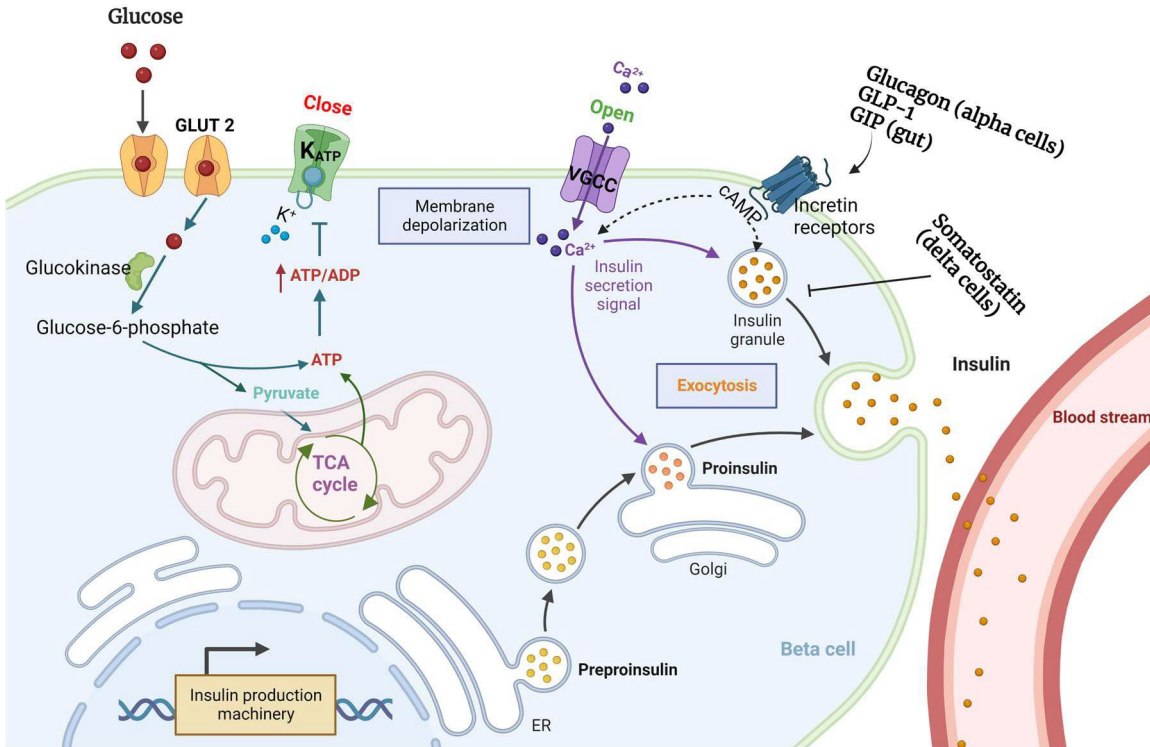


**Figure 5. Mechanism of insulin secretion.**

Insulin is secreted by pancreatic beta cells into the blood circulation. In principle, pancreatic beta cells sense and take up glucose. This glucose is then metabolized into pyruvate via glycolysis, which is transferred into mitochondria for generating ATP. As the ATP to ADP ratio is increased, it leads to the closure of ATP-sensitive potassium channels, cell membrane depolarization, and calcium influx, which together trigger insulin beta cell secretion. In addition, glucagon (secreted from alpha cells), GLP-1 (secreted from alpha cells and the gut), GIP (secreted from gut), somatostatin (secreted from delta cells) amplify glucose-stimulated insulin secretion by activating the beta cell receptors and elevating cAMP levels. (Adapted from 'Insulin Production Pathway', by BioRender.com, Retrieved from <https://app.biorender.com/biorender-templates>)

The primary physiological stimulus for beta cell insulin secretion is elevated circulating postprandial glucose, referred to as glucose-stimulated insulin secretion (GSIS). GSIS consists of two phases: a first phase and a second phase characterized as 'triggering' and 'amplifying' pathways (Campbell and Newgard, 2021; Henquin, 2009).

## *Introduction*

The 'triggering pathway' occurs within the first 20 minutes following a glucose excursion, and is primarily responsible for initiating the 'first phase' of insulin secretion. The first phase of insulin secretion plays a great role in controlling the acute secretion of insulin from the pancreatic beta cell. The basic cellular mechanisms of the triggering pathway have been well-known since the 1980s (Fig. 3) (Ashcroft et al., 1984; Cook and Hales, 1984). Glucose metabolism within the pancreatic beta cell involves glucose transport across the plasma membrane, in which the accumulation of incoming glucose is phosphorylated thus acting as a representation of extracellular glucose concentrations and triggering GSIS. The rate of glucose metabolism in the pancreatic beta cell, which is reflective of changes within circulating blood glucose levels, determines the total amount of first phase insulin secretion (Campbell and Newgard, 2021; Henquin et al., 2009; Prentki et al., 2013). Once circulating glucose levels rise, the extracellular glucose is rapidly transported into beta cells by glucose transporters. Notably, the principal glucose transporters in rodent pancreatic beta cells differ from those in humans. GLUT2 is the primary glucose transporter in rodent pancreatic beta cells, however, the GLUT2 expression in human beta cells is about 100-fold lower than in rodents. GLUT1 and GLUT3 are the major glucose transporters in the beta cells of the human pancreas (De Vos et al., 1995; McCulloch et al., 2011). After entering into beta cells, glucose is converted into glucose-6-phosphate by glucokinase. Glucokinase is a member of the hexokinase family which exhibits low affinity for glucose but high-throughput as it lacks the N-terminal domain mediating product inhibition by glucose-6-phosphate (Matschinsky, 2002; Sweet and Matschinsky, 1995; Wilson, 2003). These kinetic and regulatory characteristics enable glucokinase to govern the rate of glucose metabolism in the pancreatic beta cell and further control the secretion of insulin.

During glycolysis, glucose-6-phosphate is oxidized to pyruvate which enables adenosine triphosphate (ATP) generation. In the pancreatic beta cell, pyruvate is primarily used for mitochondrial metabolism (Khan et al., 1996; Lu et al., 2002). Pyruvate enters the tricarboxylic acid (TCA) cycle as acetyl-CoA to provide substrate for generating of ATP within the mitochondria. Beta cells contain ATP-sensitive potassium channels ( $K_{ATP}$ ), which normally are open at low glucose

## *Introduction*

levels. With the rise of ATP production, the ratio of ATP to ADP is increased, leading to the closure of these  $K_{ATP}$  channels which induces cell membrane depolarization (Gembal et al., 1993; Lim et al., 2009). The depolarized cell membrane activates voltage-gated calcium channels which stimulates calcium flux into the beta cells triggering the fusion of the insulin-containing secretory granules with the cell membrane and releasing insulin into the cell exterior by exocytosis (Dolensek et al., 2015b; Gaisano, 2017; Omar-Hmeadi and Idevall- Hagren, 2021; Takahashi et al., 2002). The triggering pathway is dependent on the  $K_{ATP}$  channel and is essential for stimulating insulin secretion. A second pathway, referred to as the 'amplifying pathway', modulates GSIS independent of  $K_{ATP}$  channel involvement. A further prolonged increase in insulin secretion in response to glucose stimulus is possible even when intracellular  $Ca^{+}$  is maximized or during stimulation with  $K_{ATP}$  channel opener diazoxide (de Wet and Proks, 2015; Gembal et al., 1993; MacDonald, 1981). Unlike the 'triggering pathway' which leads to a sharp rise of insulin levels, the 'amplifying pathway' govern insulin secretion at a lower and sustained rate during the entire course of digestion lasting for several hours, which is called the second phase of insulin secretion (Henquin et al., 2006; Ishiyama et al., 2006).

### **Intra-islet paracrine signaling effect insulin secretion**

# Introduction

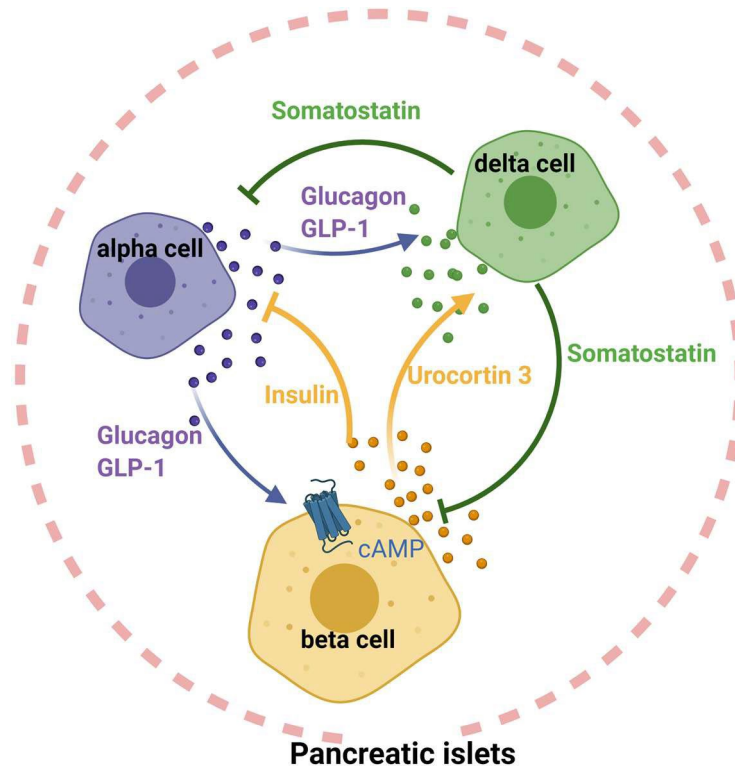


**Figure 6. Paracrine signaling network.**

The endocrine cells: alpha cells, beta cells and delta cells within pancreatic islets tightly affect each other. Insulin secreted by beta cells and somatostatin secreted by delta cells inhibits glucagon secretion. Beta cells also secrete Urocortin 3, which stimulates somatostatin secretion. Somatostatin provides negative feedback on beta cells by suppressing insulin secretion from the beta cell. Glucagon and GLP-1 secreted by alpha cells promote both insulin secretion and somatostatin secretion. (Created with BioRender.com)

In addition to the multiple metabolic signaling mechanisms, insulin secretion from pancreatic beta cells is also regulated by intra-islet paracrine signaling from pancreatic alpha cell and delta cell, which typically converge on regulating cAMP levels in beta cells (Fig. 4).

Pancreatic alpha cells primarily produce glucagon and also have the capacity to produce intra-islets glucagon-like peptide 1 (GLP-1), both of which are derived from the *proglucagon* gene (Briant et al., 2016; Campbell et al., 2020; Fava et al., 2016; Marchetti et al., 2012). Recent studies have revealed that pancreatic alpha cells regulate insulin secretion by mediating proglucagon productions via cAMP signaling (Fig. 3) (Capozzi et al., 2019; Svendsen et al., 2018; Wendt and Eliasson, 2020; Zhu et al., 2019). Disruption of glucagon output within pancreatic islets

## *Introduction*

reduces insulin secretion. The impairment in insulin secretion is recovered from additional glucagon or GLP-1 treatment. Moreover, the effect of glucagon on insulin secretion is mediated by the combination of the glucagon receptor and the GLP-1 receptor. Loss of both the glucagon and GLP-1 receptors causes an impairment on insulin secretion other than only loss of either one (Svendsen et al., 2018). Glucagon secretion from alpha cells is largely affected by paracrine factors from other endocrine cell types (Jensen et al., 2008; Kawamori et al., 2009). One of the negative regulators of glucagon secretion is insulin secreted by the pancreatic beta cells. Moreover, alpha cell activity is also regulated by delta cells via somatostatin through multiple mechanisms including the presence of the glucagon receptor on the delta cells (Adriaenssens et al., 2016; Briant et al., 2018).

Like alpha cells, delta cells mediate insulin secretion mainly by altering beta cell cAMP levels. Somatostatin secreted from the delta cells inhibits both insulin and glucagon secretion. The inhibitory effect of somatostatin is mediated by somatostatin receptors activating inhibitory G protein, which leads to the transient suppression of alpha cell and beta cell electrical activity and exocytosis (Rorsman and Huisin, 2018). Somatostatin secretion is stimulated by alpha cells via the glucagon receptor and beta cells via Urocortin 3 (Hartig and Cox, 2020).

In summary, endocrine cells: alpha cells, beta cells and delta cells are tightly regulated by each other and play an important role in controlling glucose metabolism of the body.

# Introduction

## 1.5 Effect of insulin on metabolism

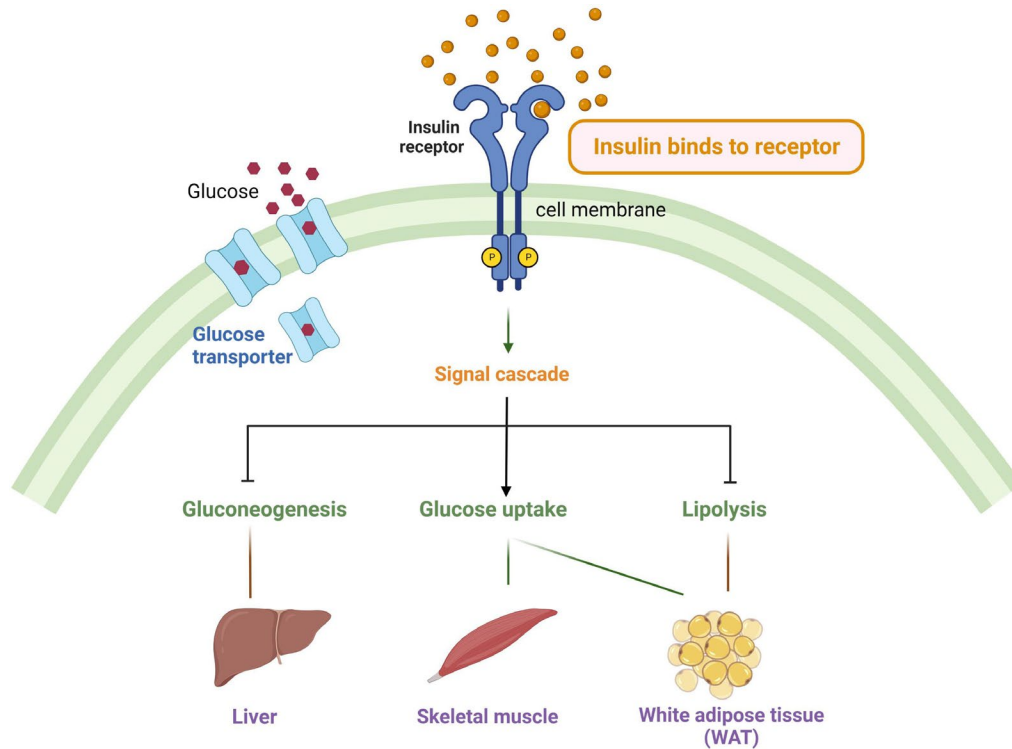


**Figure 7. Effect of insulin on carbohydrate Metabolism.**

*Insulin increases tissue glucose uptake, promotes excess glucose into fatty acids, inhibits gluconeogenesis in liver, and inhibits lipolysis in adipose tissue. (Created with BioRender.com)*

Insulin is secreted into the blood with a half-life of approximately 6 minutes. Approximately 80% of insulin is degraded by liver, the left is cleared by the kidneys and muscles (Duckworth et al., 1998).

To trigger metabolic signaling, insulin first binds and activates receptors in the target cells (Fig. 2). After insulin binds with the insulin receptor, it stimulates the translocation of glucose transporter to the cell membrane to facilitate cellular glucose uptake. The transient increase in intracellular glucose can then be used for energy production or storage. During conditions of excess glucose, insulin promotes the activity of glycogen synthase, which is an enzyme that facilitates glycogen synthesis to store excess glucose as glycogen in liver and muscle. Further, glycogen synthesis is inhibited after liver glycogen concentrations reach

## *Introduction*

5% to 6%. The remaining excess glucose that does not enter into glycogen synthesis is then converted into fat under the stimulus of insulin. For this to occur, glucose is split into pyruvate via glycolysis, in which the pyruvate molecule is then converted into acetyl coenzyme A (acetyl-CoA), and used as a substrate for fatty acid synthesis. When citrate and isocitrate anions, which are formed by the citric acid cycle, accumulate they activate the enzyme acetyl-CoA carboxylase. This enzyme initiates the first stage of fatty acids synthesis which is accompanied with the formation of malonyl-CoA from acetyl-CoA. The subsequently synthesized fatty acids in the liver are then packaged as triglycerides into very low-density lipoproteins and transported into the blood. Once the triglyceride-carrying very low-density lipoproteins reach the adipose tissue, circulating insulin will have promoted lipoprotein lipase activity, which then splits the triglycerides into fatty acids for adipocytes absorption, which is then ultimately stored as triglycerides. Inhibition of the action of hormone-sensitive lipase (HSL) by insulin is also necessary for fat storage in adipose tissue (Cohen and Spiegelman, 2016; Sears and Perry, 2015; Wong and Sul, 2010).

Another primary effect of insulin is inhibiting gluconeogenesis in the liver. Hepatic insulin action predominantly decreases the quantity and activity of gluconeogenic enzymes such as phosphoenolpyruvate carboxykinase and glucose-6-phosphatase, while the expression of these two enzymes is increased by glucagon during fasting (Barthel and Schmoll, 2003; Hatting et al., 2018).

### **1.6 Insulin and fat metabolism**

Adipose tissue is the main tissue to store excess energy. With overnutrition, the excess energy is stored as triglycerides (TG) consisting of three long-chain fatty acids and one molecule of glycerol in the lipid droplets of adipose tissue. TGs account for 80-95% of the volume of an adipocyte. Minute amounts of TGs are synthesized in adipose tissue, but mainly come from the diet or are synthesized endogenously in the liver. Triglycerides are packaged into lipoproteins and then transported into circulating blood and other tissues. Lipoproteins mainly include five different types very low density lipoprotein (VLDL), low density lipoprotein (LDL), intermediate density lipoproteins (IDL), high density lipoprotein (HDL) and

## *Introduction*

chylomicrons. Of these, chylomicrons in the lymph or VLDL in the liver, contain the highest concentration of TG. TGs synthesized in the liver are mainly transported in VLDL to the adipose tissue. Circulating TGs split into non-esterified fatty acids (NEFA, free fatty acids) through hydrolysis by lipoprotein lipase. Then fatty acid transporters shuttle the released free fatty acids into adipocytes and other peripheral tissues. The lipoprotein lipase activity is stimulated by insulin. Moreover, insulin promotes glucose uptake that further increases the production of glycerol 3-phosphate, in which free fatty acids are then esterified using the glycerol 3-phosphate to reform TG stored in lipid droplets.

Basal adipocyte lipolysis is elevated during obesity and is tightly associated with insulin resistance (Heine et al., 2018; Morigny et al., 2016). Lipolysis is a process of breaking down triglycerides into fatty acids and glycerol. There are three main enzymes that participate in three steps of lipolysis which are adipose triglyceride lipase (ATGL), hormone-sensitive lipase (HSL) and mono-glycerol lipase (MGL). ATGL initiates the first step of TG lipolysis, which is also a rate-limiting step, for the generation of diacylglycerols (DG) and FFA. Its activity is tightly regulated by two accessory proteins GCI58 that co-activates ATGL and G0S2 that inactivates ATGL. Next, HSL performs the second step of hydrolyzing DG, generating monoacylglycerols (MG) and FFA. Then, MGL catalyzes MGs, producing glycerol and the third molecule FFA (Fig. 8).

## Introduction

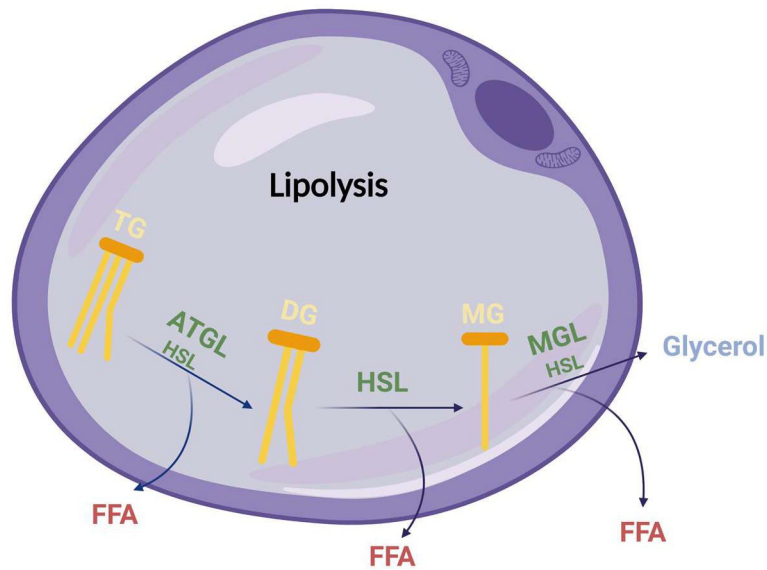


**Figure 8. Main enzymes of breaking down triglycerides in lipolysis.**

Triglycerides (TG) are first hydrolyzed by ATGL and HSL into diacylglycerols (DG), then DG is continued catalyzed by HSL into monoacylglycerols (MG). Later, MG is degraded into free fatty acid and glycerol via MGL. (Created with BioRender.com)

Lipolysis can be triggered by pro-lipolytic hormones like glucagon, growth hormone, thyroid hormone, cortisol and catecholamines. In WAT, there are two important mechanisms regulating lipolysis: the activation of ATGL by CGI-58 and the protein kinase A (PKA)-mediated phosphorylation of HSL and perilipin, both of which are the major proteins in association with lipid droplets in adipocytes. Without any stimulus, CGI-58 is bound to perilipin together, unable to bind to or activate ATGL. Moreover, both ATGL and HSL reside in the cytosol (Fig. 9). While, under the triggered state, these pro-lipolytic hormones elevate levels of cellular cAMP. Next, cAMP binds to the enzyme PKA and initiates the activity of PKA. Then PKA phosphorylates the key lipolytic proteins: perilipin and HSL, and initiates all the stages of lipolysis. HSL translocates from the cytosol to the surface of the lipid droplet following phosphorylation and binds with the phosphorylated perilipin to release CGI-58. Thus CGI-58 can bind and activate ATGL. The phosphorylation of ATGL moves from cytosol to the surface of the lipid droplet starting lipolysis. Fatty acids and glycerol are released into the cytosol in the last step of lipolysis. Glycerol coming from lipolysis enters the liver and acts as a potential carbon

## *Introduction*

source for gluconeogenesis. FFA travel the circulatory system by binding albumin, which once reaching the liver, undergo beta-oxidation to produce ATP and NADH to promote gluconeogenesis in the liver (Fig. 9) (Duncan et al., 2007; Fruhbeck et al., 2014; Morigny et al., 2016; Schweiger et al., 2014). However, unlike glucagon which is a pro-lipolytic hormone, insulin acts as an anti-lipolytic hormone regulator (FGF1 also is a lipolytic suppressor). Insulin binds to the insulin receptor and activates PI3K to stimulate the phosphorylation of phosphodiesterase 3B (PDE3B). In *Pde3b* KO brown adipocytes, the action of insulin on suppressing lipolysis is impaired. However, a mutant form of PDE3B, which disrupted the major Akt phosphorylation site, S273, also restores the ability of insulin to inhibit lipolysis (DiPilato et al., 2015). Therefore, Akt is not the only regulator that phosphorylates PDE3B, but other factors existed that contribute to its phosphorylation as well. Nevertheless, PDE3B plays a vital role in lipolysis, which accelerates the degradation of the cyclic AMP (cAMP). The resulting inhibition of PKA activity reduces the activity of lipolytic enzymes in adipocytes. (Fruhbeck et al., 2014; Girousse et al., 2013; Heine et al., 2018; Sancar et al., 2022).

# Introduction

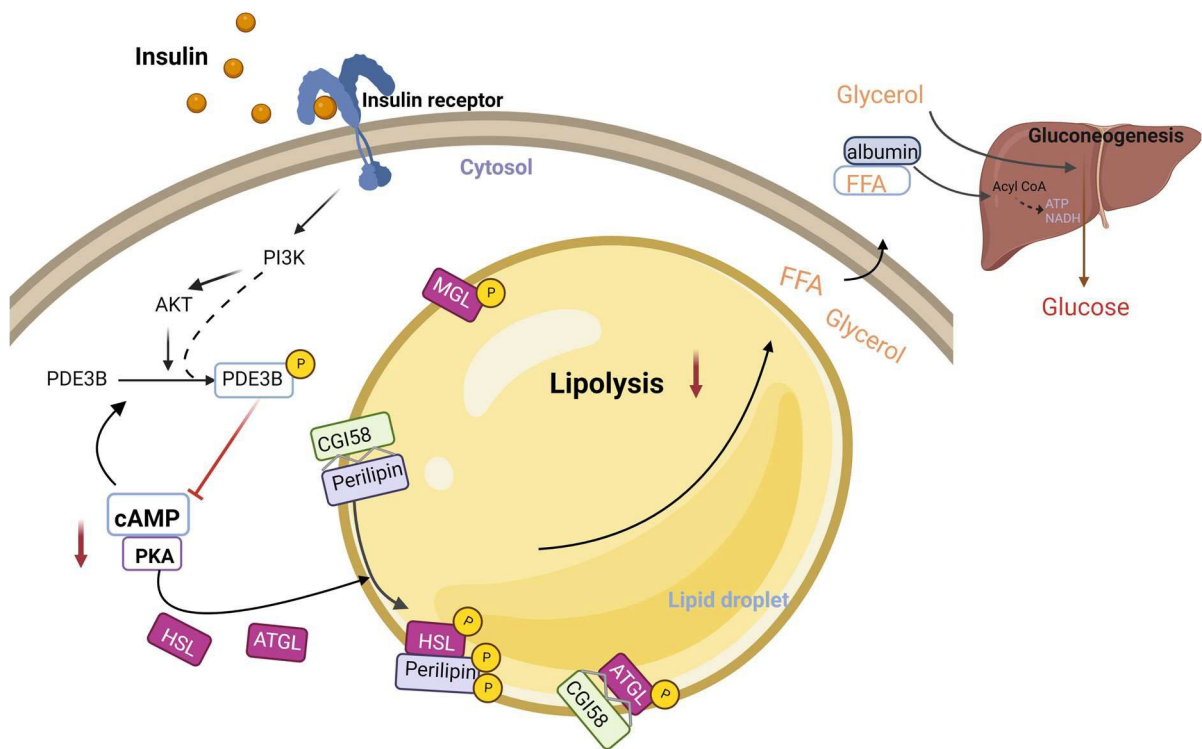


**Figure 9. Mechanism of lipolysis in adipocyte.**

Insulin induces suppression of adipose lipolysis. Insulin signaling activates PDE3B to decrease cAMP levels and then further suppresses HSL phosphorylation to suppress lipolysis. However, with pro-lipolytic hormone stimulation, lipolysis is induced. Perilipin released from CGI58 combine with HSL activating the process of TG degradation. Fatty acid and glycerol from lipolysis are released into the cytosol. (Created with BioRender.com)

## 1.7 Role of serine racemase and NMDARs in regulating insulin secretion

Peripheral insulin resistance caused by obesity is often an early stage of T2D development. In this stage, a greater islet expansion and an increased insulin secretion from pancreatic beta cells occur to compensate for insulin resistance. Later the progressive pancreatic islets dysfunction and beta cell mass loss lead to T2D (Talchai et al., 2012). Therefore, patients with T2D require additional treatment including antidiabetic drugs such as metformin, sulfonylureas, tirzepatide, and ultimately insulin replacement. However, most commonly used antidiabetic drugs fail to stop the progression of pancreatic islet dysfunction in

## *Introduction*

patients with T2D (Tahrani et al., 2011; Tokarz et al., 2018; Zhou and Melton, 2018). Moreover, sulfonylureas increase both glucose-stimulated insulin secretion and basal insulin secretion, which can trigger hypoglycemia easily. Further, occurrence of severe hypoglycemia can be life-threatening. Medicines like glucagon-like peptide-1 receptor (GLP-1R) agonists or inhibitors of the incretin-degrading dipeptidyl peptidase-4 (DPP-4) do not cause severe hypoglycemic events via increasing GSIS predominantly instead of basal insulin secretion. These drugs are suggested to potentially assist in slowing down islet dysfunction and diabetes progression. However, these treatments have not been shown to sustainably restore beta cell function or further rescue T2D progression (Kahn et al., 2014). Recently, research has explored a novel antidiabetic drug targeting the N-methyl-D-aspartate receptor (NMDAR), which was previously understood primarily for its important role in modulating synaptic plasticity and brain memory-related effects. Recent studies demonstrate improvements in pancreatic islets function, insulin secretion in response to glucose stimulation, and survival of islet cells. Further, inhibition of NMDAR prolongs the glucose-stimulated depolarized state within beta cells by increasing cytosolic  $Ca^{2+}$  concentrations. In diabetic mice, long-term dextromethorphan treatment (DXM), a non-competitive NMDAR antagonist, improves pancreatic islets insulin content, islets cell mass and blood glucose tolerance. Moreover, individuals with T2D show enhanced glucose tolerance and enhanced serum insulin concentrations after DXM treatment (Huang et al., 2017; Marquard et al., 2015; Wu et al., 2017). NMDAR also displays a role in mediating the effect of leptin to modulate pancreatic beta cell electrical activity by promoting AMP-activated protein kinase (AMPK)-dependent trafficking of  $K_{ATP}$  and Kv2.1 channels to the plasma membrane (Cochrane et al., 2021; Wu et al., 2017).

NMDAR is a tetrameric ligand-gated ion channel. NMDARs are comprised of two glycine-binding GluN1 subunits and two glutamate-binding GluN2 A-D subunits or GluN3 subunits that are additional subunits for binding Glycine and D-serine (Grand et al., 2018; Lee et al., 2014; Nong et al., 2003; Skrenkova et al., 2020). The ion channel of NMDAR is blocked by the extracellular  $Mg^{2+}$  ions at resting membrane potentials, and can be released by membrane depolarization. Thus,

## *Introduction*

the activation of NMDAR requires both membrane depolarization and binding of the agonist glutamate, and D-serine or glycine. Two co-agonists, glycine and D-serine, both are present in the extracellular space (Johnson and Ascher, 1987; Wolosker and Balu, 2020). In addition, D-serine is more effective than glycine in activating NMDARs in adult forebrain regions (Balu et al., 2013; Basu et al., 2009; Curcio et al., 2013; Papouin et al., 2012; Wolosker and Balu, 2020). D-serine is produced from L-serine via racemization by serine racemase (SRR). SRR activity can be inhibited by NMDAR in brain, which triggers the translocation of SRR from the cytosol to membranes and the cell nucleus, where the enzyme is mostly inactive (Kolodney et al., 2015). On the other side, inhibition of NMDARs by MK-801 administration increase SRR expression in the brain (Hashimoto et al., 2007). Besides the racemization reaction, SRR catalyzes the  $\alpha,\beta$ -elimination reaction from L-serine producing pyruvate and ammonia but at a slower rate. (Foltyn et al., 2005; Strisovsky et al., 2005; Wolosker et al., 1999). Recent study demonstrates that serine racemase supports the growth of colorectal tumors via producing pyruvate from serine. Inhibition of SRR suppresses the proliferation of colorectal cancer cells in mice. (Ohshima et al., 2020).

Serine is a non-essential amino acid, and mainly comes from five sources: dietary intake, glycolytic intermediate 3-phosphoglycerate, glycine, proteins and phospholipids. Restricted serine intake inhibits tumor growth by affecting mitochondrial dynamics and function. Utilization of fatty acid, glucose and glutamine is reduced in the mitochondria after serine deprivation. This indicates serine acts as a central node in the metabolic network for many aspects of cell survival and proliferation. Serine is additionally involved in influencing insulin and glucose metabolism as well. Serine levels are positively correlated with insulin secretion and sensitivity (Vangipurapu et al., 2019). Further, individuals with T1D or T2D contains lower level of serine in blood compared to non-diabetic controls (Bertea et al., 2010; Bervoets et al., 2017; Drábková et al., 2015). L-serine supplementation prevents mice from fasting-induced weight regain compare to controls under HFD but does not affect insulin secretion or glucose tolerance (Lopez-Gonzales et al., 2022). Moreover, the expression of SRR was significantly reduced in STZ-treated pancreatic islets relative to control mice but significantly

## *Introduction*

increased in pancreatic islets from 8-week-old *ob/ob* mice. Interestingly, acute D-serine supplementation enhances glucose-stimulated insulin secretion and excitatory membrane activity of pancreatic beta cells (Lockridge et al., 2021). However, mice with chronic D-serine supplementation shows impaired insulin secretion (Suwandhi et al., 2018). Deletion of SRR in the brain reverses neuronal insulin signaling inhibition by amyloid- $\beta$  oligomers (Zhou et al., 2022). SRR whole-body knockout mice show improved insulin secretion, insulin sensitivity and glucose tolerance. Although many SRR or serine functions in human have been discovered, a complete understanding of the effects of an excess or a deficiency of serine still needs to be further explored.

### **1.8 Role of glypican 4**

Obesity is one of the main causes of insulin resistance and T2D. Various cytokines and adipokines secreted by the white adipose tissue (WAT) are shown to regulate body metabolism and insulin sensitivity (Ahima and Flier, 2000; De Cat and David, 2001; Deng and Scherer, 2010). One of the adipokines is glypican-4 (Gpc4), which is a member of the six-member family of glycosylphosphatidylinositol (GPI) anchored heparan sulfate proteoglycans. Previous studies indicate that Gpc4 works as a coreceptor for growth factors like Wnt and bone morphogenetic proteins (BMPs) because of its special structure, which does not contain any transmembrane or intracellular domains (Li et al., 2014; Ning et al., 2019; Yoo et al., 2013). Recent studies demonstrate that Gpc4 levels are increased in individuals with impaired glucose tolerance but decreased in T2D individuals. Gpc4 expression in human WAT highly correlates to body mass index (BMI) and waist-to-hip ratio (WHR). Further, in subcutaneous white adipose tissue Gpc4 expression is negatively correlated with BMI and WHR. However, Gpc4 expression in visceral adipose tissue is positively correlated with BMI and WHR. Moreover, Gpc4 can be released from the surface of adipocytes and presents as a serum adipokine both in humans and mice (Deischinger et al., 2021; Mitchell, 2012; Tamori and Kasuga, 2013). Serum Gpc4 concentrations are positively correlated with body fat content and insulin resistance. In addition, studies show that Gpc4 interacts with the insulin receptor. Knockdown of Gpc4 in pre-adipocytes induces approximate 33% reduction of insulin-stimulated IR

## *Introduction*

phosphorylation in comparison with control cells (Ussar et al., 2012). Moreover, lack of insulin receptors in pancreatic beta cells promotes insulin hypersecretion and improves glucose tolerance (Skovso et al., 2022). These data suggest Gpc4 in pancreatic beta cells might play an important role in regulating insulin secretion and metabolic homeostasis.

# *Introduction*

## **1.9 Aims of the thesis**

Several studies, including the study from our lab, show that two single nucleotide polymorphisms (SNP) in serine racemase are associated with insulin secretion in humans (Suwandhi et al., 2018). Serine racemase is an enzyme that mainly catalyzes the racemization of L-serine to D-serine. Unlike L-serine, D-serine is not proteinogenic but acts as a co-agonist for the NMDA receptor, which is known to modulate membrane potential and thereby insulin secretion from beta cells (Lockridge et al., 2021; Marquard et al., 2015). Furthermore, our previous study demonstrated that chronic supplementation of D-serine to mice impairs glucose stimulated insulin secretion. Moreover, mice on a high fat diet (HFD) that chronically consumed D-serine water showed significantly lower body fat than control mice (Suwandhi et al., 2018). Whole-body knock out of SRR in mice improved glucose stimulated insulin secretion capacity (Lockridge et al., 2016). Above all, this indicates that SRR might play an important role in regulating insulin secretion and fat metabolism. As SRR is also expressed in other metabolically important tissues outside of the brain and pancreas, the observed phenotype of whole body SRR knockout mice could be due to effects in other organs. Insulin is secreted by pancreatic beta cells in islets.

**Aim 1: To answer the question ‘does serine racemase regulate fat metabolism through modulation of insulin signaling from pancreatic beta cells?’ and to elucidate the mechanism underlying the modulation of insulin secretion by SRR.**

In the proteomics analysis of pancreatic islets lacking serine racemase in beta cells, glypican 4 (Gpc4) was downregulated compared to controls. Interestingly, Ussar et al (2014) reported that Gpc4 is expressed and secreted by adipose tissue and can interact with the insulin receptor enhancing the insulin signaling. Additionally, specific loss of insulin receptor in pancreatic beta cells promotes insulin secretion and improves glucose tolerance. These data suggests that Gpc4 in pancreatic beta cells could regulate insulin secretion via modulating the interaction with insulin receptor. Therefore, in this thesis, another aim (**Aim 2**) is

## *Introduction*

**to investigate the role of Gpc4 in regulating insulin secretion in pancreatic beta cells.**

Biological aging is associated with the development of type 2 diabetes, cancer, cardiovascular and neurodegenerative diseases. Progressive telomere shortening is a hallmark of aging that is associated with the development of metabolic diseases. However, due to the severe pathologies associated with strong telomere shortening in mice, the exact effects of shortened telomeres on metabolic function remain incompletely understood. Further understanding of the metabolic alterations associated with aging is essential to develop preventive and therapeutic interventions in this high-risk population for glucose intolerance. Therefore, in this thesis, I addressed the following aim.

**Aim 3: Study the metabolic consequences of moderate telomere shortening using second-generation Terc KO mice.**

This thesis studied the metabolic consequences of moderate telomere shortening using the second-generation mice which have lost of telomerase activity in the body (Terc KO mice). This study provides important insights into the age associated development of type 2 diabetes and the metabolic syndrome.

## 2. Material and Methods

### 2.1 Animals

All animal experiments were approved by the Animal Ethics Committee of the government of Upper Bavaria (Germany). Mice were housed in a specific pathogen free facility at 20-23°C and 45-60% humidity with a 12-h light /12-h dark cycle in ventilated cage. Cages were supplemented with nesting material and were changed every week. All mice were under *ad libitum* access to water and a standard laboratory chow diet (Altromin). For dietary treatment, mice were fed with 58% high fat diet (Research Diets D12331) from 6 weeks old.

Selective loss of serine racemase (SRR) in pancreatic beta cells was generated by SRR flox/flox mice (got from McLean Hospital in Belmont, USA.) with Ins1-cre mice (Jackson Laboratories, Stock No: 026801), both on the C57BL/6J background. Srr<sup>fl/fl</sup>-Ins1-cre<sup>+</sup> (Srr<sup>ins1cre</sup>) mice and Srr<sup>fl/fl</sup>-Ins1-cre<sup>-</sup> (Srr fl/fl) mice (controls) were used for the study. Procedures for genotyping of mouse lines have been described before (Ruiz-Ojeda et al., 2021).

Selective loss of glypican 4 (Gpc4) in pancreatic beta cells was generated by Gpc4 flox/flox female mice with Ins1-cre mice, both on the C57BL/6J background. Gpc4<sup>fl/0</sup>-Ins1-cre<sup>+</sup> (Gpc4<sup>Ins1</sup>) and Gpc4<sup>fl/0</sup>-Ins1-cre<sup>-</sup> (Gpc4<sup>fl/0</sup>) are used for the study. Procedures for genotyping of mouse lines have been described before (Ruiz-Ojeda et al., 2021).

Male and female Terc (+/-) mice were bought from Jackson lab (Jackson stock: 004132). Female and male Terc (+/-) mice were firstly mated with C57BL/6N male and female mice respectively. Then Terc (+/-) litter were mated to each other. The litter from inbreeding Terc (+/-), Terc (-/-, Generation1) mice and Terc (+/+, WT) mice, were used to generate a cohort of Terc KO (second-generation) and WT mice. 53 weeks old mice of Terc KO (second-generation) and WT mice were used for experiments. Procedures for genotyping of mouse lines have been described in Jackson lab website.

Sequences of genotyping primers are following:

## Material and methods

Gene name	Forward (5' - 3')	Reverse (3' - 5')
<i>Gpc4 fl/fl</i>	TCTTCGTTGAGTTGAAGCG	GGCGAGCCCAGAAGTCATTT
<i>Srr fl/fl</i>	TGTGTGAATGTGTACATAC	ACGTGGGAACCTGCTGGATTCT
<i>Ins1 cre (Cre+)</i>	ACCCTTCACCAATGACTCCTATG	TGACTGCAGCAAATCGCTTGG
<i>Ins1 cre (Cre-)</i>	GTCAAACAGCATCTTTGTGGTC	TGACTGCAGCAAATCGCTTGG
<i>Terc Mutant</i>	ATTTGTACAGTCTGCACGACG	CTTCAATTCCTTGGCTTCG
<i>Terc WT</i>	GCACTCCTTACAAGGGACGA	CTTCAATTCCTTGGCTTCG

### 2.2 In vivo experiment

#### Glucose tolerance test (GTT)

Mice were fasted for 4 h during the light phase. Two types of GTTs were performed. Oral GTT (oGTT) where mice were orally gavaged with 20% glucose (Braun, Germany) (2 g/kg) and an intraperitoneal GTT (i.p. GTT) where mice were intraperitoneally injected with 20% glucose solution (2 g/kg). Blood glucose levels were measured from tail tip punctures using a Freestyle Freedom Lite glucometer (Abbott, Chicago, Illinois, USA) at the 0, 15, 30, 60, 90 and 120 min time points.

#### Glucose-stimulated insulin secretion test (GSIS)

Oral glucose stimulated insulin secretion test, mice were fasted for 6 hours prior to oral gavage of 4 g/kg glucose (oGSIS) or intraperitoneally injection of 3 g/kg glucose (GSIS) during the day. The blood glucose concentrations were measured in blood collected from the tail at 0 and 2, 5, 15 and 30 min time points after gavage or injection by using a FreeStyle Freedom Lite glucometer. Blood was collected from the tail into Microvette tubes (Sarstedt, Germany) at the same time points. Plasma was prepared by centrifugation (10 min at 10,000 x g at 4°C) and insulin concentrations were determined using an Ultra-Sensitive Mouse Insulin ELISA Kit (CrystalChem, USA).

## *Material and methods*

### **Insulin tolerance test (ITT)**

Mice were fasted for 4 h during the light phase and intraperitoneally injected with 0.75 (chow diet) or 1.5 (high fat diet or Terc male mice fed with chow diet) IU/kg insulin (Actrapid, Novo Nordisk, Denmark). Blood glucose levels were measured from tail tip punctures using a Freestyle Freedom Lite glucometer (Abbott) at the 0, 15, 30, 60, 90 and 120 min time points.

### **Pyruvate tolerance test (PTT)**

Mice were fasted overnight for 16 hours. 20% Pyruvate solution was prepared in Dulbecco's phosphate buffered saline (PBS) (Gibco, USA). Mice were intraperitoneally injected with 2 g/kg pyruvate and blood glucose levels were measured at 0, 15, 30, 60, 90, 120 min time points using Freestyle Freedom lite glucometer (Abbott).

### **Body composition and energy metabolism**

Body composition was analyzed with a non-invasive magnetic-resonance whole-body composition analyzer (EchoMRI).

### **Energy metabolism studies**

These studies were conducted as previously described (Lopez-Gonzales et al., 2022; Ruiz-Ojeda et al., 2021). In brief, lean and fat mass were measured using a magnetic resonance whole-body composition analyzer (EchoMRI, Houston, Texas, USA). Food intake, water intake, respiratory exchange rate (RER), energy expenditure (EE) and locomotor activity were measured continuously in 10-min intervals, after a 24 h acclimatization period, using indirect calorimetry (TSE Phenomaster, Berlin, Germany).

### **Glycosylated hemoglobin (HbA1c) measurement**

HbA1c was measured from random fed mice during the light phase without fasting by using a DCA Vantage Analyzer (Siemens, Munich, Germany)

# *Material and methods*

## **2.3 Ex vivo experiments**

### **Pancreatic islets isolation**

Mice were sacrificed by cervical dislocation and clamping the bile duct and perfuse the collagenase P (Roche) solution immediately. In brief, 1 ml of cold collagenase P solution (1 mg/ml dissolved in G-solution (HBSS (Lonza) + 1% BSA (Sigma-Aldrich)) was injected into the bile duct and the perfused pancreas was consequently dissected. Tissue pieces were incubated in a 15 ml Falcon tube with 1 ml of collagenase P solution, which is same as the injection solution, for 15 min at 37°C with a strong shaking in the middle of incubation. Then, 12 ml of the cold G-solution was filled into the falcon tubes with samples, followed by centrifugation at 1,620 rpm at room temperature. Pellet was washed with 10 ml of the G-solution. After washing step with the G-solution, the pellets were re-suspended in 5.5 ml of gradient solution – 15% of Optiprep (5 ml 10% RPMI (Lonza) + 3 ml of 40% Optiprep which diluted from 60 % Optiprep with G-solution (Sigma-Aldrich) per sample), and placed on top of 2.5 ml of the gradient solution. To form a 3-layer gradient, 6 ml of the G-solution was added on the top. Samples were then incubated for 10 min at room temperature before centrifugation at 1,700 rpm. Finally, the interphase between the upper and the middle layers of the gradient was harvested and was filtered through a 70 µm nylon filter then washed with the G-solution. Islets were handpicked by a micropipette under the microscope and cultured in RPMI 1640 medium overnight.

### **Ex vivo Glucose stimulated insulin secretion (GSIS) from pancreatic islets**

Prior to GSIS, culture medium was removed and islet microtissues were washed twice with Krebs Ringer Hepes Buffer (KRHB; 131 mM NaCl, 4.8 mM KCl, 1.3 mM CaCl<sub>2</sub>, 25 mM HEPES, 1.2 mM KH<sub>2</sub>PO<sub>4</sub>, 1.2 mM MgSO<sub>4</sub>, 1% BSA) containing 2.8 mM, glucose and equilibrated for 1 hour in the same solution. The supernatant was collected as a sample under low glucose condition), and islets were incubated for another 1 hour at 37°C with KRHB containing 16.7 mM glucose and supplements as above. The supernatant was collected as a sample under high glucose condition and stored at -20 °C. The remaining islets were lysed in 500 ul of Acid-Ethanol (70% Ethanol with 1.5% HCl 12N) using the sonicator and

## *Material and methods*

incubated at 4°C overnight. Lysed cells were centrifuged (7,000 rpm, 4°C, 10 min), and the supernatant was transferred into a new tube and stored at -20°C. Insulin concentrations were determined using the Mouse insulin ELISA (AppliChem), and secreted insulin was normalized to total insulin content.

### **Pancreatic islets mitochondrial stress test**

Day before, the Agilent Seahorse XFe96 Spheroid Microplates (Agilent Technologies #102905-100) was coated with 100 µg/ml Poly-D Lysine (Sigma #P7280). The sensor cartridge was hydrated in 200 µl of XF Calibrant in each well of the Seahorse utility plate in a non-CO<sub>2</sub> 37°C incubator overnight. Next day, on the experiment day, similar size of islets which were recovered overnight after isolation were picked into V-bottom 96 well plate with 200 µl pre-warmed RPMI 1640 medium, 25 islets per well. Afterwards, all islets were transferred from V-bottom plate into Seahorse plate with 175 µl of low glucose assay medium (2.8 mM glucose, 0.1% FBS in Agilent Seahorse XF Base Medium # 102353-100) by VIAFLO 96 machine (Integra Biosciences) at same time. Islets fall out of the pipette tip by gravity and into the central detent of each well. Then the bubbles were removed from the wells under the scope. Next, the plate was incubated in non-CO<sub>2</sub> 37°C incubator for 1 hour. Mitochondrial respiration was measured using the Seahorse XF96 extracellular flux analyzer equipped with a spheroid plate-compatible thermal tray (Agilent Technologies, Santa Clara, CA). Basal respiration was first measured in 2.8 mM glucose media. Islets were then sequentially exposed to Oligomycin A (4.5 µM at final concentration), CCCP (1 µM final concentration) and Rotenone + Antimycin A (2.5 µM final concentration). Each injection had 4 repeats of a cycle composed of mix for 2 min, wait for 2 min and measurement for 3 min. DNA content of islets from each well were measured by Quant-iT PicoGreen dsDNA Assay Kit (Life Technologies, P7589). For calculation of mouse islet bioenergetics parameters, lowest non-electron transport chain OCR values after injection of Rotenone + Antimycin A were subtracted from all OCR measurements. Non-mitochondrial oxygen consumption, basal respiration, maximal respiration, ATP production, coupling efficiency, proton leak was calculated according to the Seahorse XF Cell Mito Stress Test equations template provided by Agilent Technologies. Non-mitochondrial oxygen consumption is the

## *Material and methods*

minimum rate measurement after Rotenone + Antimycin A injection. Basal respiration was calculated by last rate measurement before first injection minus non-mitochondrial respiration rate. Maximal respiration was calculated by dividing the maximum rate measurement after CCCP injection by the non-mitochondrial respiration. Proton leak was equal to minimum rate measurement after oligomycin injection minus non-mitochondrial respiration. ATP production was determined by dividing the last rate measurement before oligomycin injection by the minimum rate measurement after oligomycin injection.

### **Electrophysiological recordings**

Thirty minutes prior to recordings, single coverslips carrying dispersed beta-cells were incubated in Krebs-Ringer-buffer (KRB) solution, containing (in mM): 138 NaCl, 5 KCl, 1.25 NaH<sub>2</sub>PO<sub>4</sub>, 2 NaHCO<sub>3</sub>, 1.2 MgCl<sub>2</sub>, 2.6 CaCl<sub>2</sub>, 2.8 D-glucose and 5 HEPES (pH 7.4). Then, they were transferred to a chamber mounted on a stage of an upright microscope (SliceScope; Scientifica) coupled with a video camera (optiMOS sCMOS; QImaging) and continuously perfused with KRB solution at a rate of ~1 mL/min by a gravity-driven perfusion system. The cells were visualized under infrared differential interference contrast (IR-DIC) optics with a 40× immersion objective using the  $\mu$ -Manager 1.4 software (Edelstein et al. 2010; DOI: 10.1002/0471142727.mb1420s92). Patching pipettes were made with thick-walled borosilicate glass (GC150F-10; Harvard Apparatus) pulled using a horizontal puller (P-1000; Sutter Instruments) and filled with an ATP-free internal solution, containing (in mM): 148 K-gluconate, 8 KCl, 10 HEPES, 1 EGTA, 2 MgCl<sub>2</sub> and 1 CaCl<sub>2</sub> (pH 7.3), resulting in a pipette tip resistance between 4 and 7 M $\Omega$ . Whole-cell recordings were performed with an EPC 10 USB Double patch-clamp amplifier (HEKA Elektronik) in voltage- and current-clamp mode. Data were acquired at 10-20 kHz and low-pass filtered at 5 kHz (Bessel) using the PatchMaster 2x90.2 software (HEKA Elektronik). Beta-cells were identified by morphology and electrophysiological fingerprints. To obtain K<sub>ATP</sub> currents, beta-cells were held at -70 mV and voltage steps ( $\pm 10$  mV for 100 ms) were applied every 10 s immediately after break-in in order to monitor the increase in whole-cell conductance during intracellular ATP washout. At its maximal response, whole-cell conductance ( $G_{\max}$ ) was calculated by measuring the current amplitude

## *Material and methods*

response to two voltage steps ( $\pm 10$  mV for 500 ms). The  $K_{ATP}$  channel antagonist tolbutamide (100  $\mu$ M) was bath-applied to obtain residual conductance ( $G_{res}$ ), thus generating  $K_{ATP}$  conductance ( $G_{KATP} = G_{max} - G_{res}$ ) normalized to the cell capacitance. Membrane potential was monitored at  $I = 0$ . Data were visualized and analyzed using custom-written codes in MATLAB (MathWorks).

### **2.4 Staining and imaging**

#### **Cryo-embedded sections preparation**

Pancreas were fixed in 4% PFA immediately after sac and were kept overnight at 4°C. Next day, wash twice with 1×PBS to remove the remaining PFA. Afterwards, tissues were cryoprotected in a sequential gradient of 7.5% and 15% sucrose for 1 hour at room temperature. Then tissues were incubated with 30% sucrose overnight at 4°C. Later on, pancreas was incubated with 30% sucrose and tissue embedding medium (Tissue-Tek O.C.T. Compound, REF 4583) 1:1 solution for 1 hour. In the end, tissues were embedded into a cryomold (Tissue Tek® Cryomold, Weckert Labortechnik, REF 4557) with embedding medium O.C.T on dry ice and stored at -80°C. Sections of 10  $\mu$ m thickness were cut from each sample, mounted on a glass slide (Thermo Fisher Scientific) and dried for 10 min at room temperature and storage at -20°C.

#### **Immunofluorescence staining and imaging**

The cryo-sections were washed for 15 min with 1×PBS 3 times to rehydrated and permeabilized in 0.5% TritonX-100 in PBS for 20 min. Afterwards, wash 5 times for 5 min in PBS. Then blocking samples with donkey blocking solution (0.1% Tween-20, 10% FCS, 0.1% BSA and 3% donkey serum) for 1 hour. Next incubate primary antibody overnight at 4°C. All antibodies were diluted with blocking solution. Rabbit monoclonal anti-insulin (1:300, Cell Signaling, Catalog Nr.3014); guinea pig polyclonal anti-glucagon (1:3000, Takara Catalog Nr.M182); rat monoclonal anti-somatostatin (1:300, Invitrogen Catalog Nr.MA5-16987). Thereafter, sections were washed 5 min firstly with 1×PBST for 4 times and last time with 1×PBS on 160 rpm shaker. Next, sections were incubated with secondary antibodies which also diluted with blocking solution for 2 hours at room temperature. Following secondary antibodies were used, donkey anti-rabbit IgG

## *Material and methods*

(H + L) secondary antibody (1:800, Alexa Fluor 555, Invitrogen A-31572), donkey anti-guinea pig (H + L) secondary antibody (1:500, Alexa Fluor 488, Dianova 706–545–148), Donkey anti Rat (1:800, Alexa Fluor 647, Dianova 712-605-150). After secondary antibody incubation, staining DAPI (1:1000 in PBS) for 20 min. Then wash 4 times for 5 min with PBST and once with PBS. In the end, the sections were mounted with fluorescence mounting medium (DAKO, S3023), dried in the dark overnight and stored at 4°C. All images were obtained with a Leica SP8 confocal microscope using LAS AF software (Leica). Images were analyzed using ImageJ software (win64,1.53c).

### **Histology and imaging**

Perigonadal fat (pgWAT), subcutaneous fat (Sub WAT) were isolated from mice and fixed with 4% paraformaldehyde (PFA) (Roth, Germany) overnight at 4°C. The tissues were dehydrated into ascending concentrations of ethanol (70-100%), cleared by xylene then embedded in paraffin (Leica, Germany). Two micrometer tissue sections were cut using a semi-automated microtome (Leica, Wetzlar, Germany) and the sections were stained with a hematoxylin and eosin (H&E) stain as previously described (Lillie et al., 1976). Imaging was done using ECLIPSE Ci microscope (Nikon, Minato city, Tokyo, Japan).

### **2.5 Adipocyte size quantification**

Three images were taken from different locations of the tissue per slides from H&E staining, and 3 slides per tissue per mouse for quantification. Adipocyte size quantification was done by the software Fiji plugin Adiposoft. The area of the adipocytes was measured in pixels and then converted to  $\mu\text{m}^2$  using Fiji.

### **2.6 Hormone and triglyceride measurement**

Serum was prepared by centrifugation for 10 min at 10,000 x g at 4°C. Insulin concentration was determined by Ultra-Sensitive Mouse Insulin ELISA Kit (CrystalChem, USA). Triglyceride contents in liver, serum and feces were measured using the Triglyceride Quantification Colorimetric/Fluorometric kit (BioVision, USA).

## **2.7 Proteomics and analysis**

### **Proteomics sample preparation**

Proteomic sample preparation for LC-MS/MS analyses were performed as described previously (Kulak et al. 2014) with minor adjustments. Samples were lysed in SDC lysis buffer (2% SDC, 100 mM Tris-HCl pH 8.5) at 95°C for 10 min at 1,000 rpm, sonicated in high mode (30 sec OFF, 30 sec ON) for 10 cycles (Bioruptor® Plus; Diagenode), protein concentration was determined by BCA, and 25 µg of protein were used for further analysis. Samples were treated with TCEP and CAA (final concentrations of 10 mM and 40 mM, respectively) at 45°C for 10 min with 1000-rpm shake, in dark, and digested with trypsin and LysC (1:40, protease: protein ratio) overnight at 37°C at 1,000 rpm shake. Later, peptides were acidified with 2% TFA, isopropanol with 1:1 volume-to-volume ratio. Custom-made StageTips with three layers of styrene divinylbenzene reversed-phase sulfonate (SDB-RPS; 3 M Empore) membranes were used for desalting and purification of the acidified samples. Peptides were loaded on the activated (100% ACN, 1% TFA in 30% Methanol, 0.2% TFA, respectively) StageTips, run through the SDB- RPS membranes, and washed by EtOAc including 1% TFA, isopropanol including 1% TFA, and 0.2% TFA, respectively. Peptides eluted from the membranes with 60-µL elution buffer (80% ACN, 1.25% NH<sub>4</sub>OH) were dried by vacuum centrifuge (40 min at 45°C) and reconstituted in 6 µL of loading buffer (2% ACN, 0.1% TFA). Peptide concentration was estimated via optical measurement at 280 nm (Nanodrop 2000; Thermo Scientific) and 500 ng material were loaded onto 50 cm in-house packed HPLC column (75 µm inner diameter, packed with 1.9 µm with C18 Reprosil particles (Dr. Maisch GmbH) at 60°C) for LC-MS/MS analysis.

### **LC-MS/MS analysis**

Proteome was analyzed using EASY-nLC 1200 (Thermo Fisher Scientific) combined with an Orbitrap Exploris 480 Mass Spectrometer (Thermo Fisher Scientific) and a nano-electrospray ion source (Thermo Fisher Scientific). Peptides were separated by reversed-phase chromatography using a binary buffer system consisting of 0.1% formic acid (buffer A) and 80% ACN in 0.1% formic acid (buffer B) with a 120 min gradient (5-30% buffer B over 95min, 30-65%

## *Material and methods*

buffer B over 5min, 65-95% buffer B over 5min, wash with 95% buffer B for 5 min) at a flow rate of 300 nL/min.

MS data were acquired using a data-dependent cycle time (1 second) scan method. Full scan MS targets were in a 300–1650 m/z scan range with a normalized automatic gain control (AGC) target %300. The data was acquired in at 60,000 resolution with 25 ms maximum injection time. Precursor ions for MS/MS scans were fragmented by higher-energy C-trap dissociation (HCD) with a normalized collision energy of 27%. MS/MS scan sets were 15,000 resolution with an AGC target %100 and a maximum injection time of 28 ms.

The raw data were processed with MaxQuant version 1.6.14.0. Default settings were kept if not stated otherwise. FDR 0.01 was used for filtering at protein, peptide and modification level. As variable modifications, acetylation (protein N-term) and oxidized methionine (M), as fixed modifications, carbamidomethyl (C) were selected. Trypsin/P and LysC proteolytic cleavages were added. Missed cleavages allowed for protein analysis was 2. “Match between runs” and Label free quantitation (LFQ) were enabled and all searches were performed against the mouse Uniprot FASTA database (2019). Perseus (version 1.6.14.0 and 1.6.2.3) was used for bioinformatics analysis. UniProtKB, Gene Ontology (GO), and the Kyoto Encyclopedia of Genes and Genomes (KEGG) annotations were included in the analysis. Data visualized using Adobe Illustrator or Graphpad Prism (version 8.0).

Quantified proteins were filtered for at least two valid values among biological replicates in at least one condition. Missing values were imputed (Gaussian normal distribution with a width of 0.3 and a downshift of 1.8). Two-sample test with student *t*-test statistics (permutation-based FDR = 0.05;  $s_0 = 0$ ) was performed in Perseus and significant proteins were hierarchical clustered by applying Euclidean as a distance measure for row clustering after normalization of median protein abundances of biological replicates by z-score. Fisher’s Exact GOBP, GOCC, GOMF and KEGG Term enrichment of significant proteins was performed against *mus musculus* gene list with 21846 items in Perseus (Benjamini Hochberg FDR truncation with 0.02 threshold value).

## Material and methods

### 2.8 RNA isolation and cDNA preparation and real-time PCR.

For the determination of gene expression, total RNA was extracted from tissue or cells by using the RNeasy mini kit (Quiagen) and cDNA synthesis (110 ng RNA, High Capacity cDNA Reverse Transcription Kit, Applied Biosystems) was performed according to the manufacturers' instructions. qPCR was performed in a CFX384 Touch (BioRad), using 300 nM forward and reverse primers and iTaq Universal SYBR Green supermix (BioRad) and analyzed using the BioRad CFX Manager 3.1 Software. The target gene expression was normalized on TATA box-binding protein (TBP) expression. Samples without Ct value were set to 50, given that TBP was expressed. The primer sequences are shown below.

Gene name	Forward (5' - 3')	Reverse (3' - 5')
<i>Actb</i>	TTGCTGACAGGATGCAGAAG	ACATCTGCTGGAAGGTGGAC
<i>Gpc4</i>	GGCAGCTGGCACTAGTTTG	AACGGTGCTTGGGAGAGAG
<i>Srr</i>	CATTGGCTTGAATACCTGGC	TGAGCAGTTTCATTCTCCCC
<i>Tbp</i>	ACCCTTCACCAATGACTCCTATG	TGACTGCAGCAAATCGCTTGG

### 2.8 Protein extraction and western blot

Tissue samples were stored in -80°C freezer after sac. The frozen tissue was put into the 2ml tube with a metal bead. Then 500 µl-700 µl RIPA buffer (50mM Tris (pH 7.4), 150mM NaCl, 1mM EDTA and 1% Triton X100 (Sigma-Aldrich)) containing 1% protease inhibitor (Sigma-Aldrich), 1% phosphatase inhibitor cocktail II (Sigma-Aldrich) and 1% phosphatase inhibitor cocktail III (Sigma-Aldrich) was added into tube. Then the tissue was homogenized by using Tissuelyser II for 2 min at 30 Hz. Next, 0.1% SDS was added and the tube was kept on ice for 10 min. Later, the tube was centrifuged at 14000g for 30 min at 4°C, and the clear supernatant was collected into a fresh tube. Then, the protein concentration was measured by Pierce BCA Protein Assay Kit (ThermoFisher scientific). The desired protein concentration was diluted with 4X sample buffer (containing 10% β-mercaptoethanol), nuclease free water and the protein lysate. Afterward, mixed

## *Material and methods*

samples were boiled for 5 min at 95°C then frozen at -20°C for western blots. The western blot was conducted as previously described (Lopez-Gonzales et al., 2022; Ruiz-Ojeda et al., 2021).

### **2.9 Telomere length quantification**

#### **DNA extraction for telomere length quantification**

One volume of phenol: chloroform: isoamyl alcohol (25:24:1) (Roth, Germany) was added to the sample followed by centrifugation for 5 min at 16,000 x g at room temperature (RT). The upper phase was collected. One microliter of 20 mg/ml glycogen (Serva, Germany), 7.5 M ammonium acetate (0.5 x sample volume) and 100% Ethanol (2.5 x (sample volume + ammonium acetate volume)) were added to the sample. The sample was then incubated at -20°C overnight. The DNA was pelleted by centrifugation at 4°C for 30 min at 16,000 x g. The supernatant was removed and 150 µl of 70% ethanol was added to the sample followed by centrifugation at 4°C for 30 min at 16,000 x g then the supernatant was discarded. This step was repeated once and the sample was left to dry at RT for 10 min. The sample was reconstituted in water.

#### **Telomere length quantification**

Using isolated enterocyte DNA, telomere length relative to *Actb* was determined by using the Absolute Mouse Telomere Length Quantification Qpcr Assay Kit (ScienCell, USA).

### **2.10 Microbiota measurement and analysis**

Fecal pellets were collected from the colon during sacrifice and initially kept on dry ice. Long-term storage was at -80°C without addition of preservatives. DNA was extracted using the ZymoBIOMICS 96 MagBead DNA Kit (Zymo Research Europe GmbH, Freiburg, Germany). In brief, samples were homogenized in lysis buffer by bead beating three times for 5 min (MiniBeadBeater 96) followed by DNA isolation according to the manufacture's instruction on a Tecan Fluent liquid handling platform. DNA was normalized and the hypervariable region V4 of the 16S rRNA (F515/R806) gene was amplified in accordance with previously described protocols (Caporaso JG et al., 2011). Amplicons were sequenced on the Illumina

## *Material and methods*

MiSeq platform (PE300) and reads were cut at 250 bp. The Usearch11 software package (<https://drive5.com/usearch/>) was used to assemble (-fastq\_mergepairs -with fastq\_maxdiffs 30), quality control, and cluster obtained reads. Quality filtering was set up with the fastq\_filter (-fastq\_maxee 1); minimum read length, 250 bp. Reads were clustered into 97% ID operational taxonomic units (OTUs). The UPARSE algorithm (Edgar RC 2013) was used to determine the OTU clusters and representative sequences. The Silva database v138 (Quast C et al., 2012) and the RDP Classifier (Wang Q et al., 2007) were used for taxonomic assignment with a bootstrap confidence cut-off of 80%. OTUs with an abundance < 0.02% were pruned. Resulting OTU absolute table was used further for statistical analyses and data visualization in R package phyloseq (McMurdie PJ et al., 2013).

### **2.11 Statistics**

One-way analysis of co-variance (ANCOVA), statistical significance was calculated using R (x64 4.1.2 version) and R studio (2021.09.2+382 version) software. All the other statistical analyses were done using GraphPad Prism 7. Data are shown as mean  $\pm$  standard error of the mean (SEM). Statistical significance was calculated using unpaired student's *t*-test or Mann-Whitney test, and multiple comparisons, one- or two-way analysis of variance (ANOVA) followed by turkey's or Sidak's multiple comparison's test. Values with p-value lower than 0.05 ( $p < 0.05$ ) were considered statistically significant. \* $p < 0.05$ , \*\* $p < 0.01$ , \*\*\* $p < 0.001$ , \*\*\*\* $p < 0.0001$ .

# Results

## 3. Results

### 3.1 Genetic deletion of *Srr* in pancreatic beta cells impairs islets architecture and improves glucose tolerance under CD.

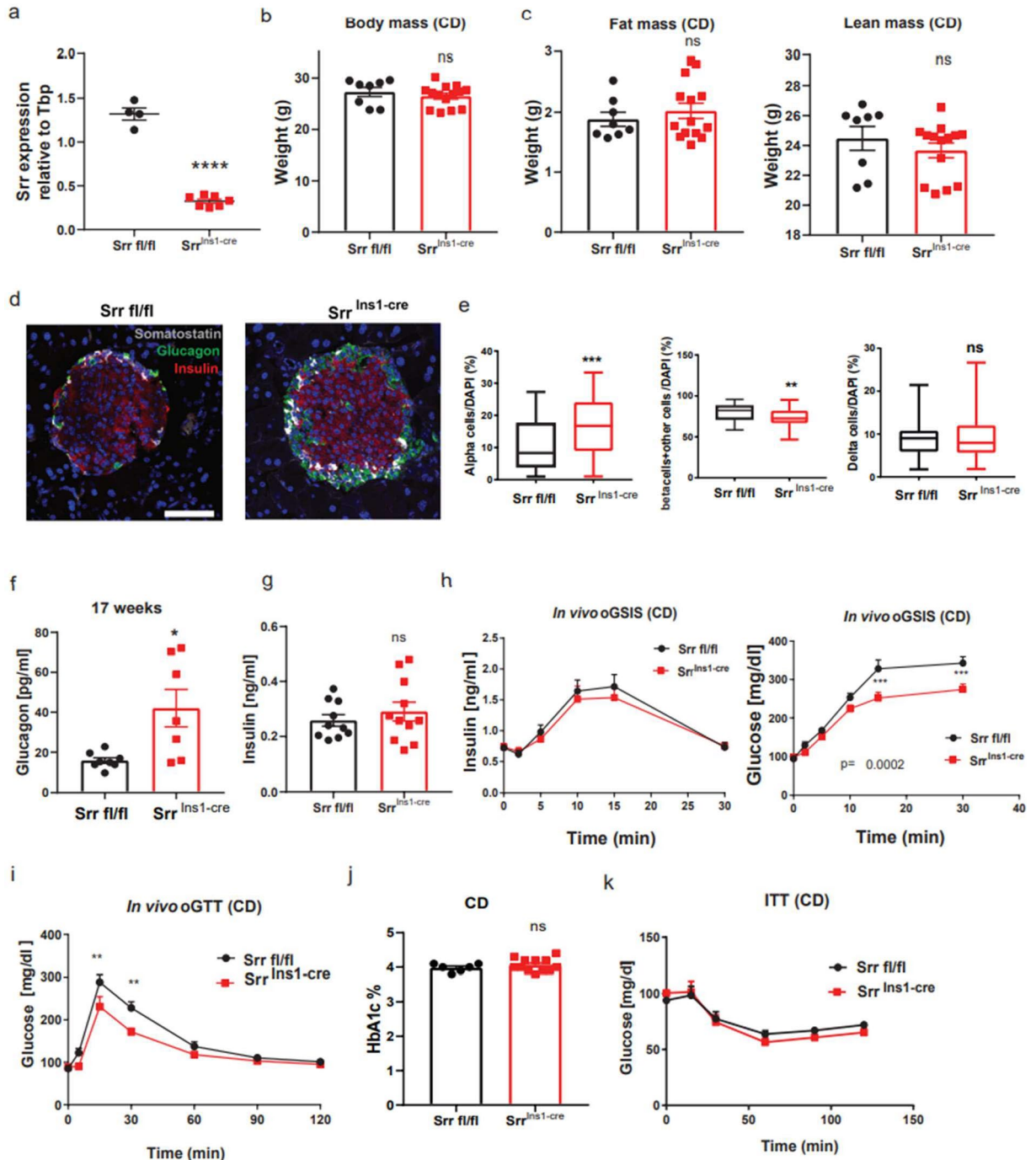


**Figure 10. Genetic deletion of *Srr* in pancreatic beta cells impairs islets architecture and improve glucose tolerance under chow diet.**

a. Knockout efficiency of *SRR* in pancreatic islets at mRNA, n= 4-7. b. Body mass (g) c. body composition (g). *Srr* fl/fl n=8, *Srr*<sup>Ins1cre</sup> n=14; 17 weeks old. d. Architecture of chow diet pancreatic

## Results

islets by immunofluorescence staining of glucagon (green, alpha cells), insulin (red, beta cells) and somatostatin (grey, delta cells). Scale bar, 75  $\mu$ m. e. Quantification of the number of alpha (left panel), beta plus other cells (middle) and delta cells (right) in islets. 43 islets from four biological replicates of *Srr fl/fl* mice, 72 islets from four biological replicates of *Srr<sup>ins1cre</sup>* mice, 28 weeks old. f. Serum glucagon level before sacrifice, *Srr fl/fl* n=8, *Srr<sup>ins1cre</sup>* n=7; 17 weeks old. g. Random insulin level in serum, *Srr fl/fl* n=10, *Srr<sup>ins1cre</sup>* n=11; 17 weeks old. h. Oral gavage glucose stimulated insulin secretion test (oGSIS), insulin level (left panel) and glucose level (right panel), *Srr fl/fl* n=10, *Srr<sup>ins1cre</sup>* n=10; 13 weeks old. i. Glucose level in oral glucose tolerance test (oGTT), *Srr fl/fl* n=10, *Srr<sup>ins1cre</sup>* n=10; 14 weeks old. All data presented as mean  $\pm$  SE. a, c, e, f, g and j were analyzed by unpaired t-test. h, i, k were analyzed by two-way ANOVA, \*p<0.05, \*\*p<0.01, \*\*\*p<0.001, \*\*\*\*p<0.0001

To examine whether serine racemase regulates fat metabolism through modulating insulin signaling from pancreatic beta cells, *Srr<sup>fl/fl</sup>-Ins1-cre<sup>+</sup>* (*Srr<sup>ins1cre</sup>*) mice with specific loss of SRR in pancreatic beta cells was used in this study. *Srr<sup>ins1cre</sup>* mice were generated by mating *Srr flox/flox* mice and *Ins1 cre* mice. *Srr<sup>fl/fl</sup>-Ins1-cre<sup>-</sup>* (*Srr fl/fl*) mice were used as controls. In *Srr fl/fl* mice, the first coding exon of serine racemase is flanked by two *LoxP* sites, without Cre recombinase expression. In *Srr<sup>ins1cre</sup>* mice, the Cre recombinase is inserted into the *Ins1* gene replacing its sequence and starting at the start codon (Thorens et al., 2015). Thus, Cre-recombinase is only expressed in the pancreatic beta cells where *ins1* is expressed to cut *LoxP* flanked sites. Therefore, serine racemase is only deleted in the pancreatic beta cells and not other tissues in *Srr<sup>ins1cre</sup>* mice. Further, the mouse model of this study was confirmed at the transcriptional level showing that SRR was efficiently deleted in pancreatic islets isolated from *Srr<sup>ins1cre</sup>* (**Fig.10a**).

*Srr<sup>ins1cre</sup>* mice exhibited normal body mass and body composition relative to the control mice (**Fig. 10b and c**). Furthermore, the architecture of the pancreatic islets was checked by immunofluorescence staining visualizing insulin-producing beta cells, glucagon-producing alpha cells, and somatostatin-producing delta cells. A significantly greater number of glucagon-positive alpha cells was observed in pancreatic islets from *Srr<sup>ins1cre</sup>* mice (**Fig. 10d, e**). Consistent with the changes observed in islet architecture, higher levels of glucagon (**Fig. 10f**) but normal insulin levels were detected in serum from *Srr<sup>ins1cre</sup>* mice compared to *Srr fl/fl* mice (**Fig. 10g**).

## Results

Thereafter, the function of pancreatic beta cells was determined by performing *in vivo* oral gavage glucose-stimulated secretion tests (oGSIS) under chow diet (CD). Surprisingly, no significant differences were observed in insulin levels between  $Srr^{ins1cre}$  and  $Srr\ fl/fl$  mice after high glucose stimulation (**Fig. 10h, left panel**). This finding suggested that the responsiveness of pancreatic beta cells to glucose stimulation in oGSIS was still maintained after SRR deletion. However, genetic deletion of SRR in pancreatic beta cells resulted in a significantly improved glucose tolerance (**Fig. 10h, right panel**), which was further confirmed by oral gavage glucose tolerance tests (oGTT) (**Fig. 10i**). In addition,  $Srr^{ins1cre}$  mice showed normal long-term global glycemic control with normal HbA1c % levels (**Fig. 10j**).  $Srr^{ins1cre}$  mice did not show significant differences in insulin tolerance compared to control mice under chow diet (**Fig. 10k**).

# Results

## 3.2 Loss of SRR in pancreatic beta cells promotes basal insulin secretion from pancreatic islets with enhanced ATP production and potassium channel trafficking observed under chow diet.

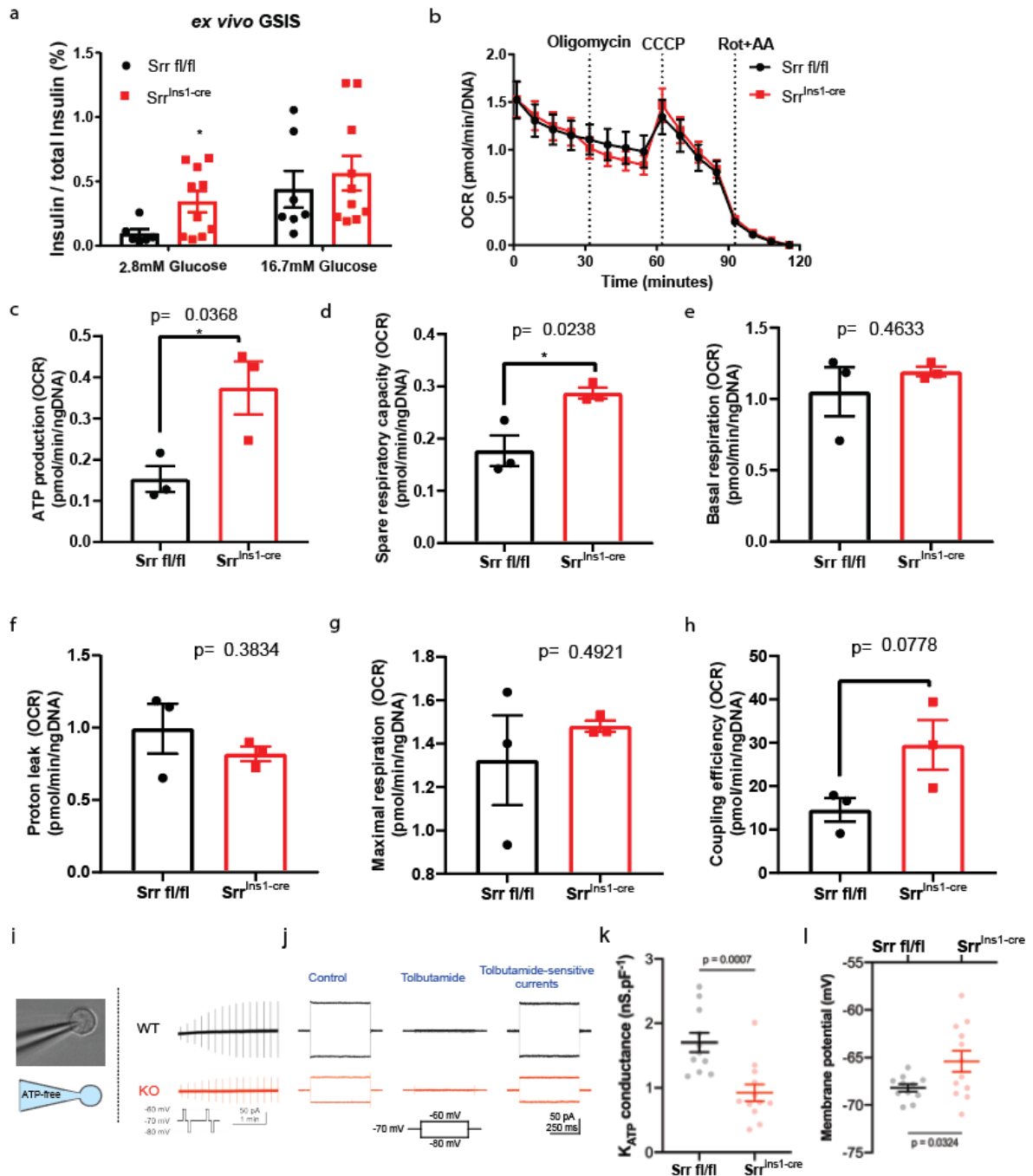


**Figure 11. Seahorse and electrical physiological tests of pancreatic islets in low glucose condition under chow diet.**

a. ex vivo glucose-stimulated insulin secretion (GSIS) in isolated islets, *Srr<sup>Ins1-cre</sup>* n=7, *Srr fl/fl* n=10. Ten islets per well. b-d. Mitochondrial stress tests of isolated pancreatic islets by seahorse under 2.8 mM glucose condition. Islets were acutely exposed to 2.8 mM glucose (final concentration),

## Results

Oligomycin A (Oligomycin), CCCP and Rotenone (Rot) + Antimycin A (AA). Twenty-five islets per well, eight replicates from three biological replicates of *Srr fl/fl* mice, nine technique replicates from three biological replicates of *Srr<sup>ins1cre</sup>* mice, 20 weeks old. b. Representative oxygen consumption rates (OCRs) traces of pancreatic islets normalized by DNA content. c. ATP production d. Spare respiratory capacity. e. Basal respiration. f. Proton leak g. Maximal respiration and h. coupling efficiency. i. Using an ATP-free pipette solution, the currents in response to voltage steps obtained from beta-cells of *Srr fl/fl* and *Srr<sup>ins1cre</sup>* mice were monitored immediately after entering in whole-cell configuration until reaching their maximal amplitude. *Srr fl/fl* n=11, *Srr<sup>ins1cre</sup>* n=12; 12 weeks old. j. Representative time course of maximum whole-cell current traces in response to voltage steps in control and in the presence of tolbutamide (100  $\mu$ M;  $K_{ATP}$  channel antagonist), and the respective subtraction of currents. k. Summary of  $K_{ATP}$  conductance l. Summary of the resting membrane potential measured after ATP washout. All data presented as mean  $\pm$  SE. Data analyzed by unpaired t-test, \* $p < 0.05$ , \*\* $p < 0.01$ , \*\*\* $p < 0.001$ , \*\*\*\* $p < 0.0001$

To exclude the compensatory influence of other tissues, an *ex vivo* glucose-stimulated insulin secretion was performed with isolated islets to detect its capacity for insulin secretion. Pancreatic islets from *Srr<sup>ins1cre</sup>* mice showed a similar response to insulin secretion to high glucose stimulation compared to *Srr fl/fl* mice. However, interestingly, under 2.8 mM low-glucose condition, a higher level of insulin was detected in isolated pancreatic islets from *Srr<sup>ins1cre</sup>* mice compared to *Srr fl/fl* mice (**Fig. 11a**). These data indicate that unlike the effects of exogenous D-serine administration or the impact of D-serine on insulin secretion via the CNS, loss of SRR and thereby endogenous D-serine production did not have this effect but modulated basal insulin secretion under low glucose levels.

An increased ratio of ATP to ADP is the initial stage of inducing insulin secretion in beta cells. Therefore, to explore how SRR promotes basal insulin secretion in pancreatic beta cells, the cellular respiration experiment was performed with isolated pancreatic islets under the 2.8 mM low glucose condition measuring oxygen consumption rates (OCRs). The proportion of basal respiration that is used to drive ATP synthesis can be estimated by adding ATP synthase inhibitor Oligomycin. An enhanced ATP production, a higher coupling efficiency (ATP production Rate/basal respiration rate \*100), and spare respiratory capacity were observed in isolated pancreatic islets from *Srr<sup>ins1cre</sup>* mice compared to control

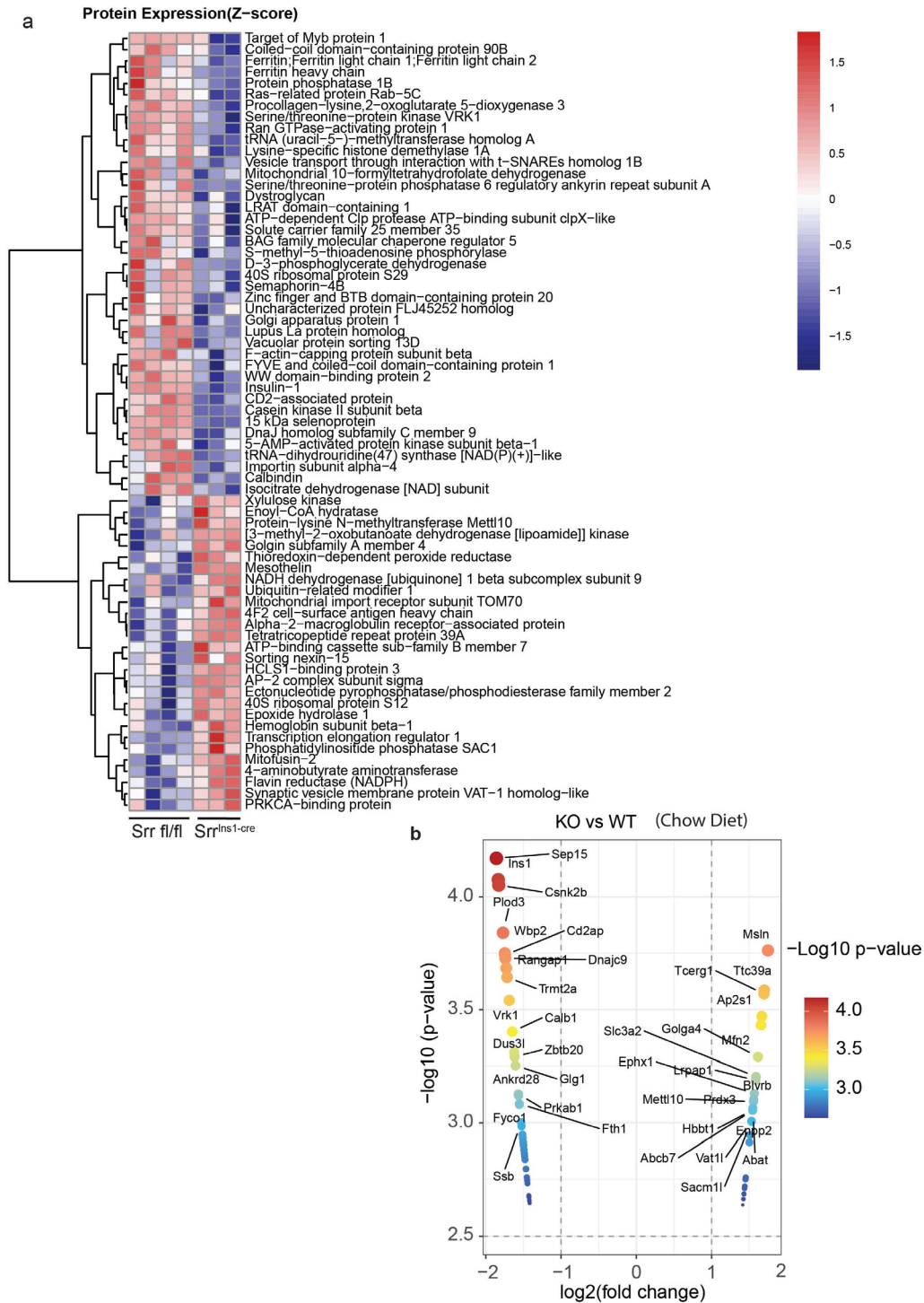
## Results

mice under 2.8 mM low glucose condition (**Fig. 11b-d**). Islets from  $Srr^{ins1cre}$  mice showed normal basal respiration but a lower proton leak under low glucose conditions compared to control mice (**Fig. 11e, f**). Further, the maximum respiratory capacity for mitochondrial substrate oxidation was checked by adding CCCP. However, no difference in maximal respiration was detected between islets of  $Srr^{ins1cre}$  mice and  $Srr$  fl/fl mice (**Fig. 11g**). This finding indicates that the higher ATP production of the islets was not primarily caused by changes in mitochondrial content, cristae density or substrate transport. In addition, an increase in the spare respiratory capacity of pancreatic islets from  $Srr^{ins1cre}$  mice compared to  $Srr$  fl/fl was observed, which indicated a stronger reserve capacity to handle mitochondrial stress (**Fig. 11h**).

Closure of  $K_{ATP}$  channels causing membrane depolarization is one of the key stages regulating the secretion of insulin from pancreatic beta cells after an increased ratio of ATP to ADP. Therefore, an electrical physiological assay in isolated pancreatic islets was applied to detect membrane depolarization. The  $K_{ATP}$  channel conductance was significantly lower, and the membrane potential were found to be greater in isolated islets of  $Srr^{ins1cre}$  mice compared to  $Srr$  fl/fl. (**Fig. 11i-l**). These data reveal an increased membrane potential under the low glucose condition, which is a potential consequence of increased mitochondrial ATP production.

# Results

## 3.3 Mitochondria function related ABC transporters, glycine-serine metabolism and amino acid metabolic process in islets were most affected after the loss of SRR in pancreatic islets observed in proteomics



# Results

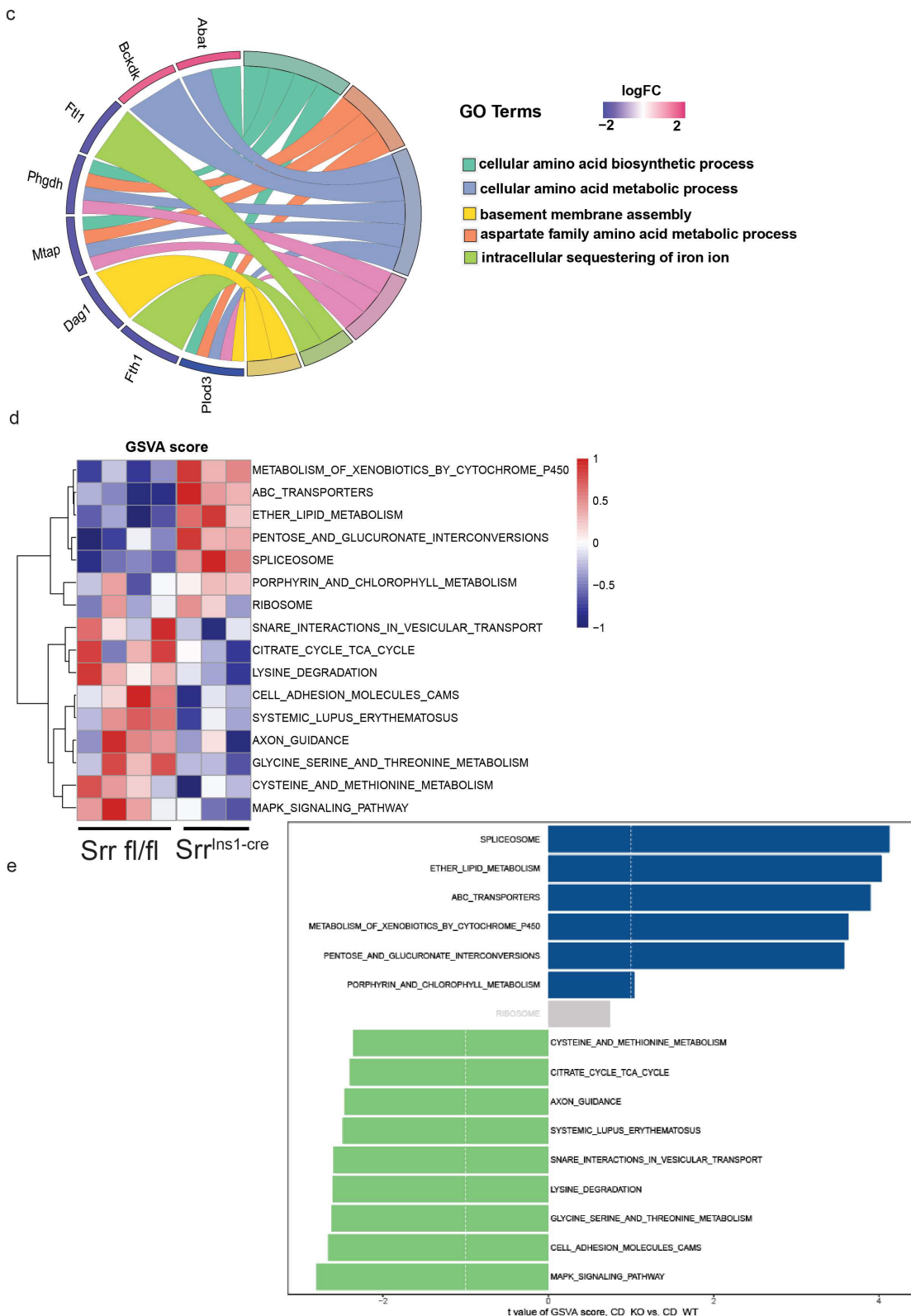


**Figure 12. Proteomics analysis of isolated pancreatic islets of *Srr<sup>ins1cre</sup>* under chow diet.** Heatmap (a, z-score) and volcano plot (b,  $\log_2$ -fold-change threshold  $\geq 0.5$  and  $p < 0.001$ ) of significantly up-regulated and down-regulated proteins in isolated pancreatic islets from *Srr<sup>ins1cre</sup>*

## Results

(KO) relative to *Srr fl/fl* (WT). c. Chord plots demonstrating most enriched GO terms with up-regulated and down-regulated proteins in isolated pancreatic islets from *Srr<sup>Ins1<sup>cre</sup></sup>* (KO) relative to *Srr fl/fl* (WT). LogFC: log 2 (fold changes). d-e. GSEA analysis: Heatmap (d) and bar plot (e). Differential distribution of signal pathway enrichment between the high risk-score (blue) and low risk-score (green) groups in isolated pancreatic islets. *Srr fl/fl* n=4, *Srr<sup>Ins1<sup>cre</sup></sup>* n=3; 17 weeks old.

To test the effect of loss of SRR in pancreatic islets on protein levels, the changes in the proteome of pancreatic islets from *Srr<sup>Ins1<sup>cre</sup></sup>* and *Srr fl/fl* mice fed with chow-diet was characterized. 4,410 proteins were identified in total. In a stringently filtered dataset of 2,559 proteins quantified at least once in two or more biological replicates, 69 of the proteins were differentially regulated in response to the loss of SRR within pancreatic islets (student's *t*-test,  $p < 0.05$ ). In addition, 28 proteins were upregulated and 41 proteins were downregulated in *Srr<sup>Ins1<sup>cre</sup></sup>* mice relative to controls. In addition, Insulin protein was found significantly downregulated in *Srr<sup>Ins1<sup>cre</sup></sup>* mice compared to the control (**Fig. 12a and b**). Proteins that underwent the greatest changes were Gene Ontology (GO)-annotated and were involved in cellular amino acid biosynthetic and metabolic processes. In addition, phosphoglycerate dehydrogenase (PHGDH), the key metabolic enzyme that catalyzes the rate-limiting step of the serine biosynthesis pathway, was downregulated in *Srr<sup>Ins1<sup>cre</sup></sup>* mice (**Fig. 12c**). Moreover, the gene set variation analysis (GSEA) showed ether lipid metabolism and ATP binding cassette (ABC) transporters pathway were enhanced in *Srr<sup>Ins1<sup>cre</sup></sup>* mice. Lysine degradation and glycine serine and threonine metabolic pathways were downregulated in *Srr<sup>Ins1<sup>cre</sup></sup>* (**Fig. 12d, e**).

# Results

## 3.4 $Srr^{Ins1cre}$ mice showed insulin resistance, glucose intolerance and an impaired islets architecture under HFD.

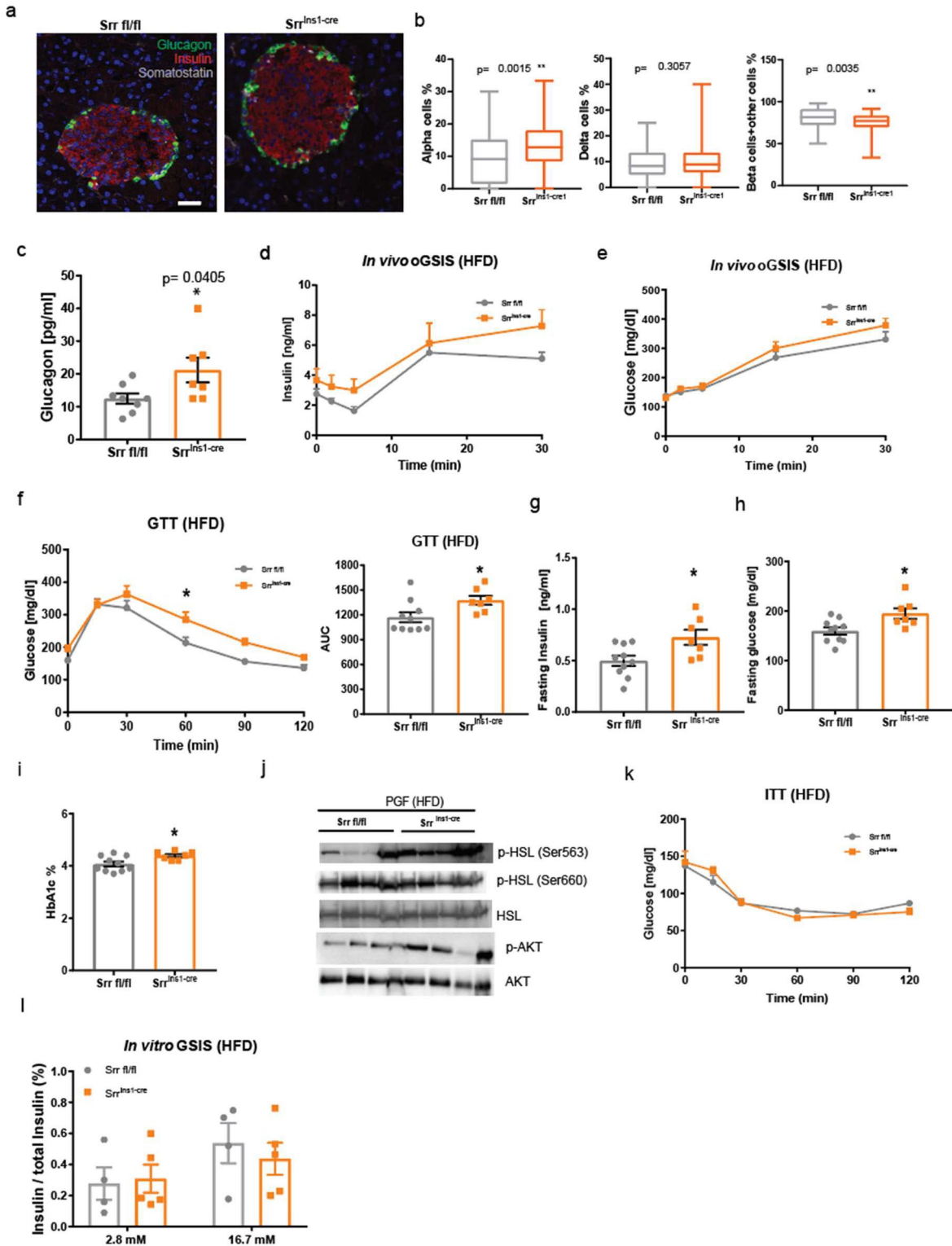


Figure 13.  $Srr^{Ins1cre}$  mice under HFD showed insulin resistance and impaired glucose tolerance with impaired islets architecture under HFD.

## Results

a. Architecture of high fat diet pancreatic islets by immunofluorescence staining of glucagon (green, alpha cells), insulin (red, beta cells) and somatostatin (grey, delta cells). Scale bar, 75  $\mu$ m. b. Quantification of the number of alpha, delta, beta plus other cells in islets. 65 islets from three biological replicates of *Srr fl/fl* mice, 80 islets from four biological replicates of *Srr<sup>ins1cre</sup>* mice fed HFD for 11 weeks. c. Glucagon level in serum before sac, *Srr fl/fl* n=8, *Srr<sup>ins1cre</sup>* n=8, fed HFD for 11 weeks. d-e, Insulin levels (d) and glucose levels (e) in oral gavage glucose-stimulated insulin secretion test (oGSIS), on 8 weeks of HFD treatment. f. Glucose levels in glucose tolerance test (GTT) (left) and area under the curve of GTT (right), on 10 weeks of HFD treatment. g. Fasting insulin levels. h. Fasting glucose levels. i. HbA1c% levels on 11 weeks of HFD treatment. d-h *Srr fl/fl* n=10, *Srr<sup>ins1cre</sup>* n=7. j. Representative western blot images for p-HSL (Ser563), p-HSL (Ser660), HSL, p-AKT and AKT in perigonadal adipose tissue (PGF) from *Srr fl/fl* and *Srr<sup>ins1cre</sup>* mice fed HFD mice for 11 weeks. k. Glucose levels in insulin tolerance test. l. ex vivo glucose stimulated insulin secretion (GSIS) in isolated islets from four *Srr<sup>ins1cre</sup>* mice and five *Srr fl/fl* mice fed HFD for 11 weeks. All data presented as mean $\pm$ SE. b,c,g and h were analyzed by unpaired t-test, d,e,f and j were analyzed by two-way ANOVA, \* $p < 0.05$ , \*\* $p < 0.01$ , \*\*\* $p < 0.001$ , \*\*\*\* $p < 0.0001$ .

The mass of pancreatic beta cells in C57BL6J mice expands and basal insulin secretion increases upon HFD feeding. Moreover, insulin is more potent in suppressing lipolysis than inducing glucose uptake. Thus, *Srr<sup>Ins1cre</sup>* mice was challenged with HFD to investigate the effects of slightly increased basal insulin secretion on body weight gain. Consistent with the finding observed under chow diet, loss of SRR in pancreatic beta cells impaired the architecture of pancreatic islets under HFD as well (**Fig. 13a**). There were more glucagon-positive cells, alpha cells, in pancreatic islets in *Srr<sup>ins1cre</sup>* mice compared to *Srr fl/fl* mice but similar numbers of delta cells and a relatively lower number of beta cells plus other cells in *Srr<sup>ins1cre</sup>* mice (**Fig. 13b**). Correspondingly, greater glucagon levels were recorded in *Srr<sup>ins1cre</sup>* mice compared to control mice (**Fig. 13c**). In line with chow diet treatment, *Srr<sup>ins1cre</sup>* mice exhibited normal responses to oral gavage glucose stimulation recording insulin secretion but the improvement in glucose tolerance effect at 15 min and 30 min time points from CD (oGSIS, **Fig. 10h**) was blunted after HFD treatment (**Fig. 13d, e**). An impaired glucose tolerance was also observed in *Srr<sup>ins1cre</sup>* mice compared to controls (**Fig. 13f**). A significant fasting hyperinsulinemia (**Fig. 13g**), fasting hyperglycemia (**Fig. 13h**), as well as a higher level of HbA1c% (**Fig. 13i**) were observed in *Srr<sup>Ins1cre</sup>* mice compared to control mice under HFD. Due to the impaired insulin action, insulin resistance

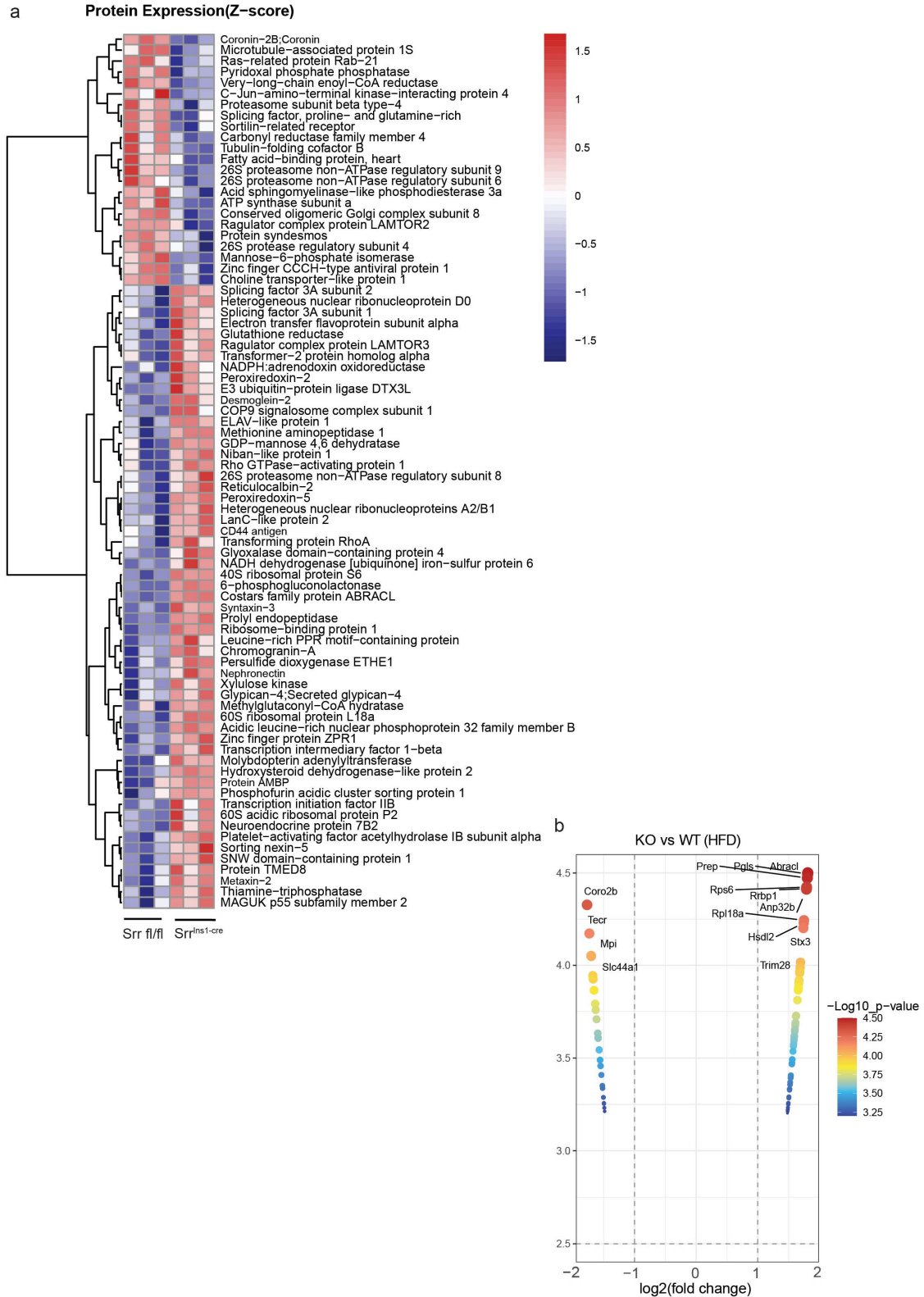
## Results

drives higher lipolysis activity (Morigny et al., 2016). HSL phosphorylation was enhanced at activation sites serine 563 and 660 residues, in perigonadal adipose tissue (PGF) from  $Srr^{ins1cre}$  mice compared to that from control in western blots. Further, AKT phosphorylation was increased in PGF from KO compared to control (**Fig. 13j**). However, no significant differences were observed between  $Srr^{ins1cre}$  mice and control mice in insulin tolerance tests under HFD (**Fig. 13k**). In summary, lipolysis was enhanced, and AKT phosphorylation was increased in PGF of  $Srr^{ins1cre}$  mice compared to SRR fl/fl. Next, the function of isolated pancreatic islets from the mice under HFD was detected. Interestingly, the effect of enhanced basal insulin secretion in  $Srr^{ins1cre}$  mice fed with HFD was not observed during the *ex vivo* glucose-stimulated insulin secretion test with isolated islets. And pancreatic islets from  $Srr^{ins1cre}$  mice showed a similar response to insulin secretion to high glucose stimulation compared to  $Srr$  fl/fl mice (**Fig. 13l**).

These data suggest that loss of SRR in pancreatic beta cells resulted in insulin resistance, and impaired systemic glucose homeostasis under HFD.

# Results

## 3.5 Proteomic analysis of islet indicates an upregulation in PPAR signaling and the biosynthesis of unsaturated fatty acids pathway.



# Results

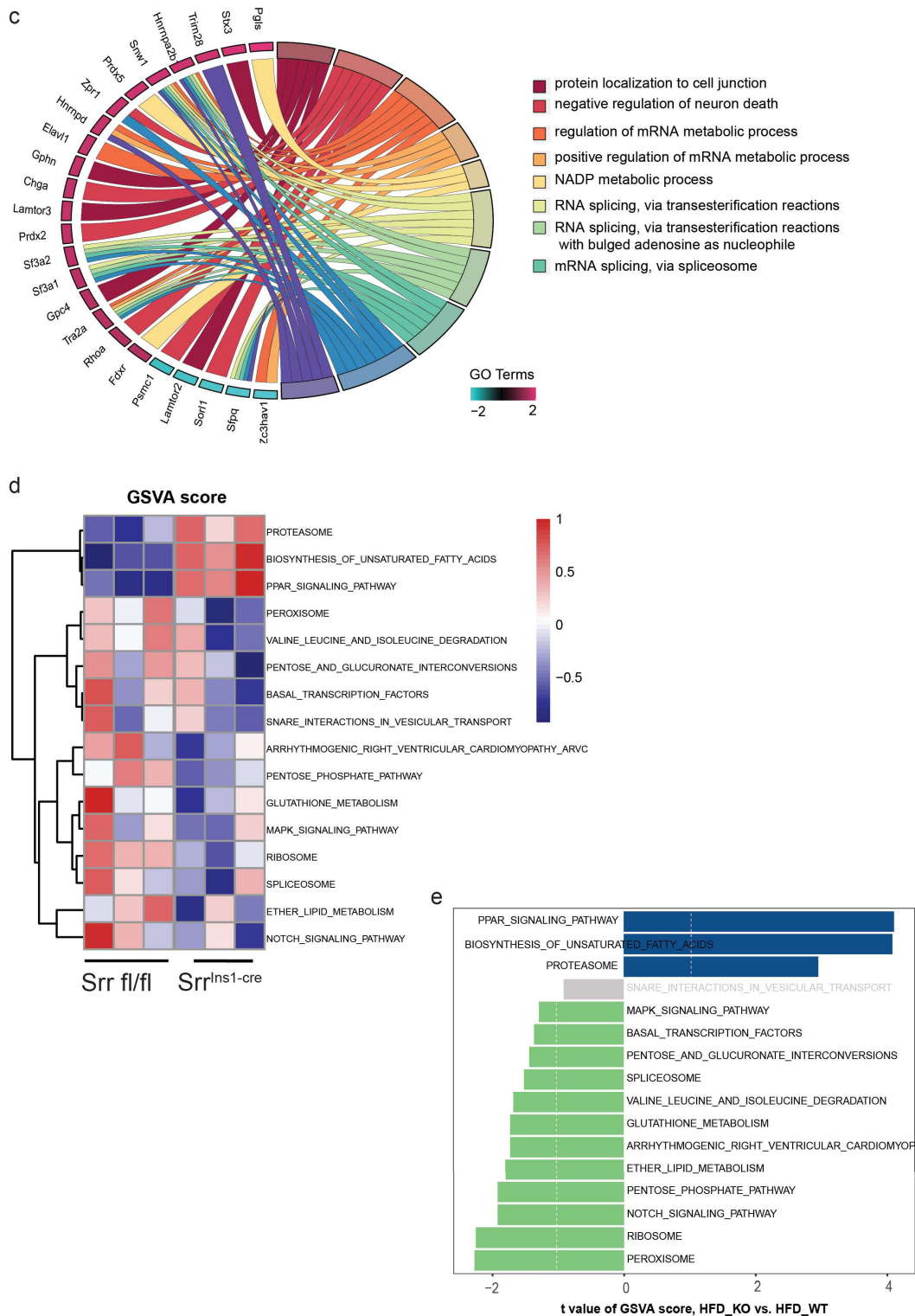


**Figure 14. Proteomics analysis of pancreatic islets from *Srr<sup>ins1-cre</sup>* under HFD**

Heatmap (a, z-score) and volcano plot (b,  $\log_2$ -fold-change threshold  $\geq 0.5$  and  $p < 0.001$ ) of significantly up-regulated and down-regulated proteins in isolated pancreatic islets from *Srr<sup>ins1-cre</sup>* (KO) relative to *Srr fl/fl* (WT). c. Chord plots demonstrating most enriched GO terms with up-regulated and down-regulated proteins in isolated pancreatic islets from *Srr<sup>ins1-cre</sup>* (KO) relative to *Srr fl/fl* (WT). LogFC:  $\log_2$  (foldchanges). d-e. GSVA analysis: Heatmap (d) and bar plot (e).

## Results

*Differential distribution of signal pathway enrichment between the high risk-score (blue) and low risk-score (green) groups in isolated pancreatic islets. n=3, fed HFD for 11 weeks.*

To further explore the effect of loss of SRR in pancreatic islets on protein levels under the HFD challenge, the changes in the pancreatic islet proteome from HFD-fed *Srr<sup>ins1cre</sup>* mice and *Srr fl/fl* mice were characterized. 4,410 proteins were identified in total. In a stringently filtered dataset of 2,321 proteins quantified at least once in two or more biological replicates of one time point, and 84 of the proteins were differentially regulated in response to the loss of SRR in pancreatic islets (student's *t*-test,  $p < 0.05$ ). In addition, 25 proteins were upregulated and 59 proteins were downregulated in *Srr<sup>ins1cre</sup>* mice relative to controls (**Fig. 14a, b**). Of the changed proteins, the top proteins were Gene Ontology (GO)-annotated as involved in protein localization to cell junction, mRNA metabolic process and NADP metabolic processes (**Fig. 14c**). Moreover, the gene set variation analysis (GSVA) showed PPAR signaling pathway activities and biosynthesis of unsaturated fatty acids were dramatically upregulated in *Srr<sup>ins1cre</sup>* mice. MAPK signaling pathway and the pentose and glucuronate interconversions pathway activities were downregulated in *Srr<sup>ins1cre</sup>* mice (**Fig. 14d, e**).

# Results

## 3.6 $Srr^{Ins1cre}$ mice show greater fat mass gain and reduced energy expenditure under HFD.

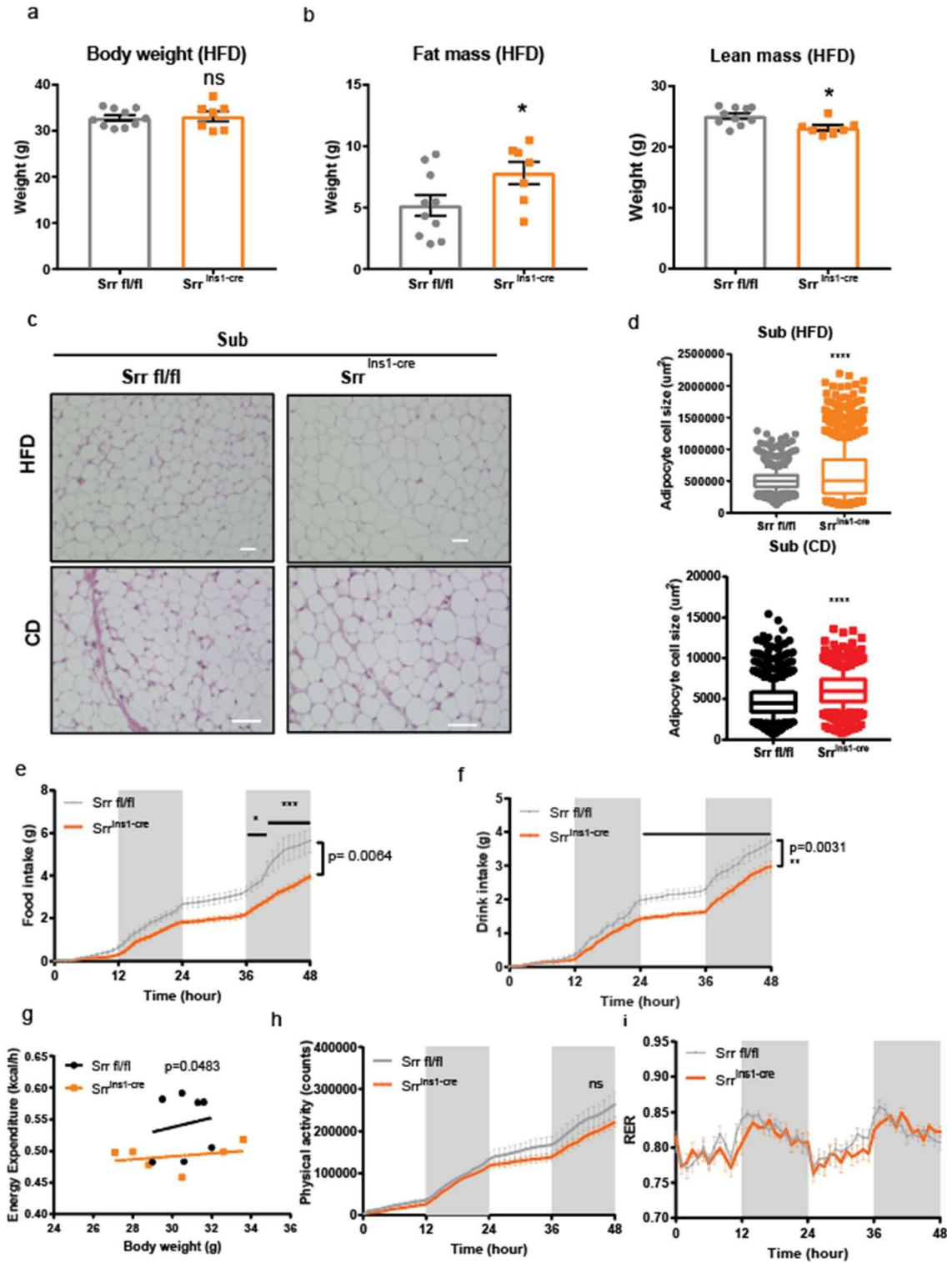


Figure 15.  $Srr^{Ins1cre}$  mice showed gain higher fat mass and reduced energy expenditure under HFD.

## Results

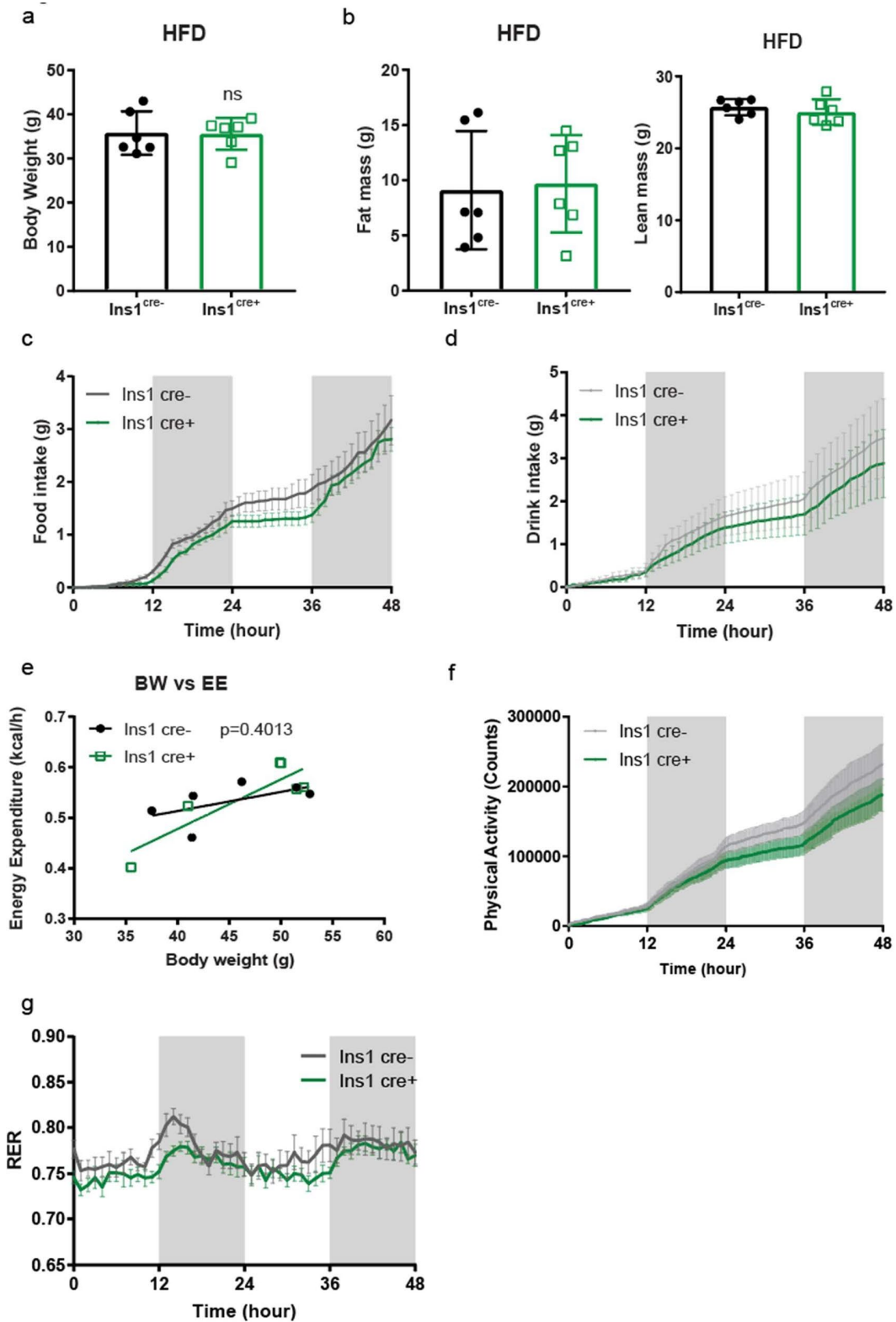
a. Body mass (g) b. Body composition (g). a-b. *Srr fl/fl* n=10, *Srr<sup>ins1cre</sup>* n=7, mice fed HFD for 11 weeks. c. Representative H&E staining of subcutaneous white adipose tissue (Sub) from HFD and CD. Scale bar, 50  $\mu$ m. d. Cell size quantification in Sub. Sub (HFD): *Srr fl/fl* n=4, *Srr<sup>ins1cre</sup>* n=3, fed HFD for 11 weeks. Sub (CD): *Srr fl/fl* n=4, *Srr<sup>ins1cre</sup>* n=5; 17 weeks old. e-i Metabolic parameter measurement by TSE metabolic cages. *Srr fl/fl* n=7, *Srr<sup>ins1cre</sup>* n=6, mice fed HFD for 8 weeks. e. Cumulative food intake (g) f. Cumulative drink intake (g) g. Body weight (g) correlated to total energy expenditure (kcal/h) h. Cumulative physical activity (counts). i. Respiratory exchange rate (RER). a,b and d were analyzed by unpaired t-test, e, f, h and i were analyzed by two-way ANOVA, g analyzed by GLM One way ANCOVA, \*p<0.05, \*\*p<0.01, \*\*\*p<0.001, \*\*\*\*p<0.0001.

Lipolysis in white adipose tissue shows negative correlation with fasting insulin levels. Corresponding with greater fasting hyperinsulinemia, a greater fat mass gain and normal body mass in *Srr<sup>ins1cre</sup>* mice was observed compared to *Srr fl/fl* mice (**Fig. 15a, b**). Further, the adipocyte size in subcutaneous white adipose tissue of *Srr<sup>ins1cre</sup>* mice was bigger compared to *Srr fl/fl* mice under both HFD and CD (**Fig. 15c, d**). Moreover, the mice were put into metabolic cages to measure indirect respiration and their basic metabolic behavior. Surprisingly, *Srr<sup>ins1cre</sup>* mice displayed a greater reduction in food intake and drink intake (**Fig. 15e, f**). Additionally, reduced energy expenditure was observed in *Srr<sup>ins1cre</sup>* mice under HFD (**Fig.15g**). However, accumulative physical activity and respiratory exchange ratio (RER) were unaltered between genotypes (**Fig. 15h, i**).

Based on the data observed above, it indicates that loss of SRR in the pancreatic beta cell causes greater fat gain and reduced energy expenditure.

# Results

## 3.7 Ins1 cre mice does not show greater fat mass gain and reduced energy expenditure under HFD.



## Results

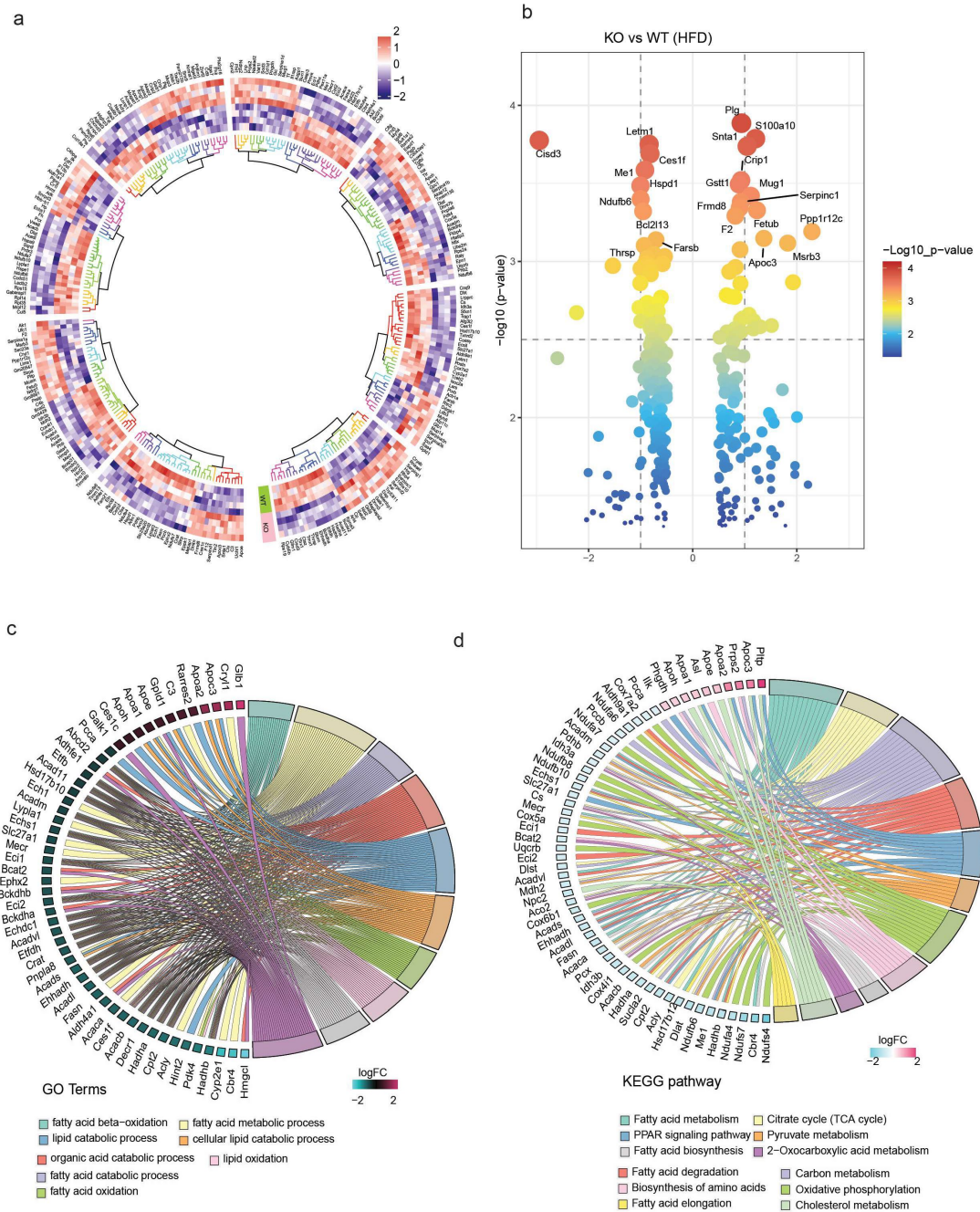
**Figure 16. *Srr<sup>Ins1cre</sup>* mice showed gain higher fat mass and reduced energy expenditure under HFD.**

a. Body mass (g). b. Body composition (g). c-g. Metabolic parameter measurement by TSE metabolic cages. c. Cumulative food intake (g) d. Cumulative drink intake (g) e. Body weight (g) correlated to total energy expenditure (kcal/h) f. Cumulative physical activity (counts). g. Respiratory exchange rate (RER). *Ins1 cre-* n=6, *Ins1 cre+* n=6, mice fed HFD for 17 weeks. All data presented as mean±SE. a-b were analyzed by unpaired t-test, c, d, f and g were analyzed by two-way ANOVA, e was analyzed by GLM One-way ANCOVA, \*p<0.05, \*\*p<0.01, \*\*\*p<0.001, \*\*\*\*p<0.0001.

To further validate effects observed above are caused by loss of SRR, the *Ins1-cre* mouse line fed with HFD was performed as control. As expected, *Ins1-cre* positive mice and *Ins1-cre* negative mice gained similar body weight and body composition under HFD (**Fig. 16a, b**). No significant difference was observed in food intake, drink intake, energy expenditure, accumulative physical activity, or RER between the *Ins1-cre* positive and negative groups (**Fig. 16c-g**). Therefore, the metabolic effects observed from *Srr<sup>Ins1cre</sup>* are not caused by the Cre-recombinase insertion in *Ins1* gene but by the loss of serine racemase in pancreatic beta cells.

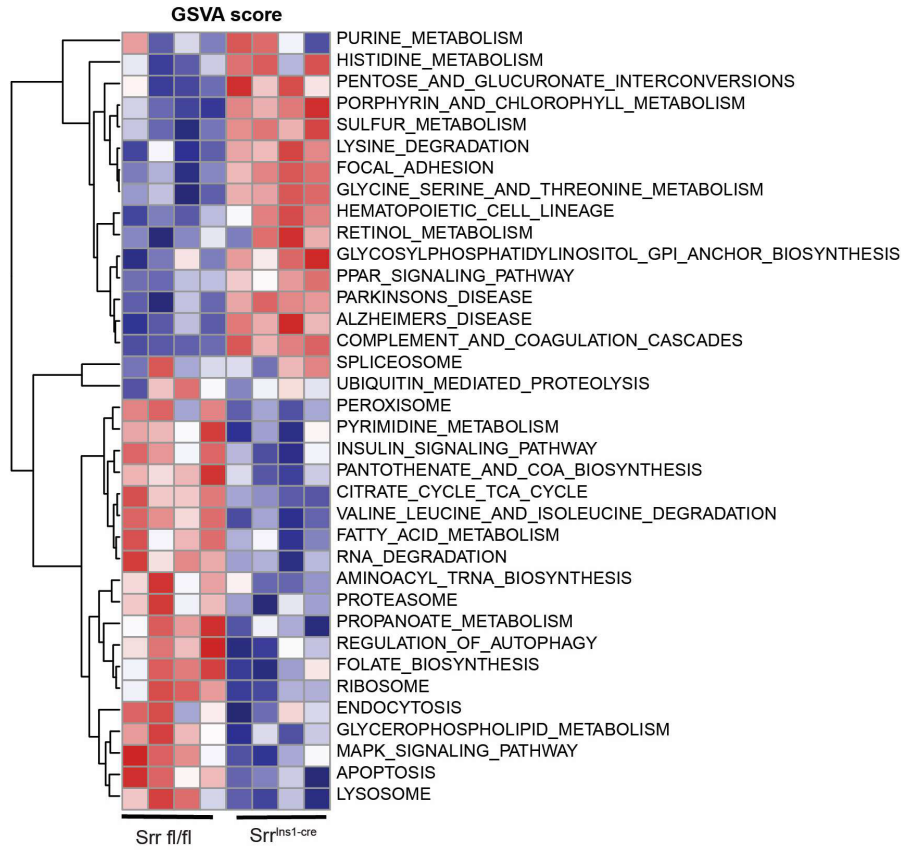
# Results

## 3.8 Proteomic analysis of subcutaneous adipose tissue from *Srr<sup>Ins1cre</sup>* under HFD indicates a downregulation in fatty acid metabolism and insulin signaling.

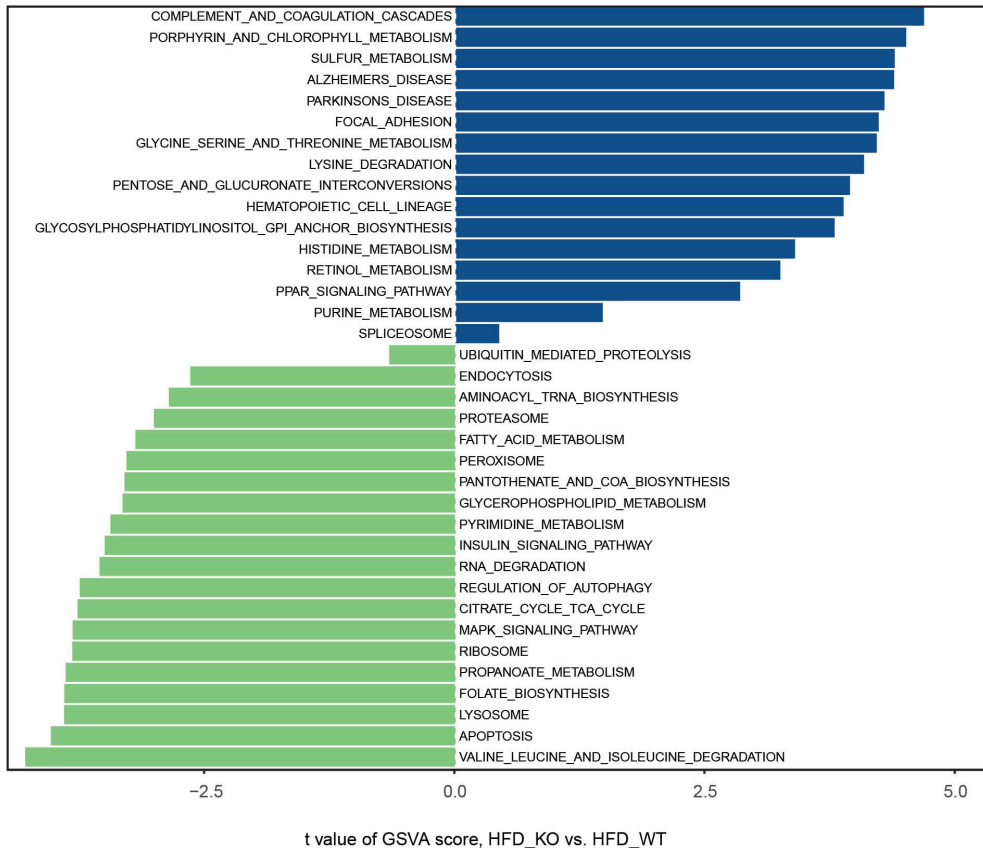


# Results

e



f



## Results

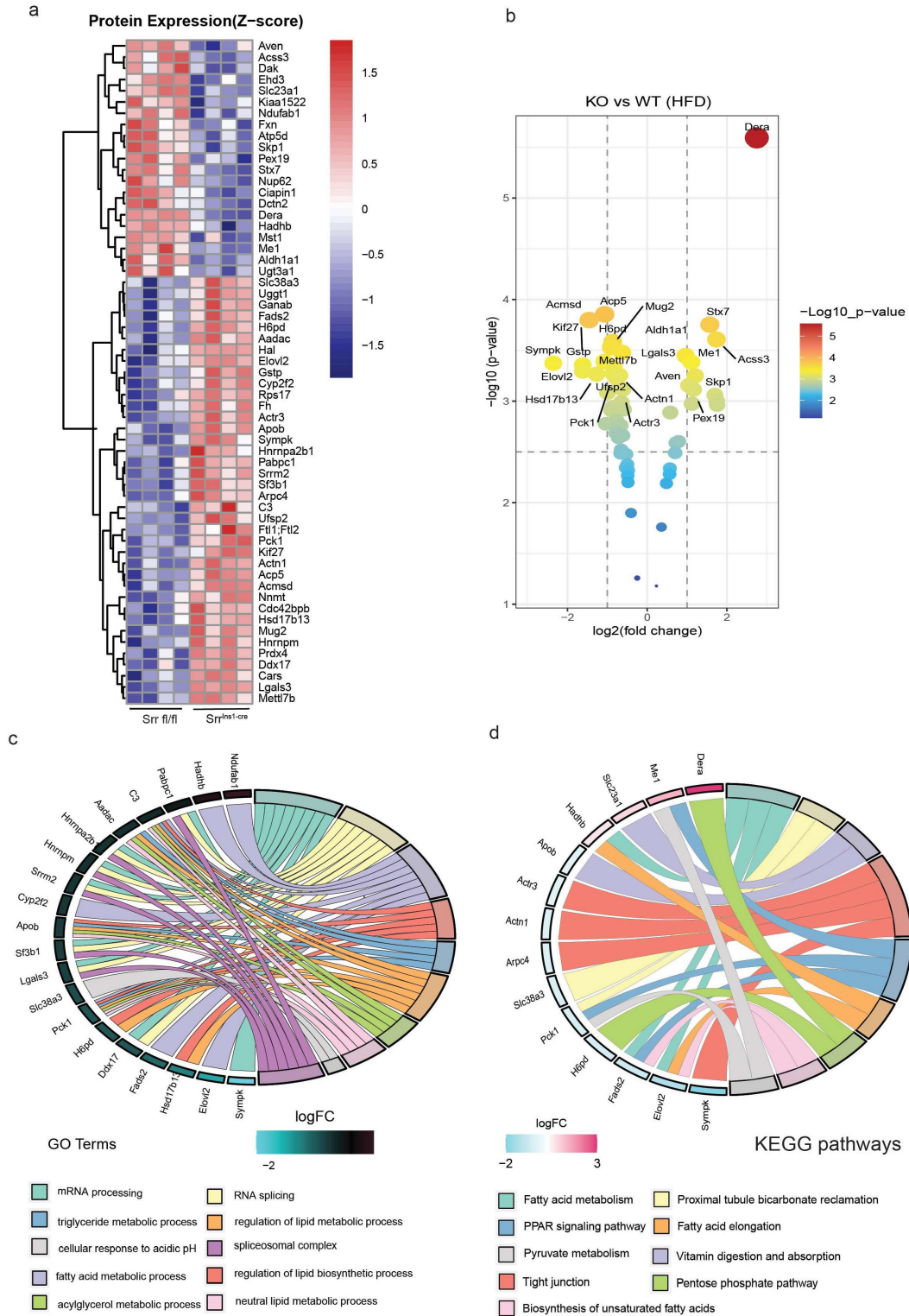
### **Figure 17. Proteomics analysis of subcutaneous white adipose tissue from $Srr^{ins1cre}$ under HFD**

Heatmap (a, z-score) and volcano plot (b,  $\log_2$ -fold-change threshold  $\geq 0.5$  and  $p < 0.001$ ) of significantly up-regulated and down-regulated proteins in subcutaneous white adipose tissue from  $Srr^{ins1cre}$  (KO) relative to  $Srr^{fl/fl}$  (WT). c. Chord plots demonstrating most enriched GO terms with up-regulated and down-regulated proteins in subcutaneous white adipose tissue from  $Srr^{ins1cre}$  (KO) relative to  $Srr^{fl/fl}$  (WT). LogFC:  $\log_2$  (foldchanges). d. Chord plots demonstrating most enriched KEGG pathways with up-regulated and down-regulated proteins in subcutaneous white adipose tissue from  $Srr^{ins1cre}$  (KO) relative to  $Srr^{fl/fl}$  (WT). e-f. GSVA analysis: Heatmap (d) and bar plot (e). Differential distribution of signal pathway enrichment between the high risk-score (blue) and low risk-score (green) groups in subcutaneous white adipose tissue.  $n=3$ , fed HFD for 11 weeks.

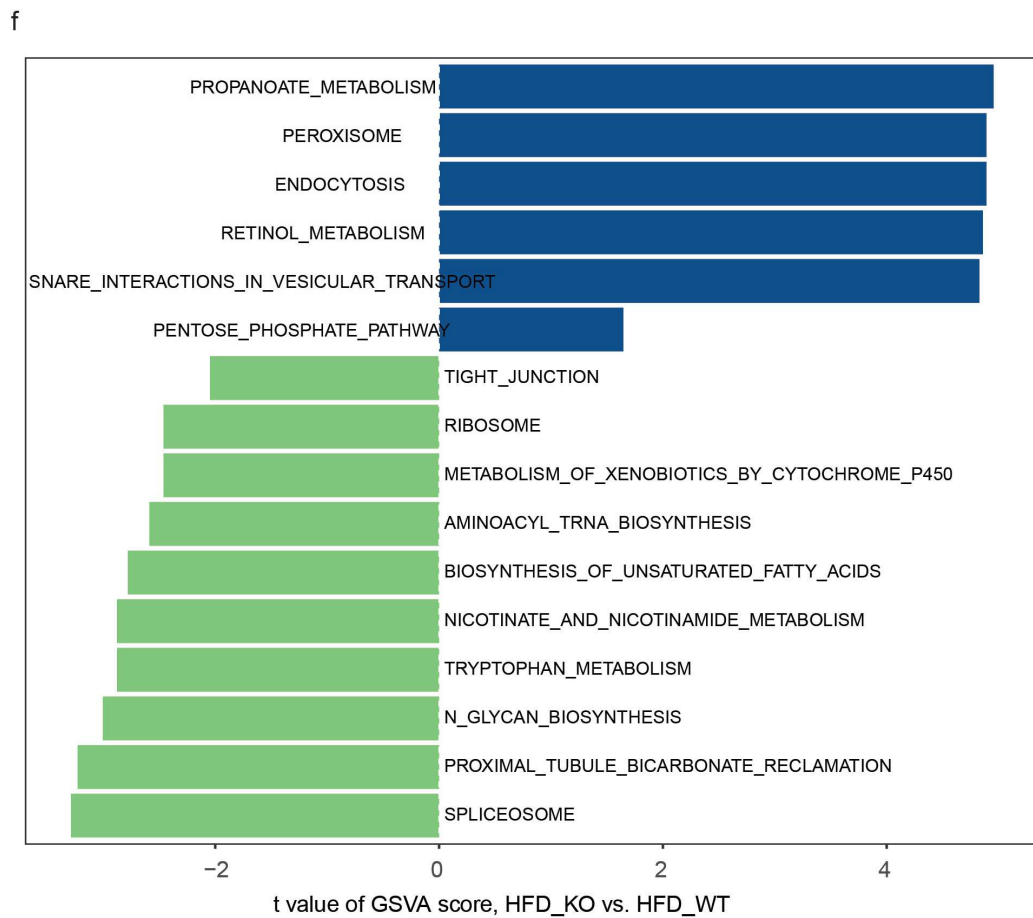
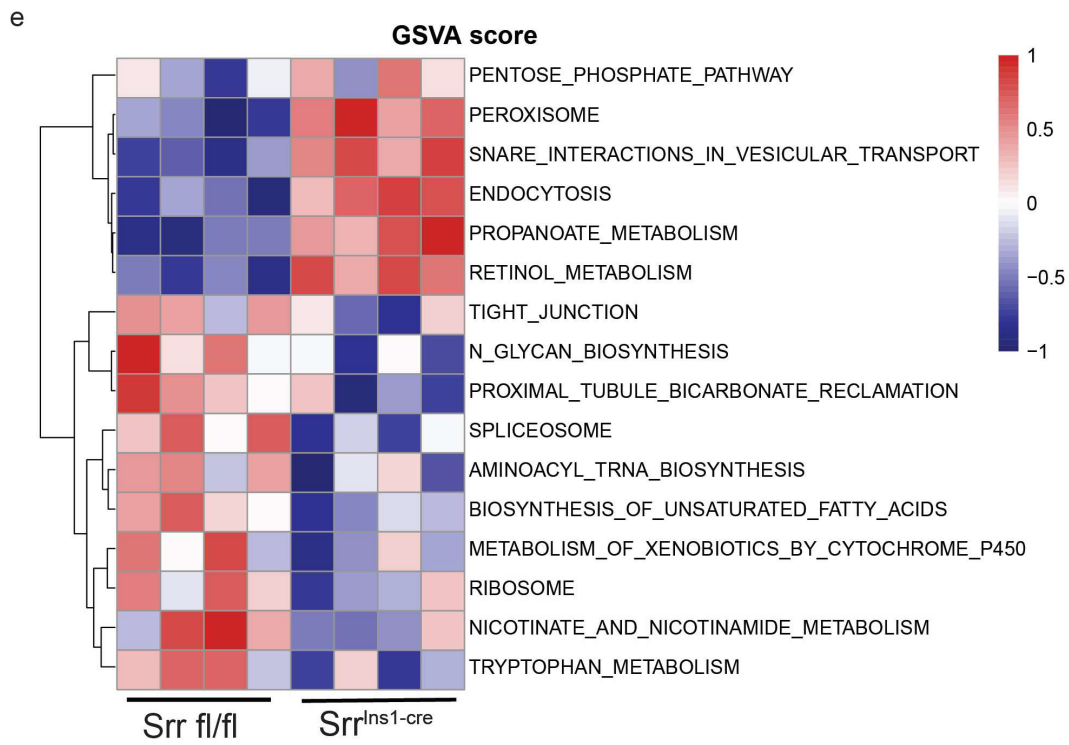
Based on results observed above, we investigated the effects on fat tissue metabolism after the loss of SRR in the pancreatic beta cell. To answer this question, the changes in the subcutaneous white adipose tissue (Sub WAT) proteome from HFD  $Srr^{ins1cre}$  mice and  $Srr^{fl/fl}$  mice was characterized. 297 proteins were differentially expressed and 135 proteins were upregulated and 162 proteins were downregulated in  $Srr^{ins1cre}$  mice compared to the control mice (**Fig. 17a, b**). Of the changed proteins, the top proteins were GO-annotated as involved in fatty acid beta-oxidation, fatty acid metabolic process, lipid catabolic process and lipid catabolic process (**Fig. 17c**). Moreover, KEGG pathway enrichment analysis indicated that the top changed proteins mainly enriched into fatty acid metabolism, citrate cycle, fatty acid degradation, carbon metabolism, and pyruvate metabolism pathways (**Fig. 17d**). The GSVA analysis showed Alzheimer disease pathway and glycine serine and threonine metabolism pathway were upregulated in KO mice. Moreover, endocytosis, fatty acid metabolism, and insulin signaling pathways were downregulated in KO mice (**Fig. 17e, f**).

# Results

## 3.9 Proteomic analysis of liver from *Srr<sup>Ins1cre</sup>* under HFD indicates fatty acid metabolism and pyruvate metabolism was top affected.



# Results



## Results

### **Figure 18. Proteomics analysis of liver from *Srr<sup>ins1cre</sup>* under HFD**

Heatmap (a, z-score) and volcano plot (b, log<sub>2</sub>-fold-change threshold  $\geq 0.5$  and  $p < 0.001$ ) of significantly up-regulated and down-regulated proteins in liver from *Srr<sup>ins1cre</sup>* (KO) relative to *Srr fl/fl* (WT). c. Chord plots demonstrating most enriched GO terms with up-regulated and down-regulated proteins in liver from *Srr<sup>ins1cre</sup>* (KO) relative to *Srr fl/fl* (WT). LogFC: log<sub>2</sub> (foldchanges). d. Chord plots demonstrating most enriched KEGG pathways with up-regulated and down-regulated proteins in liver from *Srr<sup>ins1cre</sup>* (KO) relative to *Srr fl/fl* (WT). e-f. GSEA analysis: Heatmap (d) and bar plot (e). Differential distribution of signal pathway enrichment between the high risk-score (blue) and low risk-score (green) groups in liver.  $n=3$ , fed HFD for 11 weeks.

As the liver is the central organ for fatty acid metabolism. Glycerol coming from lipolysis is a carbon source for gluconeogenesis in the liver. Fatty acids are the substrate for re-esterification within the endoplasmic reticulum to make triacylglycerol that will be secreted as VLDL. In addition, the secretion of VLDL is suppressed by insulin (Alves-Bezerra and Cohen, 2017). Therefore, the changes in liver proteome from HFD *Srr<sup>ins1cre</sup>* mice and *Srr fl/fl* mice was characterized. 59 proteins were differentially expressed and 21 proteins were upregulated and 38 proteins were downregulated in *Srr<sup>ins1cre</sup>* mice compared to the control mice (**Fig. 18a, b**). Of the changed proteins, top proteins were GO-annotated as involved in mRNA processing, RNA splicing, and triglyceride metabolic process (**Fig. 18c**). Moreover, KEGG pathway enrichment analysis indicated that the top changed proteins mainly enriched into fatty acid metabolism, PPAR signalling, fatty acid elongation, and pyruvate metabolism pathways (**Fig. 18d**). The GSEA analysis showed endocytosis pathway was one of top upregulated, and spliceosome pathway were most downregulated in *Srr<sup>ins1cre</sup>* mice (**Fig. 18f, g**).

# Results

## 3.10 Loss of Gpc4 in pancreatic beta cells does not affect body weight and body composition under CD

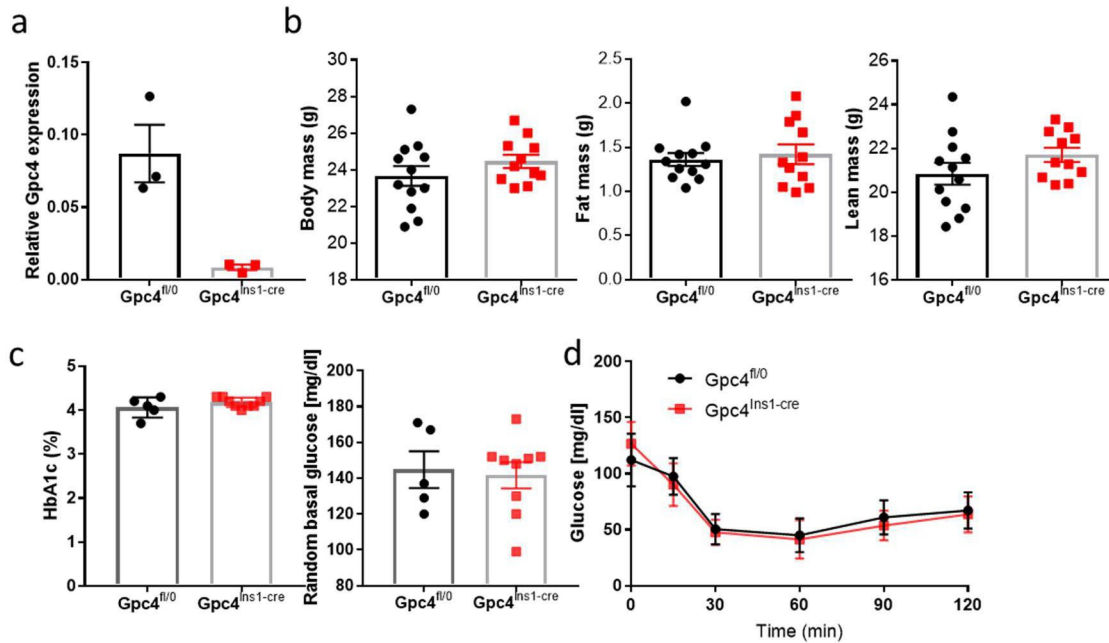


**Figure 19. Genetic deletion of Gpc4 and it does not affect body weight, body composition development and insulin sensitivity under chow diet.**

a. Knockout efficiency of Gpc4 mRNA in mouse pancreatic islets, n= 3 b. Body mass and body composition of 8 weeks old male control and knockout mice, n=11-12 c. HbA1c % and random basal glucose level of 8 weeks old knockout and control, n=5-9 d. Insulin tolerance test 12 weeks old, chow diet, 0.75 IU/kg, n=5-9

Of note, Glypican 4 (Gpc4) was shown to be downregulated in the pancreatic proteome file of  $Srr^{ins1cre}$  mice. Moreover, Gpc4 can interact with insulin receptors to enhance insulin signaling in pre-adipocyte (Ussar et al., 2012). However, the mechanism underlying the modulation of insulin secretion by Gpc4 remains to be elucidated. Furthermore, pancreatic beta cell specific loss of insulin receptor promotes insulin secretion. Therefore, Gpc4 in pancreatic beta cells might contribute to insulin secretion by modulating the interaction with the insulin receptors. Therefore, this thesis further investigates the role of Gpc4 in the regulation of insulin secretion in pancreatic beta cells.

To study the role of Gpc4 in beta cells, we generated Gpc4 beta cell specific knockout mice from the mating of Gpc4 floxed mice and Ins1 cre mice. Glypican 4 was efficiently deleted in Gpc4<sup>Ins1-cre</sup> mice compared to the Gpc4<sup>fl/0</sup> control mice

# Results

shown at the transcriptional level (**Fig. 19a**). Mice lacking Gpc4 in beta cells fed with chow diet exhibited normal body weight and body composition (**Fig. 19b**). To check long term glycemic control of the mice, HbA1c and randomly glucose levels were measured, but no significant differences was observed between two groups (**Fig. 19c**). Gpc4<sup>Ins1-cre</sup> mice exhibited normal insulin sensitivity in an insulin tolerance test (**Fig. 19d**).

## 3.11 Loss of Gpc4 in pancreatic beta cells impairs islets architecture and impairs glucose stimulate insulin secretion *in vivo* but not *in vitro* under CD

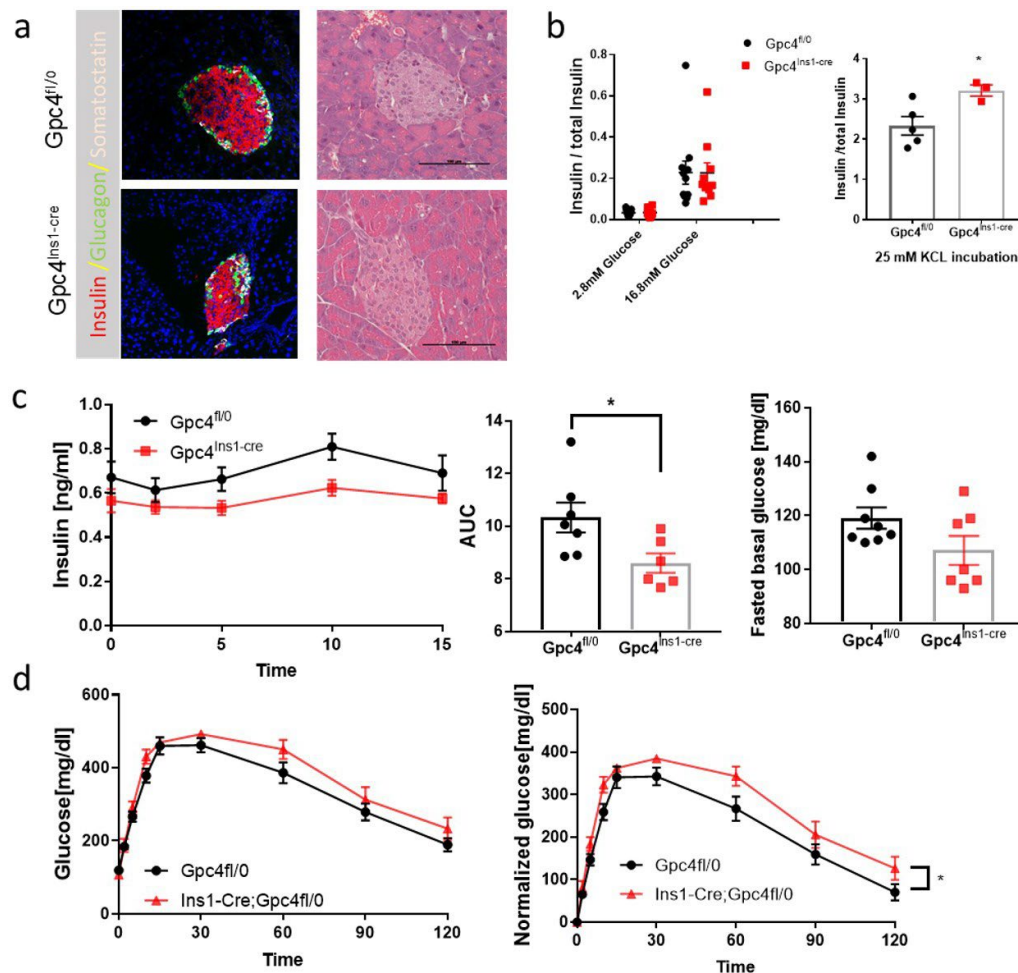


**Figure 20.** Gpc4<sup>Ins1-cre</sup> mice shows impaired islets architecture and less glucose stimulated insulin secretion *in vivo*.

a. Immunofluorescence staining 17 weeks old mice. b. In vitro GSIS, in isolated islets from KO and control mice, n= 10-11, 11 weeks old c. In vivo GSIS of 11 weeks old male control and knockout mice, n=7-9 d. Glucose tolerance test, 11 weeks old, n=7-9.

## Results

Beta cells play an important role in controlling glucose homeostasis via secreting insulin. First, the architecture of pancreatic islets was detected by immunofluorescence staining. The architecture of islets was altered with more delta and alpha cells localized to the middle of islets in *Gpc4<sup>ins1-cre</sup>* mice compared to controls (**Fig. 20a**). Based on the architecture alterations, we hypothesize that the function of pancreatic beta cells is affected as well. To test the hypothesis, first, I performed an *in vitro* GSIS from isolated islets of *Gpc4<sup>ins1-cre</sup>* and control mice. However, islets with specific loss of *Gpc4* in beta cells displayed a similar response to glucose stimulation, but had greater insulin content after 25 mM KCL incubation (unpaired *t-test*,  $p=0.0346$ , **Fig. 20b**). Interestingly, *in vivo*, *Gpc4<sup>ins1-cre</sup>* mice showed significantly less insulin secretion responding to glucose stimulation according to the area under the curve (unpaired *t-test*,  $p=0.0317$ , **Fig. 20c**). With a high dose of glucose stimulation, loss of *Gpc4* in pancreatic beta cells resulted in slightly elevated blood glucose levels as well but not fasted glucose levels (**Fig. 20c and d**). These data suggest that loss of *Gpc4* in beta cells impairs pancreatic islets architecture and insulin secretion. However, this does not appear due to a direct effect on beta cell function as no difference in insulin secretion within isolated islets from knockout and control mice, but it might be because of indirect effects via other cells or tissues.

# Results

## 3.12 *Gpc4*<sup>Ins1cre</sup> mice show greater fat mass gain and insulin resistance under HFD.

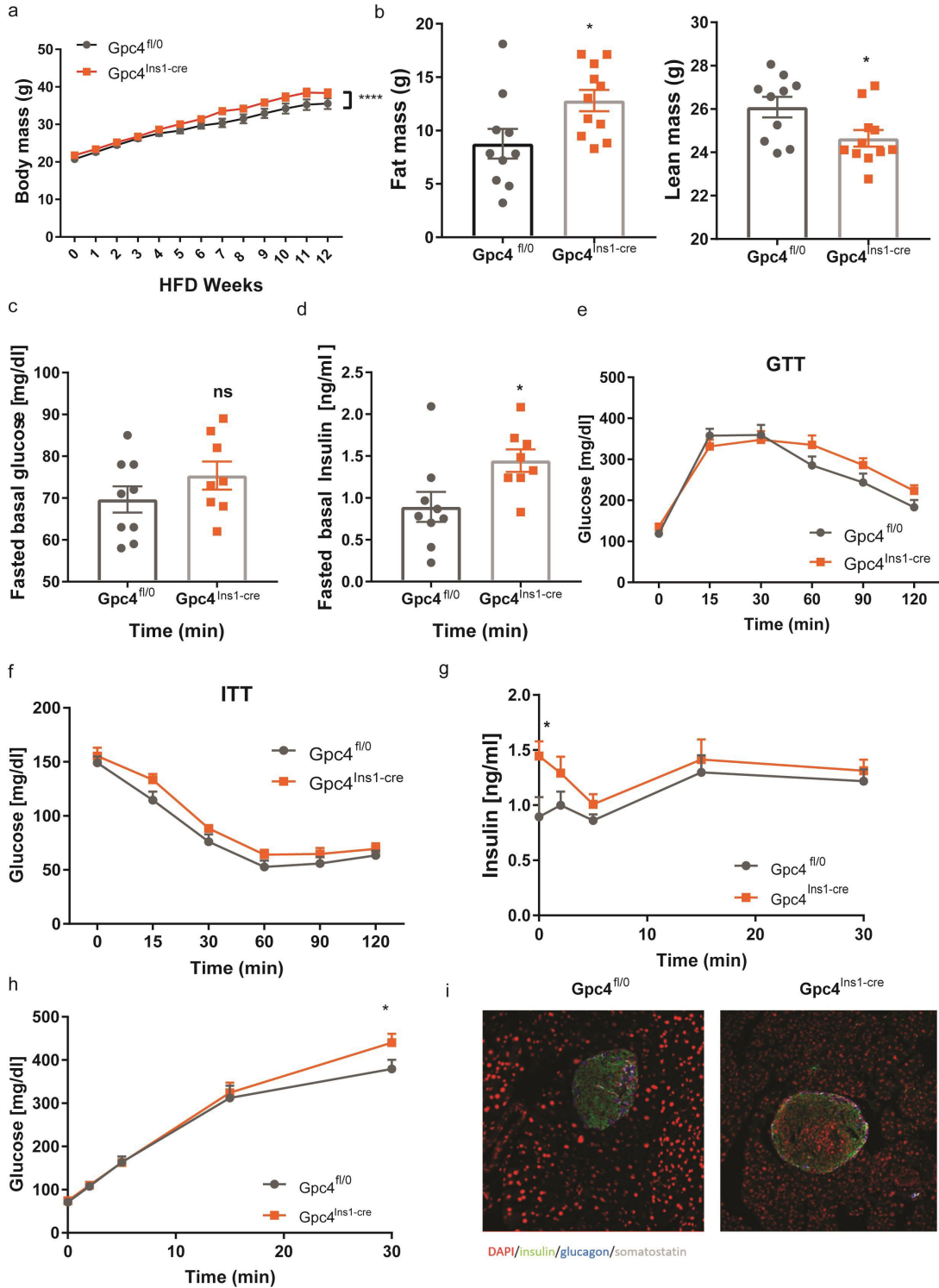


Figure 21. *Gpc4*<sup>Ins1cre</sup> mice has greater fat mass gain and insulin resistance in vivo under HFD.

## Results

*a. Body weight development under HFD. b. Body composition, fed on 12 weeks HFD c. Fasted glucose level. Fed on 9 weeks HFD. d. Fasted insulin level. Fed on 9 weeks. e. Glucose tolerance test. Fed on 8 weeks HFD. f. Insulin tolerance test. Fed on 11 weeks HFD. a-h, n= 10-11. g and h, in vivo GSIS, insulin levels (g) and glucose levels (h). Fed on 9 weeks HFD. i Architecture of pancreatic islets from control mice and Gpc4<sup>Ins1cre</sup> mice. Fed on 12 weeks HFD.*

Further, the effect of Gpc4 in pancreatic beta cells under HFD was explored. The body weight development of Gpc4<sup>Ins1cre</sup> mice and controls was recorded weekly. The body weight of Gpc4<sup>Ins1cre</sup> mice was significantly larger than the controls (two-way ANOVA, Sidak's multiple comparisons test, genotype:  $p < 0.0001$ , **Fig. 21a**). Moreover, the composition of the mice was measured by Echo MRI. Gpc4<sup>Ins1cre</sup> mice had a greater fat mass (unpaired *t-test*,  $p = 0.0274$ ) and had a lower lean mass (unpaired *t-test*,  $p = 0.0276$ ) compared with controls (**Fig. 21b**). Fat depots accumulation excess is the main factor causing insulin resistance. Therefore, the fasted basal glucose and fasted insulin levels were detected. No difference in fasted basal glucose levels was observed between Gpc4<sup>Ins1cre</sup> mice and controls (**Fig. 21c**). However, Gpc4<sup>Ins1cre</sup> mice displayed a greater level of fasted insulin compared to controls (unpaired *t-test*,  $p = 0.0287$ , **Fig. 21d**). These data indicate that Gpc4<sup>Ins1cre</sup> mice are insulin resistance. Mice were further challenged with a 2 g/kg dose of glucose and insulin injection. Surprisingly, Gpc4<sup>Ins1cre</sup> mice exhibited normal glucose tolerance (**Fig. 21e**) and normal insulin sensitivity (**Fig. 21f**). Interestingly, the mice challenged with a high dose of glucose with 3 g/kg showed normal insulin secretion response to glucose stimulation (**Fig. 21g**) but a significantly higher level of glucose at 30 min time point was observed (two-way ANOVA, Sidak's multiple comparisons test, 30 min time point,  $p = 0.0473$ , **Fig. 21h**). The architecture of the pancreatic islets under HFD was visualized by immunofluorescence staining. Interestingly, no great alterations in architecture of pancreatic islets from Gpc4<sup>Ins1cre</sup> mice was observed (**Fig. 21i**).

In summary, loss of Gpc4 in pancreatic beta cells induces greater fat mass gain and insulin resistance under HFD.

# Results

## 3.13 Terc KO mice show greater endocrine homeostasis with reduced telomere length

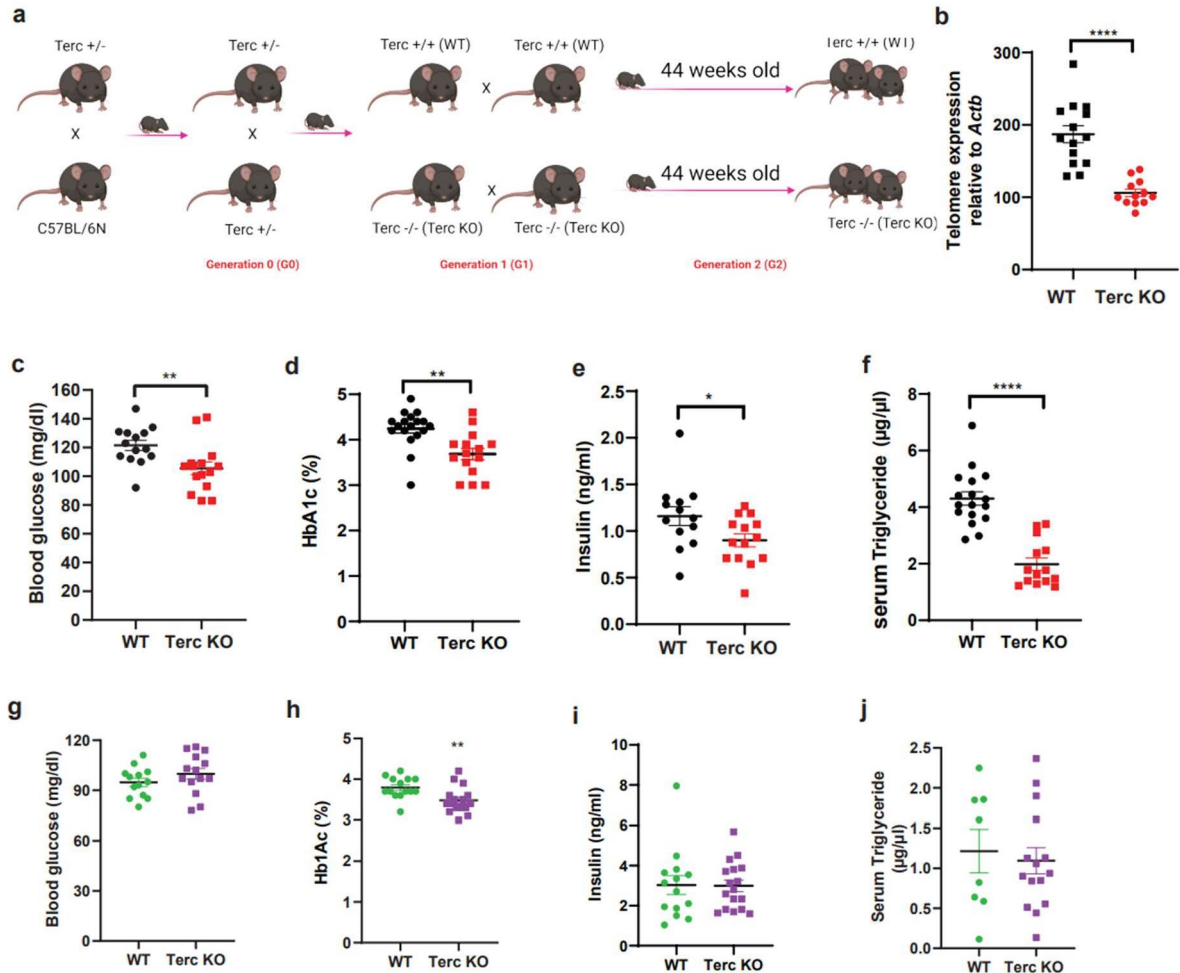


**Figure 22. Telomere shortening and metabolic characterization of *Terc* KO mice.**

*a*. Breeding scheme for second-generation *Terc* KO mice. *b*. Telomere length relative to *Actb* in male enterocytes ( $n=12$  WT,  $n=14$  KO, 14 months old, male). *c-f* male mice: black dots (WT) and red dots (*Terc* KO). *g-j* female mice: green dots (WT) and purple (*Terc* KO). *c* and *g*, Fasting glycemia in 12 months old mice ( $n=12$  WT,  $n=14$  KO). *d* and *h*, Percentage of glycosylated hemoglobin (HbA1c%) in 13 months old mice ( $n=18$  WT,  $n=15$  KO). *e* and *i*, Fasting serum insulin levels in 12 months old mice ( $n=13$  WT,  $n=14$  KO). *f* and *j*, Serum triglyceride levels in 14 months old mice ( $n=17$  WT,  $n=14$  KO). All data are shown as mean  $\pm$  SE. Statistical analysis was performed using an unpaired *t*-test. \* $p<0.05$ , \*\* $p<0.01$ , \*\*\* $p<0.001$ , \*\*\*\* $p<0.0001$ .

Glucose tolerance and insulin sensitivity declines progressively with age, and a high incidence of type 2 diabetes is observed in the elderly population. A feature of aging is the shortening of telomeres. To better understand the alterations in

## Results

insulin and glucose metabolism associated with telomere length in aging, aged (41 weeks- >10 months old) second-generation *Terc*<sup>-/-</sup> inbred mice (*Terc* KO) with telomerase deficiency were used in this study. Wild type (WT) controls are derived from the same breedings of *Terc*<sup>+/-</sup> mice and inbred as a separate cohort in parallel to *Terc*<sup>-/-</sup> (*Terc* KO) mice (**Fig. 22a**). The telomere length of *Terc* KO was significantly shorter than control mice (WT) (unpaired *t*-test,  $p < 0.0001$ ) (**Fig. 22b**). Then the long-term glycemic control of mice was further determined. A significantly lower fasting glycemia (unpaired *t*-test,  $p = 0.0038$ , **Fig. 22c**), glycosylated hemoglobin (HbA1c%) level (unpaired *t*-test,  $p = 0.0012$ , **Fig. 22d**), fasting insulineamia (unpaired *t*-test, **Fig. 22e**) and serum triglyceride levels (unpaired *t*-test,  $p < 0.0001$ ; **Fig. 22f**) in male *Terc* KO was found. In contrast to these, female *Terc* KO mice displayed a reduction in HbA1c% levels relative to controls (unpaired *t*-test,  $p = 0.0074$ ), but not in serum triglycerides and fasting glucose and insulin levels (**Fig. 22g-j**). These data suggested that unlike the typical phenotype of aged mice, moderate telomere shortening in aged mice improved glucose tolerance and insulin sensitivity.

# Results

## 3.14 Terc KO mice display improved glucose and insulin tolerance

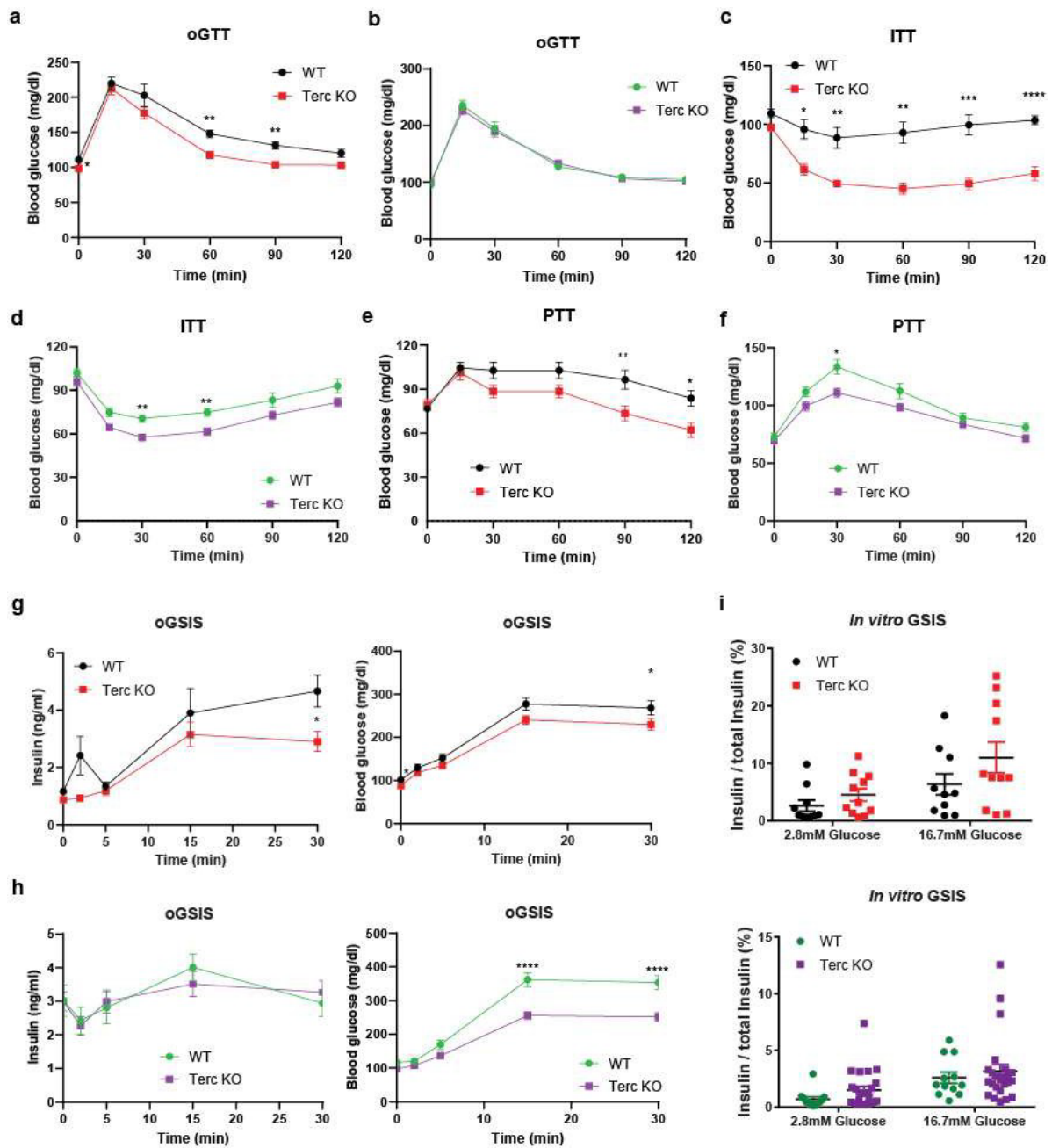


**Figure 23. Terc KO male mice show improved insulin sensitivity and glucose tolerance.**

a and b, Oral gavage glucose tolerance test (oGTT) in 12 months old Terc KO and control mice a. male mice (n=12 WT, n=14 KO) b. female mice (n=14 WT, n=14 KO). c and d, Insulin tolerance test (ITT) in 12 months Terc KO and control mice. c. male mice (n=12 WT, n=12 KO). d. female mice (n=12 WT, n=14 KO). e and f, Pyruvate tolerance test (PTT) in 13 months Terc KO and control mice. e. male mice (n=12 WT, n=11 KO). f. female mice (n=14 WT, n=13 KO). g and h. Serum insulin (left panel) and glucose levels (right panel) during an oral gavage glucose

## Results

*stimulated insulin secretion test (oGSIS) performed in 12 months old Terc KO and control mice. g. male mice (n=12 WT, n=13 KO). h. female mice (n=14 WT, n=17 KO). i. Ex vivo glucose-stimulated insulin secretion test in isolated pancreatic islets from 14 months old Terc KO and control mice. Percentage of secreted insulin compared to total insulin content. Ten islets were used per well. Upper panel shown are 10 technical replicates from five WT male mice and 11 technical replicates from five Terc male mice. Down panel shown are 12 technical replicates from four WT female mice and 24 technical replicates from five Terc KO female mice. Male mice: black dots (WT) and red dots (Terc KO). female mice: green dots (WT) and purple (Terc KO). All data are shown as mean  $\pm$  SE. Statistical analysis was performed using a two-way ANOVA and a Sidak's multiple comparison test; \* $p$ <0.05, \*\* $p$ <0.01, \*\*\* $p$ <0.001, \*\*\*\* $p$ <0.0001*

To further test the hypothesis, an oral gavage glucose tolerance test (oGTT) is performed in 12 months old Terc KO mice. We found that moderate telomere shortening caused an improved oral glucose tolerance in male (two-way ANOVA, genotype factor  $p$ =0.0066; **Fig. 23a**) but not female Terc KO mice with oral gavage of 2 g/kg glucose (**Fig. 23b**). Then, the insulin sensitivity of the mice was further investigated by performing insulin tolerance test (ITT). Significantly higher insulin sensitivity was observed in Terc KO mice than WT in both male and female mice (two-way ANOVA, genotype factor male  $p$ <0.0001 **Fig. 23c**, female  $p$ =0.0022 **Fig. 23d**).

In addition, a pyruvate tolerance test (PTT) in overnight fasted male and female Terc KO mice was performed. In male mice, Terc KO and WT mice both reached at similar level of glucose peak after 15 min pyruvate injection. Whereas, glucose levels were reduced much faster after the peak in Terc KO mice compared to WT. Moreover, in female Terc KO mice displayed a lower glucose level at 30 min and a relative lower level of blood glucose in the end as well. It reveals a moderately increased disposal of de novo generated glucose (male: 2-way ANOVA, genotype factor  $p$ =0.0424; **Fig. 23e**; female: two-way ANOVA; genotype factor  $p$ =0.0192 **Fig. 23f**), largely confirming the increased glucose tolerance and insulin sensitivity.

The study from Kuhlow suggests a direct effect of Terc deficiency on pancreatic beta cell mass and function (Kuhlow et al., 2010). To this end, the glucose stimulated insulin secretion in response to oral administration of 4 g/kg glucose which is the double dose than the oGTT was tested. A significant lower insulin

## Results

secretion was observed in Terc KO male mice than that in WT mice (**Fig. 23g** left panel: two-way ANOVA; genotype factor  $p=0.0148$ ; Sidak's multiple comparisons test at 30 min point  $p=0.0245$ ) but not in female mice (**Fig. 23h** left panel). Of note, the glucose tolerance improvement in females was observed only during glucose stimulated insulin secretion test when the glucose bolus was increased to 4 g/kg. And regarding the blood glucose responses during the test, significantly lower levels of glucose were observed in both Terc KO male mice (**Fig. 23g**, right panel: two-way ANOVA, genotype factor  $p=0.023$ ; Sidak's multiple comparisons test at 30 min point  $p=0.0396$ ) and female mice (**Fig. 23h**, right panel: two-way ANOVA, genotype factor  $p<0.0001$ ) compared to WT mice. Besides the *in vivo* experiment, the *ex vivo* experiment with isolated pancreatic islets was carried out to determine the insulin secretion capacity in response to high glucose stimulation. Isolated pancreatic islets were first incubated with 2.8 mM glucose, followed by changing into 16.7 mM glucose. During the *ex vivo* experiment, no significant difference was observed in insulin secretion in response to high glucose stimulation in islets of mice between genotypes in both genders (**Fig. 23i**).

Data mentioned above suggests moderate telomere shortening could help the body with better glucose disposal, and more insulin sensitive to maintaining glucose homeostasis compared to control mice.

# Results

## 3.15 Shorter telomere length results in a reconfiguration of the gut microbiome

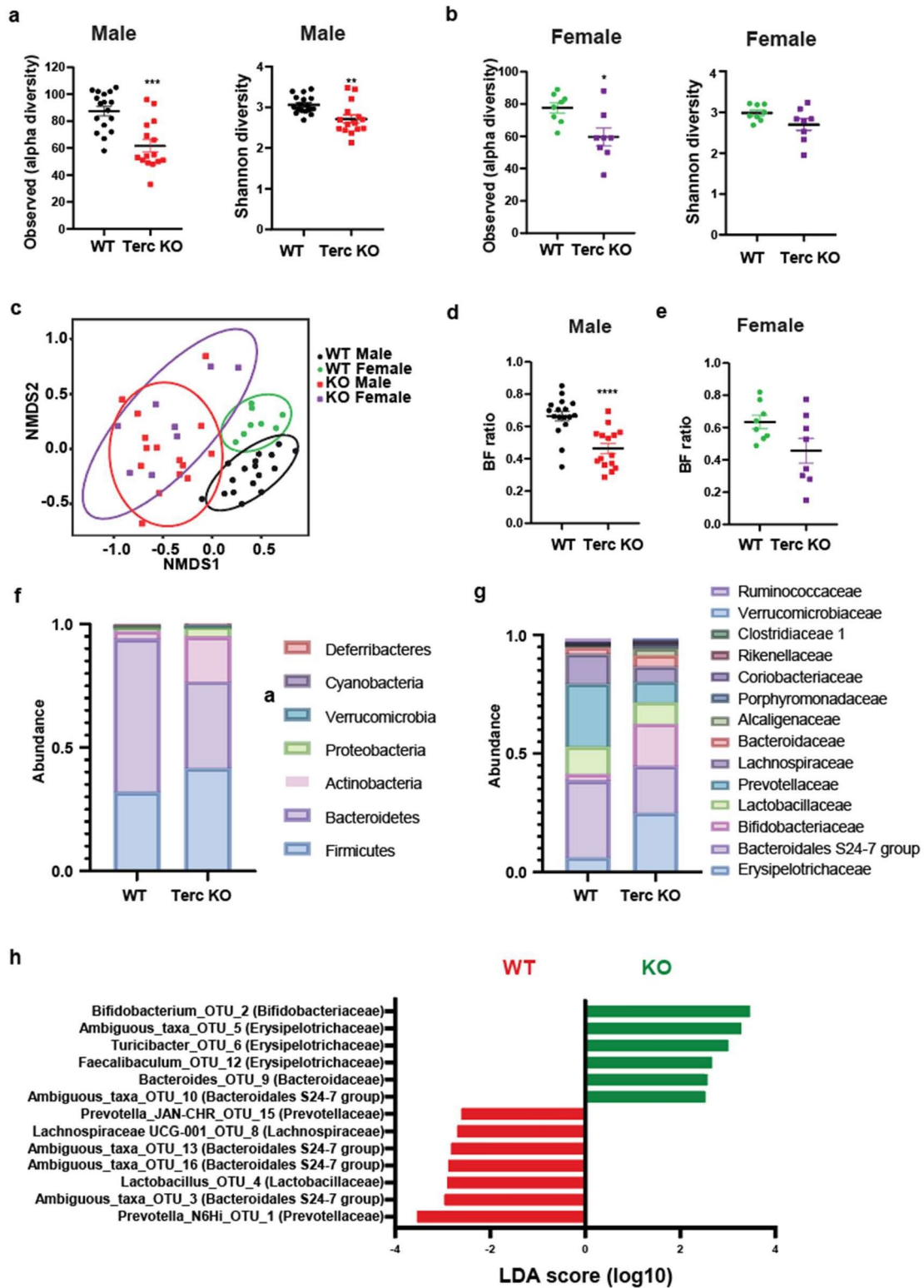


Figure 24. Shorter telomere length results in a reconfiguration of the gut microbiome via 16S rRNA sequencing analysis.

## Results

a. Alpha diversity and Shannon diversity of the male mice. b. Alpha diversity and Shannon diversity of the female mice. c. Beta diversity shown in a NMDS plot. d. Ratio of *Bacteroides*/*Firmicutes* (BF ratio) in male mice. e. Ratio of *Bacteroides*/*Firmicutes* (BF ratio) in female mice. f. Microbiota composition on phylum level. g. Microbiota composition on family level. h. LefSe analysis of microbiota changes. Fecal samples from 14 months old female ( $n=8$  WT and  $n=8$  Terc KO) and male ( $n=17$  WT and  $n=15$  Terc KO) mice. Statistical analysis were performed using an unpaired *t*-test and Mann-Whitney test, \* $p<0.05$ , \*\* $p<0.01$ , \*\*\* $p<0.001$ , \*\*\*\* $p<0.0001$ .

Changes in diet and supplementation with probiotics induce gut microbiota composition changes and an improvement in glucose homeostasis (Utzschneider et al., 2016). Therefore, the improved metabolism in Terc KO mice might be the contribution of the gut microbiome. To test the hypothesis, microbiota composition analysis of fecal samples from male mice (15 Tec KO and 17 controls) and female mice (8 Tec KO and 8 controls) was performed via 16S rRNA sequencing. The complexity of the microbial community within a sample analyzed by alpha diversity calculation revealed that male Tec KO mice had a reduced richness (**Fig. 24a** left panel, Mann-Whitney test,  $p=0.0001$ ) of the microbiota as well as a reduced Shannon diversity (**Fig. 24a** right panel, Mann-Whitney test,  $p=0.0031$ ) in comparison to the WT mice. Microbiome diversity reduction was also observed in female Tec KO mice (**Fig. 24b** left panel, Mann-Whitney test,  $p=0.02$ ), but the decrease in Shannon diversity did not reach a significant level, potentially due to the smaller sample size (**Fig. 24b** right panel). Then the similarity of the microbial community between samples by beta diversity was further analyzed showing a clear genotype-driven separation between Tec KO and WT mice (Permutational Multivariate Analysis of Variance Using Adonis, PERMANOVA,  $R^2=0.30542$ , **Fig. 24c**). Notably, differences were detectable on the phylum level as highlighted by altered *Bacteroides*/*Firmicutes* ratios in male mice (Mann-Whitney test,  $p=0.0001$ , **Fig. 24d**) and a similar trend observed in female mice (Mann-Whitney test,  $p=0.1304$ , **Fig. 24e**). Of note, a strong expansion of the Actinobacteria phylum in Tec KO mice was observed (**Fig. 24f**). Specifically, increased relative abundances of the families *Bifidobacteriaceae* and *Erysipelotrichaceae* were observed in Tec KO mice, while the families *Prevotellaceae* and *Muribaculaceae* (previously referred to Bacteroidales group S24-7) were decreased (**Fig. 24g**). A more detailed analysis of the microbiota changes using LefSe identified several “operational taxonomic

## *Results*

units" (OTUs) from the above-mentioned families that were significantly enriched in Tec KO mice, including for instance a specific OTU from the genus *Bifidobacteria* (OTU2) and the genus *Faecalibacterium* (OTU12) (**Fig. 24h**). Consistent with findings mentioned here, studies published also show these bacteria contribute to host metabolism via modulating endocrine function, improving insulin sensitivity and glucose intolerance (Aoki et al., 2017; Greiner and Bäckhed, 2011; Le et al., 2015; Portincasa et al., 2022; Qin et al., 2012; Yang et al., 2021; Zhang et al., 2013).

## **4. Discussion**

The increased rates of overweight and obesity, and its comorbidities, represents a health threat to billions of adults and children. The developmental transition from obesity to the metabolic syndrome and type 2 diabetes is mostly dependent on the occurrence of insulin resistance primarily in adipose tissue, muscle and the liver (Kolb et al., 2018). Before a diagnosis of diabetes occurs, individuals with obesity normally exhibit expanded pancreatic islet mass for the support of greater insulin secretion to compensate for peripheral insulin resistance to maintain glucose homeostasis (Alarcon et al., 2016; Czech, 2017). Without proper intervention, pancreatic beta cells then gradually become dysfunctional and lose beta cell mass, leading individuals with insulin resistance to easily develop T2D. T2D is a complex metabolic disease with many genetic factors, environmental factors, and interactions that contribute to disease development (Bonfond and Froguel, 2015; Hwang et al., 2015; Stanley, 2016; Ussar et al., 2016; Yan-Do and MacDonald, 2017). Obesity-associated diabetes goes hand in hand with complications such as hepatic steatosis, cardiovascular disorders, certain cancers, all of which consequently result in a higher morbidity and mortality risk (Sakaguchi et al., 2017). Over 90% of all diabetes cases are T2D, which is represented worldwide as 1 in 10 people living with diabetes. Therefore, a search for preventive and effective therapeutic strategies is urgently needed.

### **4.1 Serine racemase regulates insulin secretion and HFD-induced fat mass gain**

Lifestyle interventions such as dietary modification and exercise training are indicated to prevent T2D, as well as improve glucose homeostasis and the metabolic health of individual with T2D (Kolb et al., 2018). The maintenance or restoration of insulin secretion within pancreatic beta cells is one of the major objectives for treating diabetes (Estall and Srean, 2015; Henquin, 2004; Sachs et al., 2020). Various medicines such as metformin, GLP-1 receptor agonist, sulfonylureas and glitazones treat T2D as well. However, most of these drugs do not typically stop the progression of beta cell dysfunction nor restore it, ultimately increasing the risk of life-threatening hypoglycemia (Tahrani et al., 2011; Tokarz

## *Discussion*

et al., 2018; Zhou and Melton, 2018). Recently, studies have explored a new antidiabetic drug targeting the N-methyl-D-aspartate receptor (NMDAR), which has demonstrated improvements in pancreatic islet function, insulin secretion and islet cell survival by mediating electrical activity of the pancreatic beta cell membrane (Huang et al., 2017; Lockridge et al., 2021; Marquard et al., 2015). A co-agonist of NMDARs is D-serine. A previously published study from our lab has demonstrated chronic D-serine water supplementation to reduce the insulin secretory response to glucose stimulation (Suwandhi et al., 2018). Whereas, another study contrarily shows low dose D-serine supplementation, or the combination of NMDA and D-serine supplementation, to potentiate insulin secretion (Lockridge et al., 2021). D-serine is produced from the non-essential amino acid L-serine. Amino acids are critical to modulating metabolic homeostasis by participating in protein synthesis, cell signaling and energy production. Serine also acts as a central node in the metabolic network for many aspects such as cell proliferation, insulin sensitivity and glucose metabolism. Of note, L-serine is converted into D-serine through the racemization reaction of an enzyme called serine racemase (SRR). SRR was first cloned in 1999, and was found to not only catalyze racemization but also perform a parallel  $\alpha$ ,  $\beta$ -elimination reaction that generates pyruvate and ammonia (Foltyn et al., 2005; Wolosker et al., 1999). Our lab and other studies found that two SNPs (rs391300 and rs4523957) in SRR were associated with human insulin secretion and the therapeutic efficacy of metformin treatment in T2D patients. (Dong et al., 2011; Ndiaye et al., 2017; Suwandhi et al., 2018; Tsai et al., 2010). Moreover, mice with whole body SRR knockout exhibit an increase in glucose-stimulated insulin secretion and overall improvements in glucose metabolism (Lockridge et al., 2016). Therefore, here aim is to investigate the role of SRR in pancreatic beta cell insulin secretion and systemic glucose homeostasis to obtain a better understanding of the potential role of NMDARs.

### **SRR in pancreatic beta cells affects islet architecture and regulates glucose homeostasis**

Serine racemase is widely expressed in various tissues with high ubiquity. The function of SRR in the brain has been well studied. However, the role of SRR in the pancreas is still not well known yet. Transcripts of beta cell SRR have been

## *Discussion*

detected in transcriptomic screens in both mice and humans (Benner et al., 2014; Wolosker and Mori, 2012). Moreover, SRR expression in pancreatic islets in both mice and humans has been identified at the protein level by immunofluorescence staining (Lockridge et al., 2016). Here, the expression of SRR in isolated pancreatic islets of *Srr* fl/fl mice at the transcriptional level was detected. SRR was efficiently deleted in isolated pancreatic islets of *Srr*<sup>Ins1cre</sup> mice, validating the mouse model in this study.

For the typical mouse pancreatic islet, insulin-secreting beta cells form a core that is surrounded by alpha cells, delta cells and other endocrine cells. To respond to certain metabolic requirements and physiological conditions, pancreatic islets display dynamic changes in architecture (Steiner et al., 2010). Here, alterations in the architecture of pancreatic islets from *Srr*<sup>Ins1cre</sup> mice were observed. Islets from *Srr*<sup>Ins1cre</sup> mice have a greater number of alpha cells than control mice. In line with this, serum glucagon levels of *Srr*<sup>Ins1cre</sup> mice were significantly higher than those in control mice under chow diet. This observation is consistent with the study from Ohshima demonstrating serine racemase to support in cell proliferation. SRR protein expression is shown to increase in colorectal-cancer cells that exhibit rapid proliferation. Furthermore, it was demonstrated that the mechanism behind the SRR promotion of cell proliferation is due to an increase in intracellular pyruvate and the maintenance of mitochondrial mass and respiratory capacity. SRR inhibition suppresses the growth of colorectal tumors (Ohshima et al., 2020). Moreover, serine is central to regulating cell proliferation by modulating several metabolic process involving cellular biosynthesis, regulation of redox status, NADPH ratio, and lipid metabolism (Gao et al., 2018; Locasale, 2013; Mehrmohamadi et al., 2014; Nilsson et al., 2014; Ohshima et al., 2020). Restricted serine intake inhibits tumor growth, as deprivation of serine decreases utilization of fatty acids, glucose and glutamine ultimately impacting the function of mitochondria and cell proliferation (Gao et al., 2018). Phosphoglycerate dehydrogenase (PHGDH) is the key metabolic enzyme that catalyses the rate-limiting step of the serine biosynthesis pathway. In this thesis, PHGDH was found to be downregulated in the proteomic profile of pancreatic islets from *Srr*<sup>Ins1cre</sup> mice, which indicates the serine synthesis is downregulated. Decreased serine

## Discussion

synthesis may consequently affect mitochondrial dynamics and the function of mitochondria in supporting cell proliferation. Thus, mitochondria morphology should be studied to confirm this hypothesis in the future. Due to time constraints, this experiment was not done in this thesis.

The alteration of islet architecture might impact its function (Gannon et al., 2000; Roscioni et al., 2016). However, during an *in vivo* glucose stimulated insulin secretion (GSIS) test,  $Srr^{Ins1cre}$  mice fed with chow diet exhibit a normal insulin secretion response to high glucose stimulation, but also display improved glucose tolerance as measured during a glucose tolerance test.

In this study, mice are deficient in SRR in beta cells, in which D-serine synthesis is impaired. Our lab has also published another study with mice treated in the opposite experimental direction, by providing high-dose D-serine supplementation in water. Chronic D-serine supplementation through the drinking water leads to hyperglycemia and glucose intolerance, which is also consistent with our findings here to some extent (Suwandhi et al., 2018). Of note, low-dose D-serine treatment in the same experiments causes the opposite outcome by improving glucose metabolism via robust insulin secretion (Lockridge et al., 2021; Suwandhi et al., 2018). These results suggest that the underlying mechanism of D-serine on glucose and insulin metabolism is complicated, and that different concentrations of D-serine may lead to different responses. The data mentioned above indicates that loss of SRR in pancreatic beta cells enhances insulin efficiency, which is also in line with SRR whole-body knockout mice exhibiting improved insulin efficiency (Lockridge et al., 2016). However, no significant differences are observed in insulin sensitivity between  $Srr^{Ins1cre}$  mice and  $Srr^{fl/fl}$  mice in subsequent insulin tolerance tests. This might be due to the limited precision inherent to an insulin tolerance test in detecting slight differences between groups. Due to lack of equipment issues, a more precise measurement, such as a glucose clamp, for quantifying insulin secretion and insulin sensitivity was not carried out in this thesis. Consistent with observations during the *in vivo* GSIS, insulin secretion from isolated pancreatic islets during an *ex vivo* GSIS was not significantly altered between  $Srr^{Ins1cre}$  mice and  $Srr^{fl/fl}$ . However, in contrast to the SRR whole-body knockout mice that contain low D-serine concentrations,  $Srr^{Ins1cre}$  mice show an

## *Discussion*

improved insulin secretion in response to high glucose stimulation (Lockridge et al., 2016). Moreover, a combination of D-serine and NMDA supplementation potentiates insulin secretion responding to high glucose stimulation (Lockridge et al., 2021). Remarkably, these results conflict with the observations from the earlier study that NMDA receptors impair glucose stimulated insulin secretion (Marquard et al., 2015) and that a decrease in expression of SRR leads to impaired insulin secretion within the human pancreatic EndoC-bH1 beta-cell line (Ndiaye et al., 2017). These indicate that the NMDA receptors and its co-agonist D-serine have a complex role in regulating insulin secretion. Interestingly, in this study, enhanced insulin content is observed in isolated pancreatic islets from  $Srr^{Ins1cre}$  mice under 2.8 mM low glucose condition, a trend which has similarly been demonstrated in earlier studies (Lockridge et al., 2016; Marquard et al., 2015).

### **SRR in pancreatic beta cells promotes basal insulin secretion from isolated pancreatic islets with enhanced ATP production and potassium channel trafficking**

The principle mechanism of insulin secretion is that pancreatic beta cells first sense and uptake glucose via glucose transporter (GLUT2), in which the glucose is then converted into pyruvate via glycolysis, which can later enter the TCA cycle in the mitochondria to generate ATP. The rise in the ratio of ATP: ADP leads to ATP-sensitive potassium channel closure resulting in beta cell membrane depolarization. The resulting calcium influx triggers insulin secretion into systemic circulation (Ammala et al., 1991; Ashcroft et al., 1984; Cook and Hales, 1984; De Vos et al., 1995; Gremlich et al., 1995; Rorsman et al., 1991; Thorens et al., 1988). The principle mechanism of insulin secretion has been well established over 40 years, nonetheless the insulin secretion model is continuously updated to incorporate new observations of oscillatory insulin secretion (Campbell and Newgard, 2021; Prentki et al., 2013). Moreover, various hormonal (e.g. incretins) or sympathetic inputs can modulate insulin secretion (Drucker, 2006; Holst and Gromada, 2004; Svendsen et al., 2018). NMDA receptors are involved in neurotransmission, but recently are also found to be involved in regulating insulin secretion through modulation of the time span that beta cells exhibit a membrane excitatory state. Inhibition of NMDARs in mouse and human islets extends the

## Discussion

time spent in the depolarized state resulting in high beta cell cytosolic  $\text{Ca}^{2+}$  concentrations. Furthermore, acute D-serine supplementation, which is the co-agonist of NMDARs, enhances insulin secretion and increases beta cell membrane excitation. The previous study from our lab has demonstrated that  $\alpha 2$  adrenergic signaling from sympathetic nerves almost completely blocks glucose stimulated insulin secretion in mice. This has been attributed to an indirect effect of D-serine on insulin secretion through the modulation of hypothalamic-controlled insulin secretion (Suwandhi et al., 2018). Here, we show that loss of SRR, the enzyme that converts L-serine to D serine in pancreatic beta cells, results in an elevation of insulin content under low glucose condition. To further investigate the underlying mechanism, a combination of electrophysiology, proteomics and bioenergetics was applied. Greater ATP production within isolated pancreatic islets from  $\text{Srr}^{\text{Ins1cre}}$  mice was found via seahorse experiment under low glucose conditions. Further, an increased beta cell membrane potential and decreased  $\text{K}_{\text{ATP}}$  channel conductance was also observed under low glucose condition by electrophysiological experiment within isolated pancreatic islets from  $\text{Srr}^{\text{Ins1cre}}$  mice. Moreover, comparing the proteomic file of islets from  $\text{Srr}^{\text{Ins1cre}}$  mice and  $\text{Srr fl/fl}$  mice, it was found that the ATP binding cassette (ABC) transporter pathway was enhanced in  $\text{Srr}^{\text{Ins1cre}}$  mice, which supports the *ex vivo* findings that mentioned above. In addition, the pentose and glucuronate interconversion pathway that has been previously associated with T2D (Sun et al., 2014), was a top upregulated hit in the proteomic profile of islets from  $\text{Srr}^{\text{Ins1cre}}$  mice under chow diet.

### **$\text{Srr}^{\text{Ins1cre}}$ mice showed insulin resistance, glucose intolerance and a greater fat mass gain with inhibited fat metabolism under HFD.**

$\text{Srr}^{\text{Ins1cre}}$  mice fed with HFD show insulin resistance and impaired glucose tolerance.  $\text{Srr}^{\text{Ins1cre}}$  mice exhibit fasted hyperinsulinemia and hyperglycemia under HFD. Further, *ex vivo* pancreatic islets of HFD-fed mice do not exhibit the increase in basal insulin content that is associated with the chow-fed mice. Moreover, no difference in insulin secretion from isolated pancreatic islets is observed between  $\text{Srr}^{\text{Ins1cre}}$  mice and  $\text{Srr fl/fl}$  after high glucose stimulation. Insulin resistance is associated with obesity, therefore body composition of the mice was measured. As expected the  $\text{Srr}^{\text{Ins1cre}}$  mice had greater fat mass compared to control mice,

## *Discussion*

even though there were no evident body weight differences between the two groups. Further, adipocyte size in subcutaneous white adipose tissue of  $Srr^{Ins1cre}$  mice was larger compared to  $Srr^{fl/fl}$  mice under both HFD and CD.

To investigate the cause of the greater fat mass gain of  $Srr^{Ins1cre}$  mice, food intake and energy expenditure were measured within TSE metabolic cages. Surprisingly, significantly less food intake was observed in  $Srr^{Ins1cre}$  mice compared to controls. This may be due to inhibition of hypothalamus-associated orexigenic pathways in response to increased fasting insulin levels (Hu et al., 2020). Recent studies have suggested that, rather than postprandial insulin dynamics, changes in basal insulin play a more important role in regulating weight gain. The release of lipids from adipose tissue is highly sensitive to deviations in basal insulin (Speakman and Hall, 2021). The relationship between insulin levels and body fat is still not fully understood. The carbohydrate insulin model (CIM) is one of the well-known models, which focuses on the systemic effects resulting from the direct action of postprandial insulin on adipose tissue (Ludwig and Ebbeling, 2018). However, this CIM model has been challenged in clinical human studies, as well as studies in mice. Mice fed diets containing a greater proportion of carbohydrates took in fewer calories and gained less body weight, but still exhibited higher postprandial insulin levels (Hu et al., 2020). The CIM model did not accurately explain the phenotype in this case. Further, insulin is more potent in suppressing lipolysis than inducing glucose uptake. Thus, differences in basal insulin secretion, which are largely independent of dietary intake, could in fact play a grossly underappreciated role in regulating weight gain (Speakman and Hall, 2021). In this thesis, it was shown that fatty acid beta-oxidation and fatty acid/lipid metabolic and catabolic processes are among the top affected GO term categories of the WAT proteome in  $Srr^{Ins1cre}$  mice fed with HFD compared to control. Moreover, in a KEGG pathway enrichment analysis, the highest enrichment was seen in fatty acid metabolism, citrate cycle, fatty acid degradation, carbon metabolism and pyruvate metabolism pathways. Most proteins involved in fatty acid metabolism and fatty acid degradation were also down regulated, which was also supported by a GSVA analysis indicating the down regulation of fatty acid metabolism in  $Srr^{Ins1cre}$  mice. These data are in line with the finding that the degree of lipolysis in white adipose tissue is negatively

## Discussion

correlated with fasting insulin levels (Hu et al., 2020). Together, these findings provides experimental support for the hypothesis that basal insulin control is critical for regulating fat mass gain via modulating lipolysis.

### 4.2 Glypican 4 in pancreatic beta cells associates insulin secretion and insulin resistance

Gpc4 is an adipokine released from adipose tissue. Gpc4 in pre-adipocytes interacts with the insulin receptor and enhances insulin signaling and insulin sensitivity (Deischinger et al., 2021; Mitchell, 2012; Tamori and Kasuga, 2013; Ussar et al., 2012). Beta cell specific loss of insulin receptor contributes to insulin hypersecretion (Skovso et al., 2022). Interestingly, Gpc4 was shown to be downregulated in the islet proteomic file of  $Srr^{Ins1cre}$  mice compare to control mice. Here the expression of Gpc4 in pancreatic islets was demonstrated. Thus, we established  $Gpc4^{Ins1cre}$  mouse line, which specific knockout of Gpc4 in pancreatic beta cells, to investigate the mechanism underlying the modulation of insulin secretion by Gpc4. Gpc4 is efficiently deleted in the pancreatic islets at the transcriptional level in the  $Gpc4^{Ins1cre}$  mouse model. Alterations in pancreatic islet architecture in  $Gpc4^{Ins1cre}$  mice is observed. Normally the pancreatic beta cells account for 60-80% of pancreatic islet cell population and form a core that is surrounded by pancreatic alpha cells, delta cells, and other cells, which constitute about 10-20%, 5%, and 1% of the total islet cell population respectively. Interestingly, an abnormal distribution of alpha cells is observed, represented as a distributional scattering after loss of Gpc4 in pancreatic beta cells. Further, a decrease in islet size within  $Gpc4^{Ins1cre}$  mice is observed relative to control mice as established by IF staining and H&E staining. Due to time limitations, further detailed quantification of pancreatic composition experiments have not yet been done. Interestingly,  $Gpc4^{Ins1cre}$  mice display less insulin secretion in response to high glucose stimulation during *in vivo* GSIS. In line with this,  $Gpc4^{Ins1cre}$  mice also display an impaired glucose tolerance during GSIS. This observation agrees with unpublished data from our lab on Gpc4 whole body knockout mice. Whole body knockout of glypican-4 exhibit diminished glucose stimulated insulin secretion, whereas an *ex vivo* GSIS analysis indicates that pancreatic beta cell function is not affected by loss of Gpc4.

## *Discussion*

Loss of Gpc4 in pancreatic beta cells does not impact body weight or body composition under chow diet, however, it increases the rate body mass and fat mass gain under the HFD, which is a similar phenotype to the  $Srr^{Ins1cre}$  mice. To investigate if the Ins1-cre insertion system influenced HFD-induced phenotype, the phenotype of Ins1cre mouse line was characterized under HFD condition. Ins1cre mice fed with HFD do not show any differences in body mass or fat mass gain compared to control. Moreover, metabolic parameters of the Ins1cre mice are not significantly different in terms of food intake, drink intake, energy expenditure, physical activity or respiratory exchange rate. Therefore, the HFD-induced greater fat mass gain in  $Gpc4^{Ins1cre}$  mice is not effected by Ins1 insertion but by loss of Gpc4 protein in pancreatic beta cells.

Under HFD,  $Gpc4^{Ins1cre}$  mice show higher fasted basal insulin levels, but normal fasted basal glucose compared to control mice. This indicates that the loss of Gpc4 in pancreatic beta cells may cause insulin resistance in mice. Earlier studies also have shown Gpc4 to be associated with insulin sensitivity (Deischinger et al., 2021; Mitchell, 2012; Yoo et al., 2013). However, we did not observe impairments in insulin tolerance of the  $Gpc4^{Ins1cre}$  mice fed with HFD during an insulin tolerance test. This might be due the limitation of precision within the insulin tolerance test experiment. Moreover,  $Gpc4^{Ins1cre}$  and control mice exhibit similar glucose clearance in response to a high glucose stimulus during the glucose tolerance test. Interestingly, at higher concentrations of exogenously administered glucose, glucose levels of  $Gpc4^{Ins1cre}$  mice at the 30 min time point are significantly higher than that of control mice. In an associated manner, newly diagnosed T2D individuals exhibit a decrease in Gpc4, but in healthy individuals that exhibit only impairment in glucose tolerance, Gpc4 in circulation is increased in comparison to normal healthy individuals (Li et al., 2014). Together, these data indicate Gpc4 expression in pancreatic beta cells to potentially provide a positive feedback in the regulation of insulin secretion and play a role in the development of T2D.

### 4.3 Alteration in microbiota composition results in improved glucose tolerance and insulin sensitivity in *Terc* KO mice

Impaired beta-cell compensation for age-related insulin resistance may contribute to predisposing older adults to type 2 diabetes. A sign of aging is the shortening of telomeres. A greater understanding of the metabolic changes related to telomere length in aging is essential for the development of therapeutic interventions targeting the elderly population for T2D. An increase in mortality and infertility of third-generation *Terc*<sup>-/-</sup> inbred mice was observed, therefore, in this thesis, the second-generation *Terc*<sup>-/-</sup> inbred mice (*Terc* KO) was used as an accelerated aging mouse model to study their metabolic alterations. Here, we showed that moderate shortening of telomeres in second-generation C57BL/6 *Terc*<sup>-/-</sup> mice improve insulin sensitivity and glucose tolerance in both male and female mice. However, this effect does not appear to be a consequence of direct effects on cellular glucose utilization, as previously suggested (Missios et al., 2014). This thesis demonstrated that male and female *Terc* KO mice display a reconfiguration of gut microbiota, with elevated levels of Actinobacteria. Members of this family show positive effects on various metabolic parameters. For example, *Bifidobacterium longum* APC1472 improves glucose tolerance in obese mice and lowers fasting glycemia in obese/overweight individuals (Schellekens et al., 2021). Furthermore, supplementation of obese individuals with probiotics containing *Bifidobacteria* have resulted in decreased body weight and improvement in wellbeing (Michael et al., 2020). Thus, the improvement in glucose tolerance and insulin sensitivity in *Terc* KO mice may mostly be influenced by the expansion of metabolically beneficial gut microbiota in both male and female mice. In addition, sex-specific differences in individual metabolic and molecular parameters are observed. Most prominently, female mice only exhibit improved glucose tolerance when high doses of glucose (4 g/kg) are administered, whereas this effect was already observed at 2 g/kg in male mice. The most obvious explanation for this difference is the overall higher glucose tolerance and insulin sensitivity of female compared to male mice (Arslanian et al., 1991; Hedrington and Davis, 2015; Kava et al., 1989; ter Horst et al., 2015; Vital et al., 2006). This optimal metabolic state in female mice is also reflected in the serum triglyceride levels. However, the

## *Discussion*

detailed underlying mechanism is not further explored in this thesis due to the time limitation.

Overall, increased telomere shortening, either through genetic impairment in telomerase activity as described here, or via environmental effects, appears to confer beneficial effects on glucose homeostasis, which on first sight contradicts many epidemiological studies in humans. However, while describing a principle mechanism, our data should not be translated directly to humans. Moreover, further decreases in telomere length later in life, or as seen in studies using a higher number of *Terc*<sup>-/-</sup> inbred generations, has been known to cause other various organismal damages, eventually worsening glucose homeostasis among other metabolic attributes. Thus, future large scale studies in mice, or specifically designed clinical studies, will be required to unravel the transition points from beneficial to detrimental effects of telomere shortening on systemic glucose homeostasis.

## **5. Conclusion and perspectives**

Halting pancreatic beta cell dysfunction progression or restoring beta cell function is an effective therapeutic strategy for treating T2D diabetes. In this thesis, it was shown that loss of serine racemase in pancreatic beta cells induces a greater alpha cell population and impairs islet architecture. These changes may associate with the function of Serine racemase on cell proliferation via the production of pyruvate (Ohshima et al., 2020). Thus, further studies on tracking pancreatic beta cell and alpha cell proliferation, and quantifying the mitochondrial condition or pyruvate utilization, are required for a further detailed understanding of the role of serine racemase. This study also demonstrated serine racemase loss to promote insulin secretion under low glucose condition *ex vivo*. Further, this thesis revealed greater mitochondrial ATP production under low glucose condition in isolated pancreatic islets lacking serine racemase. In parallel, an increase in membrane potential under low glucose condition was observed through electrophysiological detection in isolated pancreatic islets lacking serine racemase. In line with the enhanced basal insulin secretion effect attributed to serine racemase deletion, mice lacking serine racemase in pancreatic beta cells exhibit improved glucose tolerance under chow diet, but under high fat diet exhibit hyperinsulinemia and insulin resistance and the consequences associated with increased adipose tissue lipid storage. These disparities are further confirmed by proteomic study of subcutaneous adipose tissue of HFD fed  $Srr^{Ins1cre}$  mice, which reveals fatty acid metabolism and insulin signaling components to be down regulated. In summary, data in this thesis unravels the role of SRR in the regulation of basal insulin secretion and underscores the pivotal role of basal insulin secretion in the regulation of body weight. In addition, this thesis also demonstrates that the glypican 4 potently stimulates insulin secretion in response to high glucose stimulation. Another finding in this thesis is that loss of glypican 4 in pancreatic beta cells leads to an impairment in pancreatic islets architecture and impaired glucose tolerance. Further, mice lacking glypican 4 in pancreatic beta cells demonstrate insulin resistance and greater fat mass gain under HFD. Future studies on examining the degree of lipolysis and extent glucose uptake in adipose tissue can be performed to further detail the understanding of glypican 4 in the

## *Conclusion and perspectives*

regulation of fat metabolism. Further clinical studies among healthy individuals, individuals with T2D, and individuals with obesity are required to translate the role of D-serine or glypican 4 on insulin secretion into avenues for therapeutic treatment. These findings may guide future work towards D-serine targeting or glypican 4-sensitizing therapies as treatments for diabetes.

Shortened telomeres is another factor related to the development of type 2 diabetes. Interestingly, the data in this thesis reveals that moderate telomere shortening in aged mice improves systemic metabolism. G2 generation Terc KO mice exhibit improved oral glucose tolerance and higher insulin sensitivity. Telomerase deficiency significantly alters the composition of gut microbiota with an increase in *Bifidobacteriaceae* and *Erysipelotrichaceae*, which is one of the factors responsible for the improvements in insulin sensitivity and glucose tolerance. To further explore the role of microbiota in the improvement of glucose and insulin metabolism, a study with the germ-free mice transplanted with the microbiota from Terc KO mice and control mice can be further investigated in future studies. Nevertheless, our data unravel the principle role of telomere shortening in the regulation of systemic glucose metabolism and insulin sensitivity. My study provides important insights for future murine and human aging studies of the age-associated development of type 2 diabetes and metabolic syndrome.

# References

## References

- Adriaenssens, A.E., Svendsen, B., Lam, B.Y.H., Yeo, G.S.H., Holst, J.J., Reimann, F., and Gribble, F.M. (2016). Transcriptomic profiling of pancreatic alpha, beta and delta cell populations identifies delta cells as a principal target for ghrelin in mouse islets. *Diabetologia* 59, 2156-2165.
- Ahima, R.S., and Flier, J.S. (2000). Adipose tissue as an endocrine organ. *Trends in Endocrinology & Metabolism* 11, 327-332.
- Al Khaldi, R., Mojiminiyi, O., AlMulla, F., and Abdella, N. (2015). Associations of TERC single nucleotide polymorphisms with human leukocyte telomere length and the risk of type 2 diabetes mellitus. *PloS one* 10, e0145721.
- Alarcon, C., Boland, B.B., Uchizono, Y., Moore, P.C., Peterson, B., Rajan, S., Rhodes, O.S., Noske, A.B., Haataja, L., Arvan, P., et al. (2016). Pancreatic beta-Cell Adaptive Plasticity in Obesity Increases Insulin Production but Adversely Affects Secretory Function. *Diabetes* 65, 438-450.
- Alves-Bezerra, M., and Cohen, D.E. (2017). Triglyceride Metabolism in the Liver. *Comprehensive Physiology* 8, 1-8.
- Alves-Paiva, R.M., Kajigaya, S., Feng, X., Chen, J., Desierto, M., Wong, S., Townsley, D.M., Donaies, F.S., Bertola, A., Gao, B., et al. (2018). Telomerase enzyme deficiency promotes metabolic dysfunction in murine hepatocytes upon dietary stress. *Liver Int* 38, 144-154.
- Ammala, C., Bokvist, K., Galt, S., and Rorsman, P. (1991). Inhibition of ATP-regulated K(+) channels by a photoactivatable ATP-analogue in mouse pancreatic beta-cells. *Biochim. Biophys. Acta* 1092, 347-349.
- Aoki, R., Kamikado, K., Suda, W., Takii, H., Mikami, Y., Suganuma, N., Hattori, M., and Koga, Y. (2017). A proliferative probiotic Bifidobacterium strain in the gut ameliorates progression of metabolic disorders via microbiota modulation and acetate elevation. *Scientific Reports* 7, 43522.
- Arslanian, S.A., Heil, B.V., Becker, D.J., and Drash, A.L. (1991). Sexual dimorphism in insulin sensitivity in adolescents with insulin-dependent diabetes mellitus. *J Clin Endocrinol Metab* 72, 920-926.
- Ashcroft, F.M., Harrison, D.E., and Ashcroft, S.J. (1984). Glucose induces closure of single potassium channels in isolated rat pancreatic beta-cells. *Nature* 312, 446-448.
- Autexier, C., and Lue, N.F. (2006). The structure and function of telomerase reverse transcriptase. *Annu. Rev. Biochem.* 75, 493-517.
- Backhed, F., Ding, H., Wang, T., Hooper, L.V., Koh, G.Y., Nagy, A., Semenkovich, C.F., and Gordon, J.I. (2004). The gut microbiota as an environmental factor that regulates fat storage. *Proc Natl Acad Sci U S A* 101, 15718-15723.
- Bakhti, M., Bottcher, A., and Lickert, H. (2019). Modelling the endocrine pancreas in health and disease. *Nat Rev Endocrinol* 15, 155-171.
- Balu, D.T., Li, Y., Puhl, M.D., Benneyworth, M.A., Basu, A.C., Takagi, S., Bolshakov, V.Y., and Coyle, J.T. (2013). Multiple risk pathways for schizophrenia converge in serine racemase knockout mice, a mouse model of NMDA receptor hypofunction. *Proc Natl Acad Sci U S A* 110, E2400-2409.
- Barthel, A., and Schmoll, D. (2003). Novel concepts in insulin regulation of hepatic gluconeogenesis. *American Journal of Physiology-Endocrinology And Metabolism* 285, E685-E692.

## References

- Basu, A.C., Tsai, G.E., Ma, C.L., Ehmsen, J.T., Mustafa, A.K., Han, L., Jiang, Z.I., Benneyworth, M.A., Froimowitz, M.P., Lange, N., et al. (2009). Targeted disruption of serine racemase affects glutamatergic neurotransmission and behavior. *Mol Psychiatry* 14, 719-727.
- Batterham, R.L., Le Roux, C.W., Cohen, M.A., Park, A.J., Ellis, S.M., Patterson, M., Frost, G.S., Ghatei, M.A., and Bloom, S.R. (2003). Pancreatic polypeptide reduces appetite and food intake in humans. *J Clin Endocrinol Metab* 88, 3989-3992.
- Bauer, P.V., Duca, F.A., Waise, T.M.Z., Rasmussen, B.A., Abraham, M.A., Dranse, H.J., Puri, A., O'Brien, C.A., and Lam, T.K.T. (2018). Metformin Alters Upper Small Intestinal Microbiota that Impact a Glucose-SGLT1-Sensing Glucoregulatory Pathway. *Cell Metab* 27, 101-117 e105.
- Benner, C., van der Meulen, T., Caceres, E., Tigyi, K., Donaldson, C.J., and Huising, M.O. (2014). The transcriptional landscape of mouse beta cells compared to human beta cells reveals notable species differences in long non-coding RNA and protein-coding gene expression. *BMC Genomics* 15, 620.
- Bertea, M., Rütli, M.F., Othman, A., Marti-Jaun, J., Hersberger, M., von Eckardstein, A., and Hornemann, T. (2010). Deoxysphingoid bases as plasma markers in diabetes mellitus. *Lipids in health and disease* 9, 1-7.
- Bervoets, L., Massa, G., Guedens, W., Louis, E., Noben, J.P., and Adriaenssens, P. (2017). Metabolic profiling of type 1 diabetes mellitus in children and adolescents: a case-control study. *Diabetol Metab Syndr* 9, 48.
- Blasco, M.A., Lee, H.W., Hande, M.P., Samper, E., Lansdorp, P.M., DePinho, R.A., and Greider, C.W. (1997). Telomere shortening and tumor formation by mouse cells lacking telomerase RNA. *Cell* 91, 25-34.
- Bonnefond, A., and Froguel, P. (2015). Rare and Common Genetic Events in Type 2 Diabetes: What Should Biologists Know? *Cell Metabolism* 21, 357-368.
- Briant, L., Salehi, A., Vergari, E., Zhang, Q., and Rorsman, P. (2016). Glucagon secretion from pancreatic alpha-cells. *Ups J Med Sci* 121, 113-119.
- Briant, L.J.B., Reinbothe, T.M., Spiliotis, I., Miranda, C., Rodriguez, B., and Rorsman, P. (2018). delta-cells and beta-cells are electrically coupled and regulate alpha-cell activity via somatostatin. *J Physiol* 596, 197-215.
- Burlison, J.S., Long, Q., Fujitani, Y., Wright, C.V., and Magnuson, M.A. (2008). Pdx-1 and Ptf1a concurrently determine fate specification of pancreatic multipotent progenitor cells. *Dev. Biol.* 316, 74-86.
- Campbell, J.E., and Newgard, C.B. (2021). Mechanisms controlling pancreatic islet cell function in insulin secretion. *Nat Rev Mol Cell Biol* 22, 142-158.
- Campbell, S.A., Golec, D.P., Hubert, M., Johnson, J., Salamon, N., Barr, A., MacDonald, P.E., Philippaert, K., and Light, P.E. (2020). Human islets contain a subpopulation of glucagon-like peptide-1 secreting  $\alpha$  cells that is increased in type 2 diabetes. *Molecular Metabolism* 39, 101014.
- Capozzi, M.E., Svendsen, B., Encisco, S.E., Lewandowski, S.L., Martin, M.D., Lin, H., Jaffe, J.L., Coch, R.W., Haldeman, J.M., MacDonald, P.E., et al. (2019). beta Cell tone is defined by proglucagon peptides through cAMP signaling. *JCI Insight* 4.
- Cerf, M.E. (2013). Beta cell dysfunction and insulin resistance. *Front Endocrinol (Lausanne)* 4, 37.
- Chia, C.W., Egan, J.M., and Ferrucci, L. (2018). Age-related changes in glucose metabolism, hyperglycemia, and cardiovascular risk. *Circul. Res.* 123, 886-904.

## References

- Claesson, M.J., Jeffery, I.B., Conde, S., Power, S.E., O'Connor, E.M., Cusack, S., Harris, H.M., Coakley, M., Lakshminarayanan, B., O'Sullivan, O., et al. (2012). Gut microbiota composition correlates with diet and health in the elderly. *Nature* 488, 178-184.
- Cleaver, O., and Dor, Y. (2012). Vascular instruction of pancreas development. *Development* 139, 2833-2843.
- Cochrane, V.A., Yang, Z., Dell'Acqua, M.L., and Shyng, S.L. (2021). AKAP79/150 coordinates leptin-induced PKA signaling to regulate K(ATP) channel trafficking in pancreatic  $\beta$ -cells. *J Biol Chem* 296, 100442.
- Cohen, P., and Spiegelman, B.M. (2016). Cell biology of fat storage. *Molecular biology of the cell* 27, 2523-2527.
- Coll, A.P., Chen, M., Taskar, P., Rimmington, D., Patel, S., Tadross, J.A., Cimino, I., Yang, M., Welsh, P., Virtue, S., et al. (2020). GDF15 mediates the effects of metformin on body weight and energy balance. *Nature* 578, 444-448.
- Cook, D.L., and Hales, C.N. (1984). Intracellular ATP directly blocks K<sup>+</sup> channels in pancreatic B-cells. *Nature* 311, 271-273.
- Curcio, L., Podda, M.V., Leone, L., Piacentini, R., Mastrodonato, A., Cappelletti, P., Sacchi, S., Pollegioni, L., Grassi, C., and D'Ascenzo, M. (2013). Reduced D-serine levels in the nucleus accumbens of cocaine-treated rats hinder the induction of NMDA receptor-dependent synaptic plasticity. *Brain* 136, 1216-1230.
- Czech, M.P. (2017). Insulin action and resistance in obesity and type 2 diabetes. *Nat Med* 23, 804-814.
- De Cat, B., and David, G. (2001). Developmental roles of the glypicans. In *Semin. Cell Dev. Biol.* (Elsevier), pp. 117-125.
- De Vos, A., Heimberg, H., Quartier, E., Huypens, P., Bouwens, L., Pipeleers, D., and Schuit, F. (1995). Human and rat beta cells differ in glucose transporter but not in glucokinase gene expression. *J Clin Invest* 96, 2489-2495.
- de Wet, H., and Proks, P. (2015). Molecular action of sulphonylureas on KATP channels: a real partnership between drugs and nucleotides. *Biochem. Soc. Trans.* 43, 901-907.
- DeFronzo, R.A. (1981). Glucose intolerance and aging. *Diabetes care* 4, 493-501.
- Deisinger, C., Harreiter, J., Leitner, K., Wattar, L., Baumgartner-Parzer, S., and Kautzky-Willer, A. (2021). Glypican-4 in pregnancy and its relation to glucose metabolism, insulin resistance and gestational diabetes mellitus status. *Sci Rep* 11, 23898.
- Deng, Y., and Scherer, P.E. (2010). Adipokines as novel biomarkers and regulators of the metabolic syndrome. *Ann. N. Y. Acad. Sci.* 1212, E1-E19.
- DiPilato, L.M., Ahmad, F., Harms, M., Seale, P., Manganiello, V., and Birnbaum, M.J. (2015). The Role of PDE3B Phosphorylation in the Inhibition of Lipolysis by Insulin. *Mol Cell Biol* 35, 2752-2760.
- Dolensek, J., Rupnik, M.S., and Stozer, A. (2015a). Structural similarities and differences between the human and the mouse pancreas. *Islets* 7, e1024405.
- Dolensek, J., Spelic, D., Klemen, M.S., Zalik, B., Gosak, M., Rupnik, M.S., and Stozer, A. (2015b). Membrane Potential and Calcium Dynamics in Beta Cells from Mouse Pancreas Tissue Slices: Theory, Experimentation, and Analysis. *Sensors (Basel)* 15, 27393-27419.
- Dong, M., Gong, Z.C., Dai, X.P., Lei, G.H., Lu, H.B., Fan, L., Qu, J., Zhou, H.H., and Liu, Z.Q. (2011). Serine racemase rs391300 G/A polymorphism influences

## References

- the therapeutic efficacy of metformin in Chinese patients with diabetes mellitus type 2. *Clin. Exp. Pharmacol. Physiol.* 38, 824-829.
- Drábková, P., Šanderová, J., Kovařík, J., and Kanďár, R. (2015). An assay of selected serum amino acids in patients with type 2 diabetes mellitus. *Advances in Clinical and Experimental Medicine* 24, 447-451.
- Drucker, D.J. (2006). The biology of incretin hormones. *Cell Metab* 3, 153-165.
- Duckworth, W.C., Bennett, R.G., and Hamel, F.G. (1998). Insulin degradation: progress and potential. *Endocr Rev* 19, 608-624.
- Duncan, R.E., Ahmadian, M., Jaworski, K., Sarkadi-Nagy, E., and Sul, H.S. (2007). Regulation of lipolysis in adipocytes. *Annu. Rev. Nutr.* 27, 79-101.
- Eizirik, D.L., Pasquali, L., and Cnop, M. (2020). Pancreatic beta-cells in type 1 and type 2 diabetes mellitus: different pathways to failure. *Nat Rev Endocrinol* 16, 349-362.
- Estall, J.L., and Srean, R.A. (2015). To Be(ta Cell) or Not to Be(ta cell): New Mouse Models for Studying Gene Function in the Pancreatic beta-Cell. *Endocrinology* 156, 2365-2367.
- Fava, G.E., Dong, E.W., and Wu, H. (2016). Intra-islet glucagon-like peptide 1. *Journal of Diabetes and its Complications* 30, 1651-1658.
- Finan, B., Ma, T., Ottaway, N., Müller, T.D., Habegger, K.M., Heppner, K.M., Kirchner, H., Holland, J., Hembree, J., Raver, C., et al. (2013). Unimolecular Dual Incretins Maximize Metabolic Benefits in Rodents, Monkeys, and Humans. *Science Translational Medicine* 5, 209ra151-209ra151.
- Foltyn, V.N., Bendikov, I., De Miranda, J., Panizzutti, R., Dumin, E., Shleper, M., Li, P., Toney, M.D., Kartvelishvily, E., and Wolosker, H. (2005). Serine racemase modulates intracellular D-serine levels through an alpha,beta-elimination activity. *J Biol Chem* 280, 1754-1763.
- Fruhbeck, G., Mendez-Gimenez, L., Fernandez-Formoso, J.A., Fernandez, S., and Rodriguez, A. (2014). Regulation of adipocyte lipolysis. *Nutr Res Rev* 27, 63-93.
- Fukaishi, T., Nakagawa, Y., Fukunaka, A., Sato, T., Hara, A., Nakao, K., Saito, M., Kohno, K., Miyatsuka, T., Tamaki, M., et al. (2021). Characterisation of Ppy-lineage cells clarifies the functional heterogeneity of pancreatic beta cells in mice. *Diabetologia* 64, 2803-2816.
- Gaisano, H.Y. (2017). Recent new insights into the role of SNARE and associated proteins in insulin granule exocytosis. *Diabetes Obes Metab* 19 Suppl 1, 115-123.
- Gannon, M., Ray, M.K., Van Zee, K., Rausa, F., Costa, R.H., and Wright, C.V. (2000). Persistent expression of HNF6 in islet endocrine cells causes disrupted islet architecture and loss of beta cell function. *Development* 127, 2883-2895.
- Gao, X., Lee, K., Reid, M.A., Sanderson, S.M., Qiu, C., Li, S., Liu, J., and Locasale, J.W. (2018). Serine Availability Influences Mitochondrial Dynamics and Function through Lipid Metabolism. *Cell Rep* 22, 3507-3520.
- Gembal, M., Detimary, P., Gilon, P., Gao, Z.Y., and Henquin, J.C. (1993). Mechanisms by which glucose can control insulin release independently from its action on adenosine triphosphate-sensitive K<sup>+</sup> channels in mouse B cells. *J Clin Invest* 91, 871-880.
- Gill, S.R., Pop, M., Deboy, R.T., Eckburg, P.B., Turnbaugh, P.J., Samuel, B.S., Gordon, J.I., Relman, D.A., Fraser-Liggett, C.M., and Nelson, K.E. (2006). Metagenomic analysis of the human distal gut microbiome. *Science* 312, 1355-1359.

## References

- Girousse, A., Tavernier, G., Valle, C., Moro, C., Mejhert, N., Dinel, A.L., Houssier, M., Roussel, B., Besse-Patin, A., Combes, M., et al. (2013). Partial inhibition of adipose tissue lipolysis improves glucose metabolism and insulin sensitivity without alteration of fat mass. *PLoS Biol.* 11, e1001485.
- Grand, T., Abi Gerges, S., David, M., Diana, M.A., and Paoletti, P. (2018). Unmasking GluN1/GluN3A excitatory glycine NMDA receptors. *Nat Commun* 9, 4769.
- Greiner, T., and Bäckhed, F. (2011). Effects of the gut microbiota on obesity and glucose homeostasis. *Trends Endocrinol Metab* 22, 117-123.
- Gremlich, S., Porret, A., Hani, E.H., Cherif, D., Vionnet, N., Froguel, P., and Thorens, B. (1995). Cloning, functional expression, and chromosomal localization of the human pancreatic islet glucose-dependent insulinotropic polypeptide receptor. *Diabetes* 44, 1202-1208.
- Hartig, S.M., and Cox, A.R. (2020). Paracrine signaling in islet function and survival. *J Mol Med (Berl)* 98, 451-467.
- Hashimoto, A., Yoshikawa, M., Andoh, H., Yano, H., Matsumoto, H., Kawaguchi, M., Oka, T., and Kobayashi, H. (2007). Effects of MK-801 on the expression of serine racemase and d-amino acid oxidase mRNAs and on the D-serine levels in rat brain. *Eur J Pharmacol* 555, 17-22.
- Hatting, M., Tavares, C.D., Sharabi, K., Rines, A.K., and Puigserver, P. (2018). Insulin regulation of gluconeogenesis. *Ann. N. Y. Acad. Sci.* 1411, 21-35.
- Hauge-Evans, A.C., King, A.J., Carmignac, D., Richardson, C.C., Robinson, I.C., Low, M.J., Christie, M.R., Persaud, S.J., and Jones, P.M. (2009). Somatostatin secreted by islet delta-cells fulfills multiple roles as a paracrine regulator of islet function. *Diabetes* 58, 403-411.
- Hedrington, M.S., and Davis, S.N. (2015). Sexual Dimorphism in Glucose and Lipid Metabolism during Fasting, Hypoglycemia, and Exercise. *Frontiers in Endocrinology* 6.
- Heine, M., Fischer, A.W., Schlein, C., Jung, C., Straub, L.G., Gottschling, K., Mangels, N., Yuan, Y., Nilsson, S.K., Liebscher, G., et al. (2018). Lipolysis Triggers a Systemic Insulin Response Essential for Efficient Energy Replenishment of Activated Brown Adipose Tissue in Mice. *Cell Metab.*
- Henquin, J.C. (2004). Pathways in beta-cell stimulus-secretion coupling as targets for therapeutic insulin secretagogues. *Diabetes* 53, S48-S58.
- Henquin, J.C. (2009). Regulation of insulin secretion: a matter of phase control and amplitude modulation. *Diabetologia* 52, 739-751.
- Henquin, J.C., Nenquin, M., Ravier, M.A., and Szollosi, A. (2009). Shortcomings of current models of glucose-induced insulin secretion. *Diabetes Obes Metab* 11 Suppl 4, 168-179.
- Henquin, J.C., Nenquin, M., Stienet, P., and Ahren, B. (2006). In vivo and in vitro glucose-induced biphasic insulin secretion in the mouse: pattern and role of cytoplasmic Ca<sup>2+</sup> and amplification signals in beta-cells. *Diabetes* 55, 441-451.
- Herrera, P.L. (2000). Adult insulin- and glucagon-producing cells differentiate from two independent cell lineages. *Development* 127, 2317-2322.
- Holst, J.J., and Gromada, J. (2004). Role of incretin hormones in the regulation of insulin secretion in diabetic and nondiabetic humans. *American Journal of Physiology-Endocrinology And Metabolism* 287, E199-E206.
- Hu, S., Wang, L., Togo, J., Yang, D., Xu, Y., Wu, Y., Douglas, A., and Speakman, J.R. (2020). The carbohydrate-insulin model does not explain the impact of

## References

- varying dietary macronutrients on the body weight and adiposity of mice. *Mol Metab* 32, 27-43.
- Huang, G.T., Lee, H.S., Chen, C.H., Chiou, L.L., Lin, Y.W., Lee, C.Z., Chen, D.S., and Sheu, J.C. (1998). Telomerase activity and telomere length in human hepatocellular carcinoma. *Eur J Cancer* 34, 1946-1949.
- Huang, X.T., Yue, S.J., Li, C., Huang, Y.H., Cheng, Q.M., Li, X.H., Hao, C.X., Wang, L.Z., Xu, J.P., Ji, M., et al. (2017). A Sustained Activation of Pancreatic NMDARs Is a Novel Factor of beta-Cell Apoptosis and Dysfunction. *Endocrinology* 158, 3900-3913.
- Hwang, I., Park, Y.J., Kim, Y.R., Kim, Y.N., Ka, S., Lee, H.Y., Seong, J.K., Seok, Y.J., and Kim, J.B. (2015). Alteration of gut microbiota by vancomycin and bacitracin improves insulin resistance via glucagon-like peptide 1 in diet-induced obesity. *FASEB J* 29, 2397-2411.
- Ishiyama, N., Ravier, M.A., and Henquin, J.C. (2006). Dual mechanism of the potentiation by glucose of insulin secretion induced by arginine and tolbutamide in mouse islets. *Am J Physiol Endocrinol Metab* 290, E540-549.
- Islam, M.S. (2010). The islets of Langerhans. Preface. *Adv. Exp. Med. Biol.* 654, vii-viii.
- Jacob, A.N., Salinas, K., Adams-Huet, B., and Raskin, P. (2006). Potential causes of weight gain in type 1 diabetes mellitus. *Diabetes Obes Metab* 8, 404-411.
- Jensen, M.V., Joseph, J.W., Ronnebaum, S.M., Burgess, S.C., Sherry, A.D., and Newgard, C.B. (2008). Metabolic cycling in control of glucose-stimulated insulin secretion. *Am J Physiol Endocrinol Metab* 295, E1287-1297.
- Jesudason, D.R., Monteiro, M.P., McGowan, B.M., Neary, N.M., Park, A.J., Philippou, E., Small, C.J., Frost, G.S., Ghatei, M.A., and Bloom, S.R. (2007). Low-dose pancreatic polypeptide inhibits food intake in man. *The British journal of nutrition* 97, 426-429.
- Johnson, J.W., and Ascher, P. (1987). Glycine potentiates the NMDA response in cultured mouse brain neurons. *Nature* 325, 529-531.
- Kahn, S.E., Cooper, M.E., and Del Prato, S. (2014). Pathophysiology and treatment of type 2 diabetes: perspectives on the past, present, and future. *Lancet* 383, 1068-1083.
- Kam, M.L., Nguyen, T.T., and Ngeow, J.Y. (2021). Telomere biology disorders. *NPJ genomic medicine* 6, 1-13.
- Kava, R.A., West, D.B., Lukasik, V.A., and Greenwood, M.R. (1989). Sexual dimorphism of hyperglycemia and glucose tolerance in Wistar fatty rats. *Diabetes* 38, 159-163.
- Kawamori, D., Kurpad, A.J., Hu, J., Liew, C.W., Shih, J.L., Ford, E.L., Herrera, P.L., Polonsky, K.S., McGuinness, O.P., and Kulkarni, R.N. (2009). Insulin signaling in alpha cells modulates glucagon secretion in vivo. *Cell Metab* 9, 350-361.
- Khan, A., Ling, Z.C., and Landau, B.R. (1996). Quantifying the carboxylation of pyruvate in pancreatic islets. *J Biol Chem* 271, 2539-2542.
- Kojima, S., Ueno, N., Asakawa, A., Sagiya, K., Naruo, T., Mizuno, S., and Inui, A. (2007). A role for pancreatic polypeptide in feeding and body weight regulation. *Peptides* 28, 459-463.
- Kolb, H., Stumvoll, M., Kramer, W., Kempf, K., and Martin, S. (2018). Insulin translates unfavourable lifestyle into obesity. *BMC Med* 16, 232.

## References

- Kolodney, G., Dumin, E., Safory, H., Rosenberg, D., Mori, H., Radzishevsky, I., and Wolosker, H. (2015). Nuclear Compartmentalization of Serine Racemase Regulates D-Serine Production: IMPLICATIONS FOR N-METHYL-D-ASPARTATE (NMDA) RECEPTOR ACTIVATION. *J Biol Chem* 290, 31037-31050.
- Korosi, J., McIntosh, C.H., Pederson, R.A., Demuth, H.-U., Habener, J.F., Gingerich, R., Egan, J.M., Elahi, D., and Meneilly, G.S. (2001). Effect of aging and diabetes on the enteroinsular axis. *The Journals of Gerontology Series A: Biological Sciences and Medical Sciences* 56, M575-M579.
- Kuhlow, D., Florian, S., von Figura, G., Weimer, S., Schulz, N., Petzke, K.J., Zarse, K., Pfeiffer, A.F., Rudolph, K.L., and Ristow, M. (2010). Telomerase deficiency impairs glucose metabolism and insulin secretion. *Aging (Albany NY)* 2, 650-658.
- Kuhn, C., You, S., Valette, F., Hale, G., van Endert, P., Bach, J.F., Waldmann, H., and Chatenoud, L. (2011). Human CD3 transgenic mice: preclinical testing of antibodies promoting immune tolerance. *Sci Transl Med* 3, 68ra10.
- Le, T.K.C., Hosaka, T., Nguyen, T.T., Kassu, A., Dang, T.O., Tran, H.B., Pham, T.P., Tran, Q.B., Le, T.H.H., and Pham, X.D. (2015). Bifidobacterium species lower serum glucose, increase expressions of insulin signaling proteins, and improve adipokine profile in diabetic mice. *Biomedical Research* 36, 63-70.
- Lee, C.H., Lu, W., Michel, J.C., Goehring, A., Du, J., Song, X., and Gouaux, E. (2014). NMDA receptor structures reveal subunit arrangement and pore architecture. *Nature* 511, 191-197.
- Levy, M.Z., Allsopp, R.C., Futcher, A.B., Greider, C.W., and Harley, C.B. (1992). Telomere end-replication problem and cell aging. *J. Mol. Biol.* 225, 951-960.
- Ley, R.E., Backhed, F., Turnbaugh, P., Lozupone, C.A., Knight, R.D., and Gordon, J.I. (2005). Obesity alters gut microbial ecology. *Proc Natl Acad Sci U S A* 102, 11070-11075.
- Ley, R.E., Turnbaugh, P.J., Klein, S., and Gordon, J.I. (2006). Human gut microbes associated with obesity. *Nature* 444, 1022-1023.
- Li, K., Xu, X., Hu, W., Li, M., Yang, M., Wang, Y., Luo, Y., Zhang, X., Liu, H., Li, L., et al. (2014). Glypican-4 is increased in human subjects with impaired glucose tolerance and decreased in patients with newly diagnosed type 2 diabetes. *Acta Diabetologica* 51, 981-990.
- Lillie, R.D., Pizzolato, P., and Donaldson, P.T. (1976). Hematoxylin substitutes: a survey of mordant dyes tested and consideration of the relation of their structure to performance as nuclear stains. *Stain Technol* 51, 25-41.
- Lim, A., Park, S.H., Sohn, J.W., Jeon, J.H., Park, J.H., Song, D.K., Lee, S.H., and Ho, W.K. (2009). Glucose deprivation regulates KATP channel trafficking via AMP-activated protein kinase in pancreatic beta-cells. *Diabetes* 58, 2813-2819.
- Lin, T.M., and Chance, R.E. (1974). Candidate hormones of the gut. VI. Bovine pancreatic polypeptide (BPP) and avian pancreatic polypeptide (APP). *Gastroenterology* 67, 737-738.
- Locasale, J.W. (2013). Serine, glycine and one-carbon units: cancer metabolism in full circle. *Nature Reviews Cancer* 13, 572-583.
- Lockridge, A., Gustafson, E., Wong, A., Miller, R.F., and Alejandro, E.U. (2021). Acute D-Serine Co-Agonism of beta-Cell NMDA Receptors Potentiates Glucose-Stimulated Insulin Secretion and Excitatory beta-Cell Membrane Activity. *Cells* 10.
- Lockridge, A.D., Baumann, D.C., Akhaphong, B., Abrenica, A., Miller, R.F., and Alejandro, E.U. (2016). Serine racemase is expressed in islets and contributes to the regulation of glucose homeostasis. *Islets* 8, 195-206.

## References

- Lopez-Gonzales, E., Lehmann, L., Ruiz-Ojeda, F.J., Hernandez-Bautista, R., Altun, I., Onogi, Y., Khalil, A.E., Liu, X., Israel, A., and Ussar, S. (2022). L-Serine Supplementation Blunts Fasting-Induced Weight Regain by Increasing Brown Fat Thermogenesis. *Nutrients* 14.
- Lu, D., Mulder, H., Zhao, P., Burgess, S.C., Jensen, M.V., Kamzolova, S., Newgard, C.B., and Sherry, A.D. (2002). <sup>13</sup>C NMR isotopomer analysis reveals a connection between pyruvate cycling and glucose-stimulated insulin secretion (GSIS). *Proc Natl Acad Sci U S A* 99, 2708-2713.
- Ludwig, D.S., and Ebbeling, C.B. (2018). The Carbohydrate-Insulin Model of Obesity: Beyond "Calories In, Calories Out". *JAMA Intern Med* 178, 1098-1103.
- MacDonald, M.J. (1981). High content of mitochondrial glycerol-3-phosphate dehydrogenase in pancreatic islets and its inhibition by diazoxide. *J Biol Chem* 256, 8287-8290.
- Marchetti, P., Lupi, R., Bugliani, M., Kirkpatrick, C.L., Sebastiani, G., Grieco, F.A., Del Guerra, S., D'Aleo, V., Piro, S., Marselli, L., et al. (2012). A local glucagon-like peptide 1 (GLP-1) system in human pancreatic islets. *Diabetologia* 55, 3262-3272.
- Marquard, J., Otter, S., Welters, A., Stirban, A., Fischer, A., Eglinger, J., Herebian, D., Kletke, O., Klemen, M.S., Stozler, A., et al. (2015). Characterization of pancreatic NMDA receptors as possible drug targets for diabetes treatment. *Nat Med* 21, 363-372.
- Matschinsky, F.M. (2002). Regulation of pancreatic beta-cell glucokinase: from basics to therapeutics. *Diabetes* 51 Suppl 3, S394-404.
- McCulloch, L.J., van de Bunt, M., Braun, M., Frayn, K.N., Clark, A., and Gloyn, A.L. (2011). GLUT2 (SLC2A2) is not the principal glucose transporter in human pancreatic beta cells: Implications for understanding genetic association signals at this locus. *Mol. Genet. Metab.* 104, 648-653.
- Mehrmohamadi, M., Liu, X., Shestov, Alexander A., and Locasale, Jason W. (2014). Characterization of the Usage of the Serine Metabolic Network in Human Cancer. *Cell Reports* 9, 1507-1519.
- Michael, D.R., Jack, A.A., Masetti, G., Davies, T.S., Loxley, K.E., Kerry-Smith, J., Plummer, J.F., Marchesi, J.R., Mullish, B.H., McDonald, J.A.K., et al. (2020). A randomised controlled study shows supplementation of overweight and obese adults with lactobacilli and bifidobacteria reduces bodyweight and improves well-being. *Scientific Reports* 10, 4183.
- Missios, P., Zhou, Y., Guachalla, L.M., von Figura, G., Wegner, A., Chakkarappan, S.R., Binz, T., Gompf, A., Hartleben, G., Burkhalter, M.D., et al. (2014). Glucose substitution prolongs maintenance of energy homeostasis and lifespan of telomere dysfunctional mice. *Nat Commun* 5, 4924.
- Mitchell, F. (2012). Obesity: glypican-4: role in insulin signalling. *Nat Rev Endocrinol* 8, 505.
- Monickaraj, F., Gokulakrishnan, K., Prabu, P., Sathishkumar, C., Anjana, R.M., Rajkumar, J.S., Mohan, V., and Balasubramanyam, M. (2012). Convergence of adipocyte hypertrophy, telomere shortening and hypoadiponectinemia in obese subjects and in patients with type 2 diabetes. *Clin. Biochem.* 45, 1432-1438.
- Moran, T.H. (2003). Pancreatic polypeptide: more than just another gut hormone? *Gastroenterology* 124, 1542-1544.
- Morigny, P., Houssier, M., Mouisel, E., and Langin, D. (2016). Adipocyte lipolysis and insulin resistance. *Biochimie* 125, 259-266.

## References

- Nair, K.S., Halliday, D., and Garrow, J.S. (1984). Increased energy expenditure in poorly controlled Type 1 (insulin-dependent) diabetic patients. *Diabetologia* 27, 13-16.
- Ndiaye, F.K., Ortalli, A., Canouil, M., Huyvaert, M., Salazar-Cardozo, C., Lecoecur, C., Verbanck, M., Pawlowski, V., Boutry, R., Durand, E., et al. (2017). Expression and functional assessment of candidate type 2 diabetes susceptibility genes identify four new genes contributing to human insulin secretion. *Mol Metab* 6, 459-470.
- Nilsson, R., Jain, M., Madhusudhan, N., Sheppard, N.G., Strittmatter, L., Kampf, C., Huang, J., Asplund, A., and Mootha, V.K. (2014). Metabolic enzyme expression highlights a key role for MTHFD2 and the mitochondrial folate pathway in cancer. *Nature Communications* 5.
- Ning, D.P., Xu, K., Zhu, H.J., Shan, G.L., Wang, D.M., Ping, B., Yu, Y.W., Pan, H., and Gong, F.Y. (2019). Serum Glypican 4 Levels Are Associated with Metabolic Syndrome in a Han Population from Guizhou Province, China. *Biomed Environ Sci* 32, 383-388.
- Nong, Y., Huang, Y.Q., Ju, W., Kalia, L.V., Ahmadian, G., Wang, Y.T., and Salter, M.W. (2003). Glycine binding primes NMDA receptor internalization. *Nature* 422, 302-307.
- Ohshima, K., Nojima, S., Tahara, S., Kurashige, M., Kawasaki, K., Hori, Y., Taniguchi, M., Umakoshi, Y., Okuzaki, D., Wada, N., et al. (2020). Serine racemase enhances growth of colorectal cancer by producing pyruvate from serine. *Nat Metab* 2, 81-96.
- Omar-Hmeadi, M., and Idevall-Hagren, O. (2021). Insulin granule biogenesis and exocytosis. *Cell Mol Life Sci* 78, 1957-1970.
- Pan, F.C., Brissova, M., Powers, A.C., Pfaff, S., and Wright, C.V. (2015). Inactivating the permanent neonatal diabetes gene *Mnx1* switches insulin-producing beta-cells to a delta-like fate and reveals a facultative proliferative capacity in aged beta-cells. *Development* 142, 3637-3648.
- Pan, F.C., and Wright, C. (2011). Pancreas organogenesis: from bud to plexus to gland. *Dev. Dyn.* 240, 530-565.
- Papouin, T., Ladepeche, L., Ruel, J., Sacchi, S., Labasque, M., Hanini, M., Groc, L., Pollegioni, L., Mothet, J.P., and Oliet, S.H. (2012). Synaptic and extrasynaptic NMDA receptors are gated by different endogenous coagonists. *Cell* 150, 633-646.
- Podlevsky, J.D., Bley, C.J., Omana, R.V., Qi, X., and Chen, J.J.-L. (2007). The telomerase database. *Nucleic acids research* 36, D339-D343.
- Portincasa, P., Bonfrate, L., Vacca, M., De Angelis, M., Farella, I., Lanza, E., Khalil, M., Wang, D.Q., Sperandio, M., and Di Ciaula, A. (2022). Gut Microbiota and Short Chain Fatty Acids: Implications in Glucose Homeostasis. *Int J Mol Sci* 23.
- Prentki, M., Matschinsky, F.M., and Madiraju, S.R. (2013). Metabolic signaling in fuel-induced insulin secretion. *Cell Metab* 18, 162-185.
- Purnell, J.Q., Hokanson, J.E., Marcovina, S.M., Steffes, M.W., Cleary, P.A., and Brunzell, J.D. (1998). Effect of excessive weight gain with intensive therapy of type 1 diabetes on lipid levels and blood pressure: results from the DCCT. *Diabetes Control and Complications Trial. JAMA* 280, 140-146.
- Qin, J., Li, Y., Cai, Z., Li, S., Zhu, J., Zhang, F., Liang, S., Zhang, W., Guan, Y., Shen, D., et al. (2012). A metagenome-wide association study of gut microbiota in type 2 diabetes. *Nature* 490, 55-60.

## References

- Rorsman, P., Bokvist, K., Ammala, C., Arkhammar, P., Berggren, P.O., Larsson, O., and Wahlander, K. (1991). Activation by adrenaline of a low-conductance G protein-dependent K<sup>+</sup> channel in mouse pancreatic B cells. *Nature* 349, 77-79.
- Rorsman, P., and Huisin, M.O. (2018). The somatostatin-secreting pancreatic delta-cell in health and disease. *Nat Rev Endocrinol* 14, 404-414.
- Roscioni, S.S., Migliorini, A., Gegg, M., and Lickert, H. (2016). Impact of islet architecture on  $\beta$ -cell heterogeneity, plasticity and function. *Nature Reviews Endocrinology* 12, 695-709.
- Ruiz-Ojeda, F.J., Wang, J., Backer, T., Krueger, M., Zamani, S., Rosowski, S., Gruber, T., Onogi, Y., Feuchtinger, A., Schulz, T.J., et al. (2021). Active integrins regulate white adipose tissue insulin sensitivity and brown fat thermogenesis. *Mol Metab* 45, 101147.
- Sachs, S., Bastidas-Ponce, A., Tritschler, S., Bakhti, M., Böttcher, A., Sánchez-Garrido, M.A., Tarquis-Medina, M., Kleinert, M., Fischer, K., Jall, S., et al. (2020). Targeted pharmacological therapy restores  $\beta$ -cell function for diabetes remission. *Nature Metabolism* 2, 192-209.
- Sakaguchi, M., Fujisaka, S., Cai, W., Winnay, J.N., Konishi, M., O'Neill, B.T., Li, M., Garcia-Martin, R., Takahashi, H., Hu, J., et al. (2017). Adipocyte Dynamics and Reversible Metabolic Syndrome in Mice with an Inducible Adipocyte-Specific Deletion of the Insulin Receptor. *Cell Metab* 25, 448-462.
- Sakula, A. (1988). Paul Langerhans (1847-1888): a centenary tribute. *J. R. Soc. Med.* 81, 414-415.
- Sancar, G., Liu, S., Gasser, E., Alvarez, J.G., Moutos, C., Kim, K., van Zutphen, T., Wang, Y., Huddy, T.F., Ross, B., et al. (2022). FGF1 and insulin control lipolysis by convergent pathways. *Cell Metab* 34, 171-183 e176.
- Saretzki, G. (2018). Telomeres, telomerase and ageing. *Biochemistry and Cell Biology of Ageing: Part I Biomedical Science*, 221-308.
- Schellekens, H., Torres-Fuentes, C., van de Wouw, M., Long-Smith, C.M., Mitchell, A., Strain, C., Berding, K., Bastiaanssen, T.F.S., Rea, K., Golubeva, A.V., et al. (2021). *Bifidobacterium longum* counters the effects of obesity: Partial successful translation from rodent to human. *EBioMedicine* 63, 103176.
- Schweiger, M., Eichmann, T.O., Taschler, U., Zimmermann, R., Zechner, R., and Lass, A. (2014). Measurement of lipolysis. *Methods Enzymol.* 538, 171-193.
- Scrocchi, L.A., and Drucker, D.J. (1998). Effects of aging and a high fat diet on body weight and glucose tolerance in glucagon-like peptide-1 receptor<sup>-/-</sup> mice. *Endocrinology* 139, 3127-3132.
- Sears, B., and Perry, M. (2015). The role of fatty acids in insulin resistance. *Lipids in health and disease* 14, 1-9.
- Skrenkova, K., Song, J.M., Kortus, S., Kolcheva, M., Netolicky, J., Hemelikova, K., Kaniakova, M., Krausova, B.H., Kucera, T., Korabecny, J., et al. (2020). The pathogenic S688Y mutation in the ligand-binding domain of the GluN1 subunit regulates the properties of NMDA receptors. *Sci Rep* 10, 18576.
- Speakman, J.R., and Hall, K.D. (2021). Carbohydrates, insulin, and obesity. *Science* 372, 577-578.
- Stanley, C.A. (2016). Perspective on the Genetics and Diagnosis of Congenital Hyperinsulinism Disorders. *J Clin Endocrinol Metab* 101, 815-826.
- Steiner, D.J., Kim, A., Miller, K., and Hara, M. (2010). Pancreatic islet plasticity: interspecies comparison of islet architecture and composition. *Islets* 2, 135-145.

## References

- Strisovsky, K., Jiraskova, J., Mikulova, A., Rulisek, L., and Konvalinka, J. (2005). Dual substrate and reaction specificity in mouse serine racemase: identification of high-affinity dicarboxylate substrate and inhibitors and analysis of the beta-eliminase activity. *Biochemistry* 44, 13091-13100.
- Sun, H., Zhang, S., Zhang, A., Yan, G., Wu, X., Han, Y., and Wang, X. (2014). Metabolomic analysis of diet-induced type 2 diabetes using UPLC/MS integrated with pattern recognition approach. *PLoS One* 9, e93384.
- Suwandhi, L., Hausmann, S., Braun, A., Gruber, T., Heinzmann, S.S., Galvez, E.J.C., Buck, A., Legutko, B., Israel, A., Feuchtinger, A., et al. (2018). Chronic d-serine supplementation impairs insulin secretion. *Mol Metab* 16, 191-202.
- Svendsen, B., Larsen, O., Gabe, M.B.N., Christiansen, C.B., Rosenkilde, M.M., Drucker, D.J., and Holst, J.J. (2018). Insulin Secretion Depends on Intra-islet Glucagon Signaling. *Cell Rep* 25, 1127-1134 e1122.
- Sweet, I.R., and Matschinsky, F.M. (1995). Mathematical model of beta-cell glucose metabolism and insulin release. I. Glucokinase as glucosensor hypothesis. *Am J Physiol* 268, E775-788.
- Tahrani, A.A., Bailey, C.J., Del Prato, S., and Barnett, A.H. (2011). Management of type 2 diabetes: new and future developments in treatment. *Lancet* 378, 182-197.
- Takahashi, N., Kishimoto, T., Nemoto, T., Kadowaki, T., and Kasai, H.J.S. (2002). Fusion pore dynamics and insulin granule exocytosis in the pancreatic islet. *297*, 1349-1352.
- Talchai, C., Xuan, S., Lin, H.V., Sussel, L., and Accili, D. (2012). Pancreatic beta cell dedifferentiation as a mechanism of diabetic beta cell failure. *Cell* 150, 1223-1234.
- Tamori, Y., and Kasuga, M. (2013). Glypican-4 is a new comer of adipokines working as insulin sensitizer. *J Diabetes Investig* 4, 250-251.
- ter Horst, K.W., Gilijamse, P.W., de Weijer, B.A., Kilicarslan, M., Ackermans, M.T., Nederveen, A.J., Nieuwdorp, M., Romijn, J.A., and Serlie, M.J. (2015). Sexual Dimorphism in Hepatic, Adipose Tissue, and Peripheral Tissue Insulin Sensitivity in Obese Humans. *Frontiers in Endocrinology* 6.
- Thorens, B. (2014). Neural regulation of pancreatic islet cell mass and function. *Diabetes Obes Metab* 16 Suppl 1, 87-95.
- Thorens, B., Sarkar, H.K., Kaback, H.R., and Lodish, H.F. (1988). Cloning and functional expression in bacteria of a novel glucose transporter present in liver, intestine, kidney, and beta-pancreatic islet cells. *Cell* 55, 281-290.
- Thorens, B., Tarussio, D., Maestro, M.A., Rovira, M., Heikkilä, E., and Ferrer, J. (2015). Ins1(Cre) knock-in mice for beta cell-specific gene recombination. *Diabetologia* 58, 558-565.
- Tokarz, V.L., MacDonald, P.E., and Klip, A. (2018). The cell biology of systemic insulin function. *J Cell Biol* 217, 2273-2289.
- Tsai, F.J., Yang, C.F., Chen, C.C., Chuang, L.M., Lu, C.H., Chang, C.T., Wang, T.Y., Chen, R.H., Shiu, C.F., Liu, Y.M., et al. (2010). A genome-wide association study identifies susceptibility variants for type 2 diabetes in Han Chinese. *PLoS Genet* 6, e1000847.
- Ussar, S., Bezy, O., Bluher, M., and Kahn, C.R. (2012). Glypican-4 enhances insulin signaling via interaction with the insulin receptor and serves as a novel adipokine. *Diabetes* 61, 2289-2298.

## References

- Ussar, S., Fujisaka, S., and Kahn, C.R. (2016). Interactions between host genetics and gut microbiome in diabetes and metabolic syndrome. *Mol Metab* 5, 795-803.
- Utzschneider, K.M., Kratz, M., Damman, C.J., and Hullar, M. (2016). Mechanisms Linking the Gut Microbiome and Glucose Metabolism. *J Clin Endocrinol Metab* 101, 1445-1454.
- Vangipurapu, J., Stancáková, A., Smith, U., Kuusisto, J., and Laakso, M. (2019). Nine amino acids are associated with decreased insulin secretion and elevated glucose levels in a 7.4-year follow-up study of 5,181 Finnish men. *Diabetes* 68, 1353-1358.
- Villasenor, A., Chong, D.C., Henkemeyer, M., and Cleaver, O. (2010). Epithelial dynamics of pancreatic branching morphogenesis. *Development* 137, 4295-4305.
- Vital, P., Larrieta, E., and Hiriart, M. (2006). Sexual dimorphism in insulin sensitivity and susceptibility to develop diabetes in rats. *J Endocrinol* 190, 425-432.
- Wendt, A., and Eliasson, L. (2020). Pancreatic  $\alpha$ -cells - The unsung heroes in islet function. *Semin. Cell Dev. Biol.* 103, 41-50.
- Wilson, J.E. (2003). Isozymes of mammalian hexokinase: structure, subcellular localization and metabolic function. *J Exp Biol* 206, 2049-2057.
- Wolosker, H., and Balu, D.T. (2020). D-Serine as the gatekeeper of NMDA receptor activity: implications for the pharmacologic management of anxiety disorders. *Transl Psychiatry* 10, 184.
- Wolosker, H., and Mori, H. (2012). Serine racemase: an unconventional enzyme for an unconventional transmitter. *Amino Acids* 43, 1895-1904.
- Wolosker, H., Sheth, K.N., Takahashi, M., Mothet, J.P., Brady, R.O., Jr., Ferris, C.D., and Snyder, S.H. (1999). Purification of serine racemase: biosynthesis of the neuromodulator D-serine. *Proc Natl Acad Sci U S A* 96, 721-725.
- Wong, R.H., and Sul, H.S. (2010). Insulin signaling in fatty acid and fat synthesis: a transcriptional perspective. *Curr. Opin. Pharm.* 10, 684-691.
- Wren, A.M., Seal, L.J., Cohen, M.A., Brynes, A.E., Frost, G.S., Murphy, K.G., Dhillon, W.S., Ghatei, M.A., and Bloom, S.R. (2001). Ghrelin enhances appetite and increases food intake in humans. *J Clin Endocrinol Metab* 86, 5992.
- Wu, Y., Fortin, D.A., Cochrane, V.A., Chen, P.C., and Shyng, S.L. (2017). NMDA receptors mediate leptin signaling and regulate potassium channel trafficking in pancreatic beta-cells. *J Biol Chem* 292, 15512-15524.
- Yan-Do, R., and MacDonald, P.E. (2017). Impaired "Glycine"-mia in Type 2 Diabetes and Potential Mechanisms Contributing to Glucose Homeostasis. *Endocrinology* 158, 1064-1073.
- Yang, G., Wei, J., Liu, P., Zhang, Q., Tian, Y., Hou, G., Meng, L., Xin, Y., and Jiang, X. (2021). Role of the gut microbiota in type 2 diabetes and related diseases. *Metabolism* 117, 154712.
- Yoo, H.J., Hwang, S.Y., Cho, G.J., Hong, H.C., Choi, H.Y., Hwang, T.G., Kim, S.M., Bluher, M., Youn, B.S., Baik, S.H., et al. (2013). Association of glypican-4 with body fat distribution, insulin resistance, and nonalcoholic fatty liver disease. *J Clin Endocrinol Metab* 98, 2897-2901.
- Zhang, X., Shen, D., Fang, Z., Jie, Z., Qiu, X., Zhang, C., Chen, Y., and Ji, L. (2013). Human Gut Microbiota Changes Reveal the Progression of Glucose Intolerance. *PLOS ONE* 8, e71108.

## *References*

- Zhao, Y., Zhou, Y., Xiao, M., Huang, Y., Qi, M., Kong, Z., Chi, J., Che, K., Lv, W., Dong, B., et al. (2022). Impaired glucose tolerance is associated with enhanced postprandial pancreatic polypeptide secretion. *Journal of diabetes* 14, 334-344.
- Zhou, J., Zhang, Z., Yang, Y., Liao, F., Zhou, P., Wang, Y., Zhang, H., Jiang, H., Alinejad, T., Shan, G., et al. (2022). Deletion of serine racemase reverses neuronal insulin signaling inhibition by amyloid-beta oligomers. *J Neurochem*.
- Zhou, Q., and Melton, D.A. (2018). Pancreas regeneration. *Nature* 557, 351-358.
- Zhu, L., Dattaroy, D., Pham, J., Wang, L., Barella, L.F., Cui, Y., Wilkins, K.J., Roth, B.L., Hochgeschwender, U., Matschinsky, F.M., et al. (2019). Intra-islet glucagon signaling is critical for maintaining glucose homeostasis. *JCI Insight* 5.

# *Acknowledgements*

## **Acknowledgements**

I would like to thank all the people who gives me supports in any aspects to complete my PhD.

First of all, I would like to give a big thanks to my supervisor **Siegfried Ussar** who provides me the opportunity to be here, IDO, to get my PhD. Thanks for providing great projects to me and always sharing your great ideas with us. Thanks for your patience and teaching allowing me to grow up to be strong. I learned a lot from you in both ways, work and life. Like, always believe and accept the data you got no matter whether you like it or not but just try to find a way to explain it. The tips for getting along with others, for example, collaborators, animal caretakers, and administrators. These all will help me a lot in my future life. In the end, I want to say that your sense of humor makes our lab life or lab meetings more relaxed and much more fun.

Thanks to my committee members: **Prof. Dr. Till Strowig** and **Prof. Dr. Martin Klingenspor** for the great supervise and support during my PhD study. Special thanks to Prof. Dr. Till Strowig for his great support of Terc project, especially the microbiota part. Thanks to Prof. Dr. Martin Klingenspor for the great suggestions regarding TSE data analysis.

I am really glad to be a member of the Adipocyte and Metabolism group and thanks all our group members. First of all, I would like to thank **Ahmed Elagamy Khalil**, help me to complete the Terc project together. You are always very kind to provide help at lab and always gentle to carry all the heavy stuff for me when we work together. Thanks **Andreas Isreal**, helps me a lot, cutting tons of paraffin pancreas sections and supporting me to do GSIS, my most often but a bit suffering experiment. Thanks for helping with getting my driving license as well. I would also like to thank my former colleague **René Hernández-Bautista**. Thanks for your help during my PhD: helping with the Gpc4 project; teaching me lots of techniques, GTT, ITT, dissections; paper writing; Spanish as well as my driver license. We practice parking during weekends. Thanks for being my teacher for lab technique, I am really happy to be your “calculators” at lab as well. Big thanks to **Yasuhiro Onogi**, our science and cake advisor. Thanks for helping my experiments and

## *Acknowledgements*

manuscript writing. I appreciate the time with you chatting and discussing science, career, cake baking and...that often happened at our empty office and with a cup of water while we stay very late for works. Another thanks to **Francisco Javier Ruiz-Ojeda**, for helping my projects a lot, especially the SRR project. My first GIS experiment is taught by you. I will miss our lunchtime chatting together with other colleagues, which sometimes becomes Spanish learning time. Thanks **Xiaocheng Yan** for helping with my project especially for the mice work. Really happy to know you here, and enjoy the time we travel around together. Thanks for your accompany in different countries and different cities. Thanks **Elena López-Gonzales** for the help within these years especially for my Terc project. I would also like to thank **Inderjeet Singh** for the help at lab, especially for the mice work of my project. Thanks **Irem Altun** for the help and suggestions during these years, and always glad to have discussions on any topics no matter life or science with you. Thanks **Samira Zamani, Ruth Karlina** for the help at lab. Thanks my fresh colleague **Lingru Kang**, happy to work with you and have fun with you.

I would like to thank my collaborators to make these work possible. Thanks **Cahuê De Bernardis Murat, Dr. Cristina García Cáceres Özüm Sehnaz Caliskan, Dr. Natalie Krahmer, Natalia Prudente de Mello, Prof. Dr. Fabiana Perocchi, Liwei Zhang, Prof. Dr. Susanna Hoffman, Uthayakumar Muthukumarasamy**.

I also would like to thank all other members of IDO. Thanks to our director of our institute **PD Dr. Timo Müller** especially for the suggestions for TSE data analysis. I would like to thank **Dr. Aaron Nvikoff** provides great suggestions for my PhD work, helps for proofreading my thesis and polishing my writing. Out of science, I will miss the Isar river parties during the weekend with hot dog, spike ball. Always have a lot of fun with you. Thanks to my second 'English supervisor' **Callum Couplan**, helps a lot with my manuscript writings. Out of work, enjoyed the time hiking and having fun together. Thanks Dr. Qian zhang, Dr. Gerald Grandl, Franziska Lechner, Dr. Tim Gruber, Dr. Luke Harrison, Konxhe Kulaj, Dr. Alexandra Harger.

Thanks to people from IDR, Dr. Weiwei Xu, Anett Seelig, Dr. Marta Tarquis, Dr. Aimee Bastidas Ponce, Julia provide me the opportunity to learn islets isolation,

## *Acknowledgements*

*ex vivo*, *in vivo* GSIS experiments, IF staining of islets. Thanks Dr. Xianming Wang, Dr. Mostafa Bakhti for providing helps as well.

In the end, the biggest thank to my family, my dad, mom and sisters who support me at any time from any aspects. Without you, I won't be here. Thank you.

## Publications and presentations

1. **Liu, X.**, Khalil, A. E. M. M., Muthukumarasamy, U., Onogi, Y., Yan, X., Singh, I., Lopez-Gonzales, E., Israel, A., Serrano, A. C., Strowig, T., & Ussar, S. Reduced intestinal lipid absorption improves glucose metabolism in aged G2-Terc knockout mice. **BMC biology**. **2023**
2. **Liu, X.**, Jin, Z., Summers, S., Deros, D., Li, M., Li, B., Li, L., and Speakman, J.R. Calorie restriction and calorie dilution have different impacts on body fat, metabolism, behavior, and hypothalamic gene expression. **Cell Rep**. **2022**
3. Lopez-Gonzales, E., Lehmann, L., Ruiz-Ojeda, F.J., Hernandez-Bautista, R., Altun, I., Onogi, Y., Khalil, A.E., **Liu, X.**, Israel, A., and Ussar, S. L-Serine Supplementation Blunts Fasting-Induced Weight Regain by Increasing Brown Fat Thermogenesis. **Nutrients**. **2022**
4. Zhang Q, Delessa CT, Augustin R, Bakhti M, Colldén G, Drucker DJ, Feuchtinger A, Caceres CG, Grandl G, Harger A, Herzig S, Hofmann S, Holleman CL, Jastroch M, Keipert S, Kleinert M, Knerr PJ, Kulaj K, Legutko B, Lickert H, **Liu X**, Luippold G, Lutter D, Malogajski E, Medina MT, Mowery SA, Blutke A, Perez-Tilve D, Salinno C, Seherer L, DiMarchi RD, Tschöp MH, Stemmer K, Finan B, Wolfrum C, Müller TD. The glucose-dependent insulintropic polypeptide (GIP) regulates body weight and food intake via CNS-GIPR signaling. **Cell Metab**. **2021**
5. Mei J, Böhlend C, Geiger A, Baur I, Berner K, Heuer S, **Liu X**, Mataite L, Melo-Narváez MC, Özkaya E, Rupp A, Siebenwirth C, Thoma F, Kling MF, Friedl AA. Development of a model for fibroblast-led collective migration from breast cancer cell spheroids to study radiation effects on invasiveness. **Radiat Oncol**. **2021**
6. Zhao, Z.J., Deros, D., Gerrard, A., Wen, J., **Liu, X.**, Tan, S., Hambly, C., and Speakman, J.R. Limits to sustained energy intake. XXX. Constraint or restraint? Manipulations of food supply show peak food intake in lactation is constrained. **J Exp Biol**. **2020**
7. Li B, Li L, Li M, Lam SM, Wang G, Wu Y, Zhang H, Niu C, Zhang X, **Liu X**, Hambly C, Jin W, Shui G, Speakman JR. Microbiota Depletion Impairs

## *Publications and presentations*

Thermogenesis of Brown Adipose Tissue and Browning of White Adipose Tissue. **Cell Rep. 2019**

8. Keystone Symposia Conference, Obesity and Adipose Tissue Biology J7, Banff, Canada. Poster, 2019.02
9. Obesity week, San Diego, US. Poster. 2022.11